THE SPECIFICATION AND PATTERNING OF THE DROSOPHILA EGG CHAMBER

BY

Lan Lan

B.S., Huazhong University of Science and Technology, 2002

Submitted to the graduate degree program in Molecular Biosciences
and the Graduate Faculty of the University of Kansas
in partial fulfillment of the requirements for the degree of
Doctor of Philosophy

Committee members: _____
Chairperson – Robert S. Cohen

_____
Victoria L. Corbin

_____
Erik A. Lundquist

_____
Kristi L. Neufeld

_____
Robert E. Ward

_____
Joy K. Ward

Date defended: November 30, 2010

_____

The Dissertation Committee for Lan Lan certifies
that this is the approved version of the following dissertation:

THE SPECIFICATION AND PATTERNING OF THE DROSOPHILA EGG CHAMBER

Committee members:

_____
Chairperson – Robert S. Cohen

_____
Victoria L. Corbin

_____
Erik A. Lundquist

_____
Kristi L. Neufeld

_____
Robert E. Ward

_____
Joy K. Ward

Date approved: December 6, 2010

_____

ABSTRACT

The generation of cell polarity through the localization of specific mRNAs and proteins to discrete subcellular sites is fundamental to asymmetric cell division, tissue morphogenesis, cell migration, and most other developmental processes. While many different localized mRNAs and proteins have been described, the mechanisms by which such molecules become localized are only poorly understood.

In the first part of this dissertation, I describe my efforts to unravel the mechanism by which *gurken (grk)* mRNA becomes localized to the anterodorsal corner of the *Drosophila* oocyte during mid-oogenesis. Such localization is a key step in the polarization of the mature *Drosophila* egg and future embryo; defects in *grk* mRNA localization result in the production of depolarized eggs that give rise to embryos that fail to specify ectodermal, endodermal and mesodermal germ layers and die before hatching. I show, using a transgenic fly assay system, that a conserved sequence element within the *grk* mRNA, called the GLS (*grk* localization sequence) is essential for anterodorsal localization. My studies indicate that the GLS functions by mediating the association of *grk* transcripts with a minus end directed microtubule (MT) motor protein, most probably cytoplasmic dynein. Although MT minus ends are enriched around the nuclear membrane in the oocyte's anterodorsal corner, MT minus ends are also abundant along other regions of the anterior cortex. My data force reconsideration of previous models of *grk* mRNA localization which propose that *grk* mRNA transport complexes specifically associate with that subset of MTs whose minus ends are concentrated around the oocyte nucleus. Indeed my data suggest that *grk* mRNA transport particles associate with all MT populations equally and that anterodorsal localization is brought about through repeated

rounds of MT association and anterior transport accompanied by specific trapping of the mRNA at the anterodorsal cortex. The mechanism by which *grk* becomes trapped is unclear, but probably requires at least one RNA element in addition to the GLS.

The second part of the dissertation is focused on the mechanism by which Rab11, a small GTPase best known for its role in trafficking vesicles from recycling endosomes to the plasma membrane, polarizes *Drosophila* germline stem cells (GSCs). Specifically, I present my characterization of a new Rab11 effector, dRip11 (*Drosophila* Rab11-family interacting protein). First, I show that dRip11 binds to Rab11 in vitro. Second, I identify a region within the Rab11 protein that is required for binding to dRip11. Third, I show that dRip11 has overlapping expression pattern with Rab11 in GSCs and border cells within the *Drosophila* ovary. Finally, I describe my attempt to generate and analyze dRip11 mutations.

ACKNOWLEDGEMENTS

Finishing the graduate school and writing the dissertation is never an easy journey for me, without all the help and encouragement from numerous people, I could never have come to this point.

First and the foremost, I would like to thank my mentor Dr. Robert Cohen, who gives me tremendous support, guidance and encouragement. I could not find the best word to express my deepest thanks to him. He is always been so patient to read and revise all my writings over and over. He can always solve any kinds of questions and doubts I had. I feel so lucky to be guided by him during my graduate school.

Second, I would like to thank everyone that was and is in the Cohen lab that helped me with my projects. Especially I would like to thank former postdoc researcher Dr. Shengyin Lin, former technician Sui Zhang and my labmate Jiang Xu for all the suggestions and helpful discussions.

Third, I would also like to acknowledge members of my graduate committee, Dr. Erik Lundquist, Dr. Robert Ward, Dr. Victoria Corbin, Dr. Kristi Neufeld, Dr. Jennifer Gleason, Dr. Yoshiaki Azuma and Dr. Joy Ward for all their advice and suggestions, and/or for reading my dissertation.

Last but not least, I would like to thank my parents and my grandparents, who are or were so supportive in my pursuing my childhood dream. Without them, I could not have been here and finish my PhD far away from home in the US.

TABLE OF CONTENTS

LIST OF FIGURES

LIST OF TABLES

Chapter I

Introduction

1. *DROSOPHILA* OOGENESIS

The *Drosophila* female contains a pair of ovaries (Fig. 1.1A) in which oogenesis takes place (Bastock and St Johnston, 2008). Each ovary is composed of about 15 tube-like structures called ovarioles (Fig. 1.1C and boxed area in Fig. 1.1A), with each ovariole consisting of an anterior compartment, called the germarium (Fig. 1.1B), and a posterior compartment, called the vitellarium (Fig. 1.1C). Oogenesis begins in germarial region 1, the anterior-most of three germarial subcompartments, when a germline stem cell (GSC) divides asymmetrically to give an anterior daughter, which regenerate the stem cell and a posterior cystoblast, which goes on to divide and differentiate. Each germarium contains 2-3 GSCs, which together with neighboring somatic cap, sheath and terminal filament cells define the germline stem cell niche (Kirilly and Xie, 2007; Song et al., 2002). The somatic niche cells provide chemical cues that help maintain stem cell identity. Each GSC is attached to niche cap cells by adherens junctions and such attachments are required for the maintenance of GSC identity (Bogard et al., 2007; Kirilly and Xie, 2007; Song et al., 2002). Because GSCs divide along the anteroposterior axis of the germarium, only the anterior daughter inherits the adherens junctions and retains GSC identity. The posterior daughter (i. e., the cystoblast) divides 4 times with incomplete cytokenesis to produce a 16-cell cyst that moves posteriorly and enters region 2a.

All 16 germline cyst cells are interconnected to each other via a series of 15 cytoplasmic bridges called ring canals, the remnants of incomplete cytokenesis during cyst formation： the two first-generation cells, referred to as pro-oocytes, have 4 ring canals each, the two second generation cells have 3 each, the four third generation cells

have 2 each, and the eight fourth generation cells have 1 each. One of the two cells with four ring canals becomes the oocyte, while the other 15 cells adopt the nurse cell fate, which are responsible for the synthesis of the majority of the RNAs and proteins found in the developing oocyte, mature egg, and future embryo (Becalska and Gavis, 2009). The oocyte is determined in region 2a as evident by its accumulation of specific marker proteins, such as Orb, K10, Bicaudal-D (BicD), and Egalitarian (Egl) (Huynh and St Johnston, 2004). The other pro-oocyte begins to accumulate oocyte-specific markers, but such markers ultimately become concentrated in a single cell—the oocyte.

In germarial region 2b, the oocyte-nurse cell cyst flattens to form a one-cell thick disc that extends the whole diameter of the germarium, with the oocyte positioned in the center. Two or three somatic stem cells reside along the wall of the germarium at the boundary of regions 2a and 2b, and give rise to three types of somatic follicle cells, namely, main body follicle cells, polar cells, and stalk cells (Horne-Badovinac and Bilder, 2005). As the germline cyst enters germarial region 3, it becomes encased in a monolayer of follicle cells to form a stage 1 egg chamber (Fig. 1.1B). This monolayer is composed of about 80 main body follicle cells, and 4 polar cells, 2 each at the posterior and anterior ends of the egg chamber (Dobens and Raftery, 2000; Horne-Badovinac and Bilder, 2005). The main body follicle cells have well-defined apical and basal surfaces and resemble conventional epithelial cells, whereas the polar cells have a teardrop shape and do not elaborate a distinctive apical-basal polarity. The stage 1 egg chamber subsequently buds from the germarium into the vitellarium, where it continues to move posteriorly and matures through 13 morphologically distinct stages (stages 2-14) (Bastock and St Johnston, 2008; Horne-Badovinac and Bilder, 2005). Each budding egg

chamber is separated from the next by 6-10 stalk cells, which are initially arranged as a two-cell wide column but intercalate into a single-cell wide column, or stalk, by stage 3. The stalk cells are subsequently targeted for programmed cell death and are not visible after stage 5 or 6 (Dobens and Raftery, 2000). While germline cells and polar cells do not divide during egg chamber maturation, the main-body follicle cells divide 4 times to maintain coverage of the germline cyst which grows throughout oogenesis (Horne-Badovinac and Bilder, 2005).

Nurse cells endo-replicate their DNA during each stage of oogenesis, reaching a chromosome ploidy of ~1000 by stage 9, while the oocyte remains diploid. The nurse cells are highly metabolically active during these early and middle stages of egg chamber maturation. The oocyte is metabolically inactive during these stages and most of its growth is due to its uptake of yolk protein, which is secreted into the surrounding hemolymph by follicle cells during stages 7-9. During early stage 9, the oocyte nucleus undergoes a distinct migration to the anterior cortex, orthogonal to the egg chamber's anteroposterior axis, thereby defines the dorsoventral axis of the oocyte, egg chamber and future embryo. The RNAs of certain key regulatory proteins (e.g., *gurken*, *bicoid*, and *oskar*) are selectively transported from nurse cells into the oocyte during stages 1-9 of oogenesis, but most molecules are retained in nurse cells until stage 11, when nurse cells indiscriminately dump their entire cytoplasmic contents into the oocyte (Cooley and Theurkauf, 1994).

Beginning at stage 9 of oogenesis, the 2 anterior polar cells and 6-8 neighboring main body follicle cells delaminate from the epithelium to form a "border cell" cluster (Fig. 1.1D). This cluster subsequently migrates posteriorly through the nurse cell cluster

until it reaches the oocyte's anterior surface. The border cells then migrate dorsally, i. e., toward the oocyte nucleus (Horne-Badovinac and Bilder, 2005; Montell, 2003), where they secrete the micropyle and operculum, specialized components of the eggshell designed for sperm entry and embryo hatching, respectively. The oocyte continues to grow during these stages and by stage 10, accounts for about half of the total egg chamber volume. Beginning at stage 10B, main body follicle cells start to secrete the eggshell and extrachorionic layers (Horne-Badovinac and Bilder, 2005). Nurse and follicle cells are subsequently targeted for cell death, and the oocyte is fertilized as it passes through the oviduct and is oviposited (Horne-Badovinac and Bilder, 2005).

2. POLARITY IN OOGENESIS

The freshly laid *Drosophila* egg is highly polarized. As alluded to above, such polarity arises slowly over the course of oogenesis and can be traced back to the earliest steps.

In the germarium, for example, the GSCs divide along the anteroposterior axis of the ovariole, such that the posterior cystoblast is displaced from the niche by a one-cell diameter distance. Decapentaplegic (Dpp), the *Drosophila* Bone morphogenetic protein 4 (BMP4) homolog, is secreted from niche cells which flank the anterior end of the germarium, and is required for maintenance of GSC identity. Because Dpp is a short-range signal, the cystoblast does not receive sufficient quantities of the Dpp signal to maintain GSC identity, and instead differentiates (Bogard et al., 2007; Ohlstein et al., 2004; Xie and Spradling, 2000). The GSC is itself polarized as evident by the anterior localization of the fusome (also called the spectrosome in GSCs), a membrane- and

spectrin-rich germline-specific organelle. The anterior localization of the fusome is important in the maintenance of the adherens junctions between GSCs and niche cap cells as it facilitates the polarized trafficking of E-Cadherin (E-Cad) from the fusome to the niche-facing surface of the GSC.

The asymmetric position of the fusome within the GSC also facilitates the polarization/positioning of the cystoblast and germline cyst, and is critical for oocyte determination (Huynh and St Johnston, 2004). When a GSC divides, the fusome anchors one pole of the mitotic spindle. Since the fusome is located at the anterior cortex of the GSC, such anchoring orients the plane of division perpendicular to the anteroposterior axis of the germarium, thus ensuring the birth of both an anterior and a posterior cell. Prior to cytokinesis, the fusome spreads along the microtubule spindle, with about two-thirds of it remaining in the GSC (anterior daughter cell) and one-third of it being donated to the posterior cystoblast (Huynh and St Johnston, 2004). During the first cystoblast division, the fusome again anchors a single mitotic spindle. New fusome material known as a "plug" is assembled at the spindle mid-body, where it presumably has a role in arresting cytokinesis. In this way, one of the first two cystocytes has more fusome material than the other; it has all of the original fusome plus half of the plug, while the other cystocyte has just half of the plug. The original fusome subsequently fuses with the plug to form a single fusome that although shared by both cystocytes, is of greater volume in one of the two cystocytes (Huynh and St Johnston, 2004). This general scheme of mitotic spindle anchoring, fusome plug formation, and fusome fusion is continued through the final three rounds of mitosis, such that the entire 16-cell cluster is interconnected by a stereotypically branched fusome structure, with one cell containing

more fusome than any of the others (Deng and Lin, 1997; Huynh and St Johnston, 2004; Roth and Lynch, 2009). This cell goes on to become the oocyte, although the exact role of the fusome in oocyte determination is obscure. Once the oocyte is determined, the fusome is disassembled and replaced with a polarized microtubule (MT) cytoskeleton, nucleated by a microtubule organization center (MTOC) located in the oocyte (Roth and Lynch, 2009). MTs extend anteriorly from this MTOC and provide a means for the selective transport for RNAs, proteins, vesicles, and other materials from nurse cells into the oocyte (Becalska and Gavis, 2009; Cooley and Theurkauf, 1994; Roth and Lynch, 2009).

The enrichment of the fusome in a single cystocyte is not only important for oocyte determination, but also for the subsequent positioning of the oocyte to the posterior end of the nurse cell cluster. Such positioning is dependant on homotypic interactions between E-Cad molecules located on the surface of the oocyte and posterior polar follicle cells (Fig. 1.2A) (Gonzalez-Reyes and St Johnston, 1998). E-Cad is also present on the surface of nurse cells, however, because E-Cad is enriched on the surface of the oocyte, the oocyte efficiently out competes nurse cells for adhesion to posterior follicle cells. The recent finding that E-Cad transits through the fusome en route to the plasma membrane provides an explanation for its enrichment on the surface of the oocyte, and thus, the specification of the egg chamber's anteroposterior axis.

Oocyte positioning and the specification of the egg chamber's anteroposterior axis are necessary for the specification of the oocyte's anteroposterior and, in turn, dorsoventral axes. The anteroposterior axis is specified during stage 6/7, when Gurken protein is secreted from the oocyte and induces neighboring follicle cells to adopt the

posterior cell fate through activation of Torpedo (the *Drosophila* EGF receptor) (Gonzalez-Reyes et al., 1995; Neuman-Silberberg and Schupbach, 1996; Nilson and Schupbach, 1999), which is expressed on the oocyte-facing surface of all follicle cells. Follicle cells at the anterior of the egg chamber do not receive any of the Gurken signal and adopt the default anterior follicle cell fate. Posterior follicle cells send an unknown signal back to the oocyte that acts locally both to dismantle the oocyte's MTOC and to prevent the formation of new (posterior) MTOCs (Theurkauf et al., 1992). Concomitantly, multiple new MTOCs are formed along the anterior and anterior-lateral cortexes of the oocyte and nucleate a polarized MT network (Theurkauf et al., 1992), with minus ends enriched at the anterior end of the oocyte and plus ends pointed towards the posterior pole of the cell (Clark et al., 1997; St Johnston, 2005). This new microtubule network provides the necessary polarity for the subsequent transport of *bicoid* and *oskar* mRNA to opposite poles of the oocyte. These RNAs encode morphogens that specify head and abdominal segments in the future embryo.

The polarization of the microtubule cytoskeleton, triggered by Gurken signaling, also plays an essential role in the specification of the dorsoventral axis (Roth, 2003). Shortly after MT reorganization, the oocyte nucleus is transported to a point along the anterior cortex, orthogonal to the anteroposterior axis of the cell (Roth et al., 1995). Such transport is MT- and cytoplasmic dynein dependent, and random in nature in as much as the oocyte can be transported to any of the many MTOCs that encircle the oocyte's anterior (Fig. 1.2B). *gurken* mRNA is subsequently localized above the nucleus in the anterodorsal (AD) corner of the oocyte (Neuman-Silberberg and Schupbach, 1993), where it is translated and secreted (Serano et al., 1995), inducing neighboring follicle

cells to adopt the dorsal cell fate, again through activation of Torpedo (Roth, 2003). Follicle cells that do not receive the Gurken signal adopt the default, ventral cell fate (Fig. 1.2B). Dorsal and ventral follicle cells differentially signal the oocyte, elaborating dorsoventral polarity within the oocyte that is essential for specification of the dorsoventral axis of the future embryo (Gonzalez-Reyes et al., 1995).

3. RNA LOCALIZATION

The subcellular localization of RNA figures prominently in the polarization of the oocyte and specification of the future embryo's body plan. Approximately 10% of the RNAs found in the oocyte are localized to specific subcellular sites. The vast majority of these "localized" RNAs are transcribed in nurse cells and transported in a dynein- and MT-dependant manner into the oocyte during stages 1-7 (Becalska and Gavis, 2009; Duncan and Warrior, 2002; Januschke et al., 2002). The transported RNAs initially accumulate at the oocyte's prominent MTOC at the cell's posterior pole (see above). Coincident with MT reorganization at stage 7, the transported RNAs are relocated to the oocyte's anterior cortex, where they adopt a characteristic ring-shape distribution pattern (Fig. 1.2C). Such relocalization is also MT- and cytoplasmic dynein-dependant (Duncan and Warrior, 2002; Januschke et al., 2002). While most RNAs remain at the oocyte's anterior cortex until stage 10B, when MTs are again reorganized and cytoplasmic streaming is induced, some RNAs remain at the anterior cortex only transiently and are instead relocalized to the oocyte's posterior pole (e.g., *oskar* and *nanos*) or AD corner (e.g., *gurken*). While transport into the oocyte and localization to the oocyte's anterior cortex appears to be accounted for by a single motor complex, multiple different

localization machineries appear to account for RNA localization to the oocyte's posterior pole and AD corner. For example, *oskar*'s localization to the posterior pole is powered by Kinesin I (Zimyanin et al., 2008), a plus end-directed motor protein, and is dependant on a poorly understood anchoring complex that includes Oskar protein and Rab11 activities (see below) (Dollar et al., 2002). In contrast, *nanos* RNA is localized to the posterior pole via a diffusion-trap mechanism that is dependant on Oskar protein (Forrest and Gavis, 2003). The localization of *gurken* RNA to the oocyte's AD corner appears to involve both MT-dependant transport (Delanoue et al., 2007) and a trapping mechanism (see below).

4. RNA LOCALIZATION ELEMENTS

All RNA localization events are governed by specific RNA-protein interactions. The RNA target sites of these regulatory proteins are referred to as RLEs (RNA localization elements). One of the best-characterized RLEs is the 44 nucleotide TLS (Transport/Localization Sequence), located in the 3′ UTR of *K10* mRNA (Serano and Cohen, 1995). The TLS forms a stem-loop secondary structure and is required and sufficient for the transport of *K10* mRNA into the oocyte as well as its subsequent localization to the oocyte's anterior cortex. The stem-loop secondary structure is critical for localization activity. Mutations that alter the predicted base-pairing pattern disrupt localization activity, however, second-site mutations that restore the predicted base-pairing pattern also restore localization activity (Serano and Cohen, 1995). The TLS mediates *K10* RNA localization by binding to Egalitarian (Egl), a component of the cytoplasmic dynein motor complex (Dienstbier et al., 2009). Curiously, the TLS is found

in only one other localized ovarian RNA (*orb*), even though all localized ovarian RNAs exhibit *K10*/*orb*-like localization patterns through stage 7/8, i.e., through formation of the anterior ring (Cohen et al., 2005). Whether these other RNAs contain cryptic TLS-like RLEs or associate with the cytoplasmic dynein motor complex in novel ways is not clear. It is however, noteworthy that neither the BLE1 (*bicoid* localization element 1) (Macdonald et al., 1993) nor WLE3 (*wingless* localization element) (dos Santos et al., 2008) RLEs, both of which mediate *K10*/*orb*-like localization, share recognizable similarities to each other and/or to the TLS.

The RLEs and localization machineries that are responsible for the movement of *gurken* RNA from the anterior cortex to oocyte's AD corner have been the subject of intense study, but are still only poorly understood. *gurken* mRNA contains at least two RLEs that mediate its transport from nurse cells to the oocyte and subsequent relocalization to the oocyte's anterior cortex (Saunders and Cohen, 1999; Thio et al., 2000). These elements presumably facilitate direct or indirect association of *gurken* RNA with cytoplasmic dynein, as cytoplasmic dynein mutants are defective in *gurken* RNA localization (Delanoue et al., 2007; Rom et al., 2007). One of these RLEs is the GLS (*gurken* localization sequence), which is located within the protein coding region of *gurken* transcript and forms a stem-loop 2º structure (Van De Bor et al., 2005). The GLS is required for efficient transport of *gurken* transcripts into the oocyte and, concomitant with MT re-organization at stage 7, the localization of the RNA to the oocyte's anterior cortex. The GLS is also required for AD localization, but it is not sufficient for such localization. At least two other RLEs are required for *gurken* RNA localization, one or more situated in the 5´UTR and one or more others in the 3´UTR of the *gurken* transcript

(Saunders and Cohen, 1999; Thio et al., 2000). The exact roles of these other elements are not clear, but at least one appears to be required for RNA transport into the oocyte. Giving that *gurken* RNA ultimately becomes tightly associated with the oocyte nucleus, it is generally thought that one or more *gurken* RLEs are involved in the anchoring of *gurken* transcripts to the nucleus and/or a neighboring structure. Previous studies have suggested that the nucleus nucleates a subset of microtubules and that the GLS somehow direct cytoplasmic dynein to this subset resulting in directed transport to the oocyte's AD corner (Van De Bor et al, 2005). My data presented in Chapter 2 do not support this idea and are more in line with a model in which *gurken* AD localization is brought about by repeated rounds of anterior transport coupled with specific (GLS-mediated) trapping at or near the oocyte nucleus.

5. PROTEIN LOCALIZATION AND MEMBRANE TRAFFICKING

Eukaryotic cells define a wide variety of different membrane compartments and have evolved the ability to move proteins and other molecules from one compartment to another, through a process known as membrane trafficking. There are four steps in membrane trafficking: 1) the budding of the vesicle from the donor membrane, 2) transport of the vesicle to a target membrane, 3) the docking of the vesicle to the target membrane and, 4) the fusion of the vesicle with the target membrane (Fig. 1.3). The small Rab GTPases play critical roles in each of these steps (Stenmark, 2009; Zerial and McBride, 2001).

The Rab (Ras-related protein in brain) (Touchot et al., 1987) GTPases constitute the largest branch of the Ras GTPase superfamily. There are over 70 Rabs in mammals

(Colicelli, 2004), 31 in *Drosophila* (Zhang et al., 2007), and 11 in yeast where they are known as Sec/Ypt proteins (Zerial and McBride, 2001). Each Rab localizes to a different set of membrane domains and mediates a distinct trafficking event (Stenmark, 2009). For example, Rab 5 localizes to the plasma membrane and early endosome and mediates the first step of endocytosis. Similarly, Rab 2 localizes to pre-Golgi compartments and is responsible for Golgi to ER (endoplasmic reticulum) trafficking, while Rab11 localizes to recycling endosomes and the plasma membrane and controls trafficking of vesicles from recycling endosomes to the plasma membrane, the final leg of endocytic recycling (Stenmark, 2009).

Like other Ras superfamily members, Rab proteins function as molecular switches by cycling between active GTP-bound and inactive GDP-bound states. This switch is controlled by guanosine nucleotide exchange factors (GEFs), which activate Rabs by replacing GDP with GTP, and by GTPase-activating protein (GAPs), which inactivate Rabs by stimulating their intrinsic GTP hydrolysis activity (Fig. 1.3) (Schwartz et al., 2007; Stenmark, 2009; Zerial and McBride, 2001). Other proteins called Rab effectors bind to active GTP-bound Rabs in almost all the cases and assist them in their trafficking activities (Shirane and Nakayama, 2006; Stenmark, 2009). The emerging view is that each Rab interacts with 4 different effector proteins (EI-EIV), with each effector mediating a distinct trafficking step (Fig. 1.3, with Rab11 effectors shown in the red). Upon activation by its corresponding GEF, the Rab protein binds its cognate EI effector or effector complex, which facilitates cargo selection and budding. One well-characterized EI effector is Tip47 (Carroll et al., 2001). The likely EI effector of Rab11 is nuclear fallout (Nuf) (Riggs et al., 2003). The activated Rab protein next binds its

cognate EII effector, which in all examined cases are motor proteins or a member of a motor protein complex. Rab11 has two EII effector proteins, myosin motor MyoV and dRip11 (Li et al., 2007), which form a complex. The EIII (docking) effector for Rab11 is Sec15 (Zhang et al., 2004), which is a component of exocyst (TerBush et al., 1996), which also serves as a docking complex for Rab8 vesicles in the secretory pathway (Mazelova et al., 2009). EIV effectors appear to work by mediating interactions between SNARE protein family membranes located on the vesicle (v-SNARE) and target (t-SNARE) membranes. A candidate EIV effector for Rab11 is lethal giant larvae (lgl), which is the homolog of yeast Sro7p, which mediates interactions between v-SNARE/t-SNARE complex formation (Lehman et al., 1999).

GAP proteins are presumably localized to target membranes and return the Rab proteins to their inactive states and prepare them for extraction by GDI (GDP dissociation inhibitor). Reinsertion of the GDP-Rab into the membrane requires displacement of GDI by GDF (GDI displacement factor) (Fig. 1.3) (Schwartz et al., 2007; Stenmark, 2009).

Rab11, as mentioned earlier, localizes to the recycling endosome and controls trafficking of vesicles from recycling endosomes to the plasma membrane. However, Rab11 traffics different cargoes in different cell types, and thus regulates a wide variety of cellular processes. Examples of Rab11 tissue-specific functions are listed in Fig. 1.4. In the germarium, Rab11 functions in GSC maintenance by recycling DE-Cadherin to the anterior side of the GSC, thus maintaining GSC's connection with niche cap cells (Fig. 1.4A). In a Rab11 null mutant, GSCs lose their connection to cap cells, promoting their differentiation, and thus, GSC loss and female infertility (Bogard et al., 2007). A second example of Rab11 function is organelle biogenesis. In the sensory neuron cell lineage, the

amount of the Rab11 effector, Nuf, that segregates to pIIa and pIIb sister cells determines the size of the recycling endosome that such cells elaborate and, ultimately, their developmental fate; the pIIb cell becomes a Notch signaling cell and the pIIa cell a Notch receiving cell as only the pIIb cell can recycle Delta, which is necessary for its ability to activate Notch (Emery et al., 2005; Jafar-Nejad et al., 2005) (Fig. 1.4B). A third example of Rab11 function is in cell division or cellularization. Rab11 is required along with Nuf to coordinate remodeling of actin filaments and addition of new membrane to form the cleavage furrow (Fig. 1.4C) (Pelissier et al., 2003). Rab11 also function in cell migration. For example, in border cell migration in *Drosophila* egg chambers, Rab11 recycles adhesion molecules such as DE-Cadherin to the leading edge of a migrating cell, as it builds and maintains its connections with surrounding cells along the way (Fig. 1.4D).

This dissertation focuses on several polarity events during *Drosophila* oogenesis. Chapter II is focused on *gurken* mRNA localization and explores the function of the *gurken* localization sequence (GLS). Chapter III described the cloning and characterization of a putative Rab11 effector, dRip11. In Appendix, Chapter V and VI are focused on Rab11 and its role in maintaining polarity in specific cells: Chapter V describes the role of Rab11 in maintaining GSC identity; Chapter VI discusses Rab11's function in follicle cell fate specification.

Figure 1.1 *Drosophila* oogenesis. (**A**) Schematic diagram of *Drosophila* ovaries. Each ovary consists of 16-20 tube-like compartments, called ovarioles. A single ovariole is boxed and shown in detail in **C**. (**B**) Germarium (Bogard et al., 2007). Different regions of germarium are highlighted underneath. TF: terminal filament, CC: cap cell, ESC: escort cell, FC: follicle cell. Black: germline stem cell (GSC), red: spectrosome (in GSC)/ fusome (in cystoblast or cyst), green: oocyte, blue: ring canal. (**C**) A single ovariole. The anterior compartment of the ovariole is known as the germarium. The germarium contains germline and somatic stem cells, which divide and differentiate to give rise to egg chambers, which then bud from the germarium to enter the posterior compartment of the ovariole, where they proceed to mature. Egg chamber maturation is a continuous process, but is divided into 14 morphologically distinct steps for convenience. Most ovarioles contain 6 or 7 egg chambers, arranged single file with the oldest the farthest (most posterior) from the germarium. As highlighted in the diagram, each egg chamber consists of an inner germline cyst, which includes a posterior oocyte and 15 sister nurse cells, and an outer layer of somatically-derived follicle cells that include main-body epithelial cells, and two polar cells at each end of the egg chamber. Each egg chamber is separated from the next by 6-8 stalk cells, which, like polar and main-body epithelial cells, are derived from somatic stem cells. (**D**) During stage 8/9 of oogenesis the anterior polar cells plus 6-8 neighboring main-body epithelial cells delaminated from the epithelium to become border cells, which migrate posteriorly over the next 2-3 stages and ultimately come to rest at the anterior end of the oocyte.

A is adapted from http://flybase.bio.indiana.edu/reports/FBim0000078.html

Figure 1.1

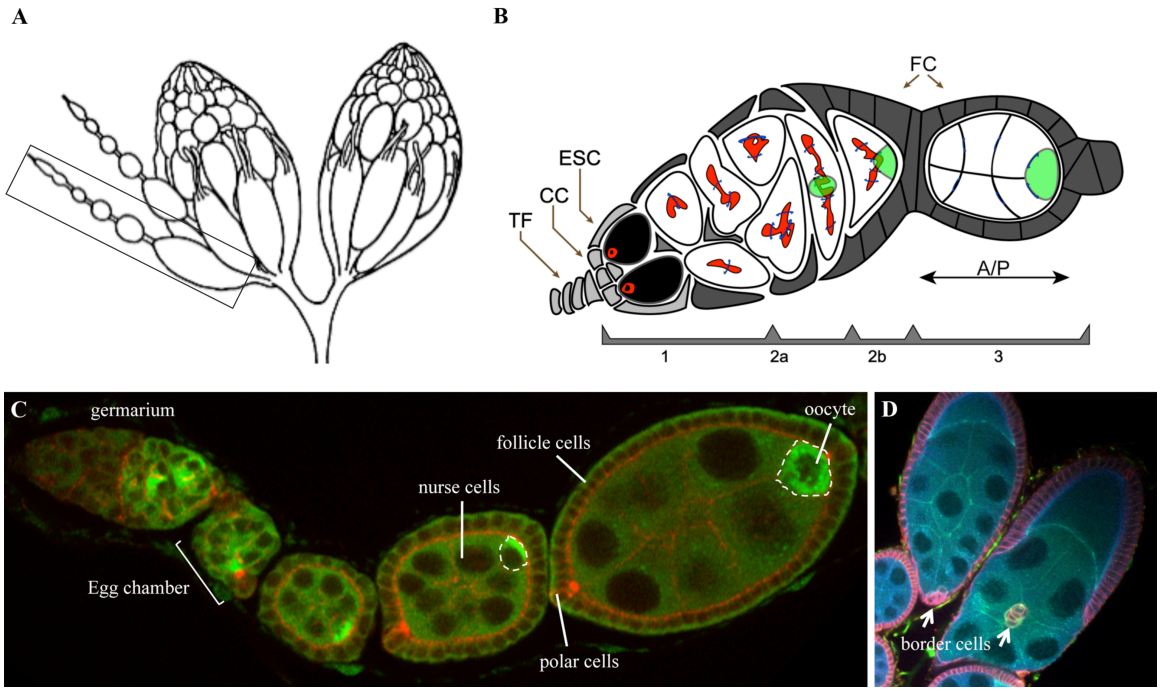
A
B
FC
ESC
CC
TF
A/P
1
2a
2b
3
C
germarium
oocyte
follicle cells
nurse cells
Egg chamber
polar cells
D
border cells

Figure 1.2 *Drosophila* egg chamber is polarized. (**A**) Wild-type expression patterns of endogenous E-Cadherin (E-Cad) in red and Orb protein, which is expressed only in the oocyte, in green, are revealed by immunofluorescence. E-Cad is enriched in the surface of the oocyte and the posterior follicle cells, thus maintains the connection between them, and ensures the posterior position of the oocyte. (**B**) After microtubule (MT) (red) reorganization, MT plus ends (+) pointed towards the posterior pole of the oocyte and the minus ends (-) to the anterior. The oocyte nucleus (N) is transported from the posterior pole along the MT to one random corner of the anterior cortex. (**C**) mRNAs that are transported from the nurse cells into the oocyte in an earlier step relocalize to the anterior cortex of the oocyte due to MT reorganization and form a ring-shape distribution pattern. One of the mRNAs (K10 mRNA) is shown here by whole mount *in situ* hybridization.

Figure 1.2

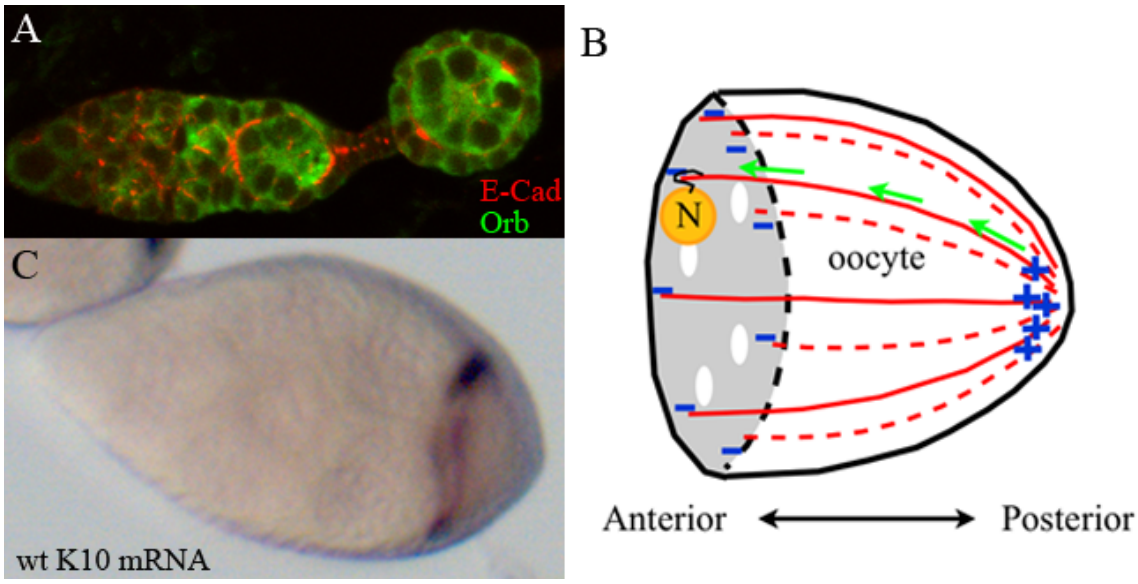

Figure 1.3 Rab effectors assist Rab proteins in every step of Membrane trafficking. The four putative effector classes are abbreviated as EI-EIV, with Rab11 representatives shown in the red text. Upon activation by its corresponding GEF, the Rab protein binds its cognate EI effector or effector complex, which facilitates cargo selection and budding. One well-characterized EI effector is Tip47. The likely EI effector of Rab11 is nuclear fallout (Nuf). The activated Rab protein next binds its cognate EII effector, which in all examined cases are motor proteins or a member of a motor protein complex. Rab11 has two EII effector proteins, myosin motor MyoV and dRip11, which form a complex. The EIII (docking) effector for Rab11 is Sec15, which is a component of exocyst, which also serves as a docking complex for Rab8 vesicles in the secretory pathway. EIV effectors appear to work by mediating interactions between SNARE protein family membranes located on the vesicle (v-SNARE) and target (t-SNARE) membranes. A candidate EIV effector for Rab11 is lethal giant larvae (lgl), which is the homolog of yeast Sro7p, which mediates interactions between v-SNARE/t-SNARE complex formation.

GDI: GDP dissociation inhibitor; GDF: GDI displacement factor; GEF: guanosinee nucleotide exchange factor; GAP: GTPase-activating protein.

Figure 1.3

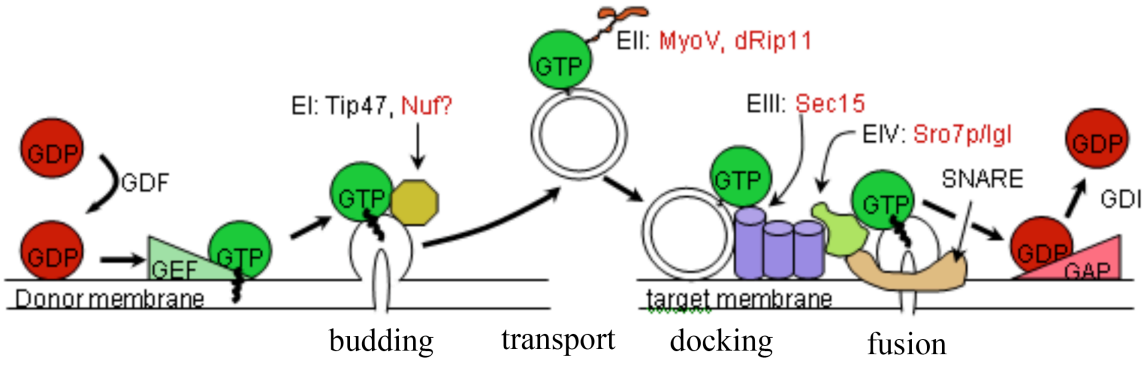
GTP
EII: MyoV, dRip11
EI: Tip47, Nuf?
EIII: Sec15
EIV: Sro7p/Igl
GDP
GDF
GDP
GTP
GTP
GTP
SNARE
GDI
GDP
GEF
GTP
GAP
Donor membrane
target membrane
budding
transport
docking
fusion

Figure 1.4 Rab11 traffics different cargoes in different cell types, thus regulates a wide variety of cellular processes. (**A**) In the germarium, Rab11 functions in GSC maintenance by recycling DE-Cadherin to the anterior side of the GSC, thus maintaining GSC's connection with niche cap cells. In a Rab11 null mutant, GSCs lose their connection to cap cells, promoting their differentiation, and thus, GSC loss and female infertility. (**B**) Rab11 functions in organelle biogenesis. In the sensory neuron cell lineage, the amount of the Rab11 effector, Nuf, that segregates to pIIa and pIIb sister cells determines the size of the recycling endosome that such cells elaborate and, ultimately, their developmental fate; the pIIb cell becomes a Notch signaling cell and the pIIa cell a Notch receiving cell as only the pIIb cell can recycle Delta, which is necessary for its ability to activate Notch. (**C**) In cell division or cellularization, Rab11 is required with the help of Nuf to coordinate remodeling of actin filaments and addition of new membrane to form the cleavage furrow. (**D**) Rab11 function in cell migration. In border cell migration in *Drosophila* egg chambers, Rab11 recycles adhesion molecules such as DE-Cadherin to the leading edge of a migrating cell, thus building and maintaining its connections with surrounding cells along the way.

N: nucleus; RE: recycling endosome; GSC: germline stem cell; EE: early endosome.

Modified from van Ijzendoorn, S.C., J Cell Sci 119, 1679-1681 (2006)

Figure 1.4

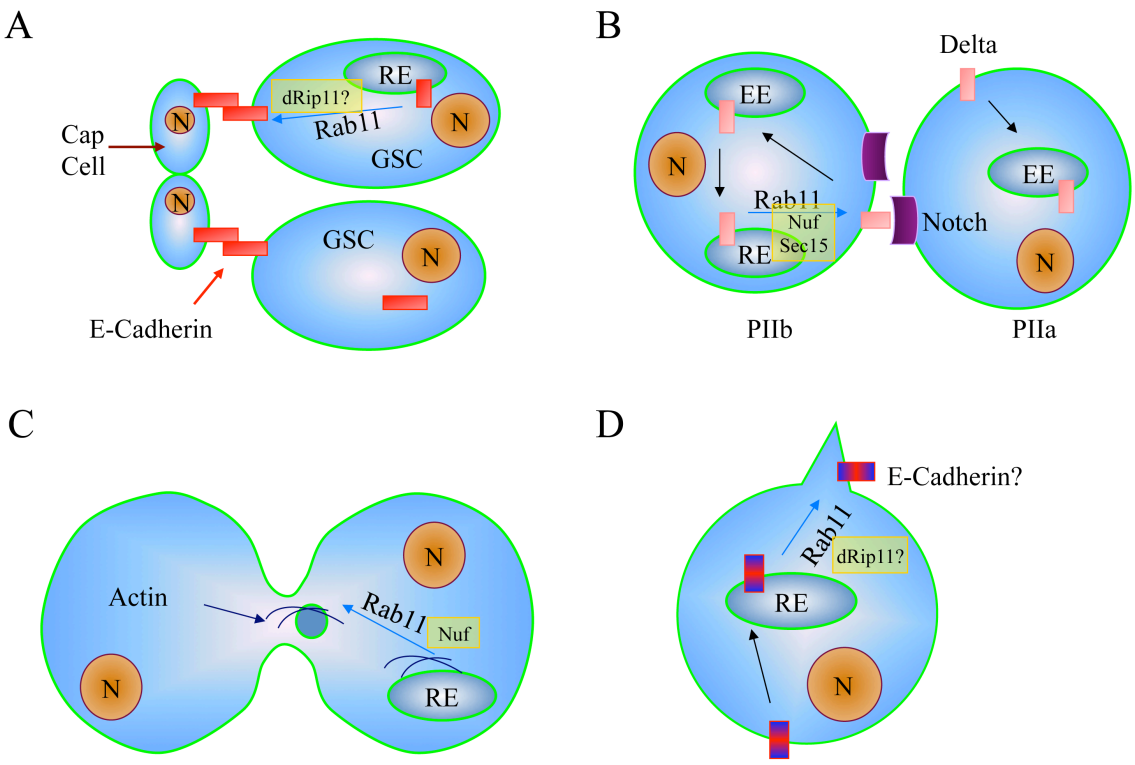
A
RE
dRip11?
Rab11
N
N
Cap
Cell
GSC
N
GSC
N
E-Cadherin
B
Delta
EE
N
Rab11
Nuf
Sec15
RE
Notch
EE
N
PIIb
PIIa
C
Actin
N
Rab11
Nuf
N
RE
D
E-Cadherin?
Rab11
dRip11?
RE
N

REFERENCES

1. Bastock, R., and St Johnston, D. (2008). *Drosophila* oogenesis. Curr Biol *18*, R1082-1087.
2. Becalska, A.N., and Gavis, E.R. (2009). Lighting up mRNA localization in *Drosophila* oogenesis. Development *136*, 2493-2503.
3. Bogard, N., Lan, L., Xu, J., and Cohen, R.S. (2007). Rab11 maintains connections between germline stem cells and niche cells in the *Drosophila* ovary. Development *134*, 3413-3418.
4. Carroll, K.S., Hanna, J., Simon, I., Krise, J., Barbero, P., and Pfeffer, S.R. (2001). Role of Rab9 GTPase in facilitating receptor recruitment by TIP47. Science *292*, 1373-1376.
5. Clark, I.E., Jan, L.Y., and Jan, Y.N. (1997). Reciprocal localization of Nod and kinesin fusion proteins indicates microtubule polarity in the *Drosophila* oocyte, epithelium, neuron and muscle. Development *124*, 461-470.
6. Cohen, R.S., Zhang, S., and Dollar, G.L. (2005). The positional, structural, and sequence requirements of the *Drosophila* TLS RNA localization element. RNA *11*, 1017-1029.
7. Colicelli, J. (2004). Human RAS superfamily proteins and related GTPases. Sci STKE *2004*, RE13.
8. Cooley, L., and Theurkauf, W.E. (1994). Cytoskeletal functions during *Drosophila* oogenesis. Science *266*, 590-596.

9. Delanoue, R., Herpers, B., Soetaert, J., Davis, I., and Rabouille, C. (2007). *Drosophila* Squid/hnRNP helps Dynein switch from a gurken mRNA transport motor to an ultrastructural static anchor in sponge bodies. Dev Cell *13*, 523-538.
10. Deng, W., and Lin, H. (1997). Spectrosomes and fusomes anchor mitotic spindles during asymmetric germ cell divisions and facilitate the formation of a polarized microtubule array for oocyte specification in *Drosophila*. Dev Biol *189*, 79-94.
11. Dienstbier, M., Boehl, F., Li, X., and Bullock, S.L. (2009). Egalitarian is a selective RNA-binding protein linking mRNA localization signals to the dynein motor. Genes Dev *23*, 1546-1558.
12. Dobens, L.L., and Raftery, L.A. (2000). Integration of epithelial patterning and morphogenesis in *Drosophila* ovarian follicle cells. Dev Dyn *218*, 80-93.
13. Dollar, G., Struckhoff, E., Michaud, J., and Cohen, R.S. (2002). Rab11 polarization of the *Drosophila* oocyte: a novel link between membrane trafficking, microtubule organization, and oskar mRNA localization and translation. Development *129*, 517-526.
14. dos Santos, G., Simmonds, A.J., and Krause, H.M. (2008). A stem-loop structure in the wingless transcript defines a consensus motif for apical RNA transport. Development *135*, 133-143.
15. Duncan, J.E., and Warrior, R. (2002). The cytoplasmic dynein and kinesin motors have interdependent roles in patterning the *Drosophila* oocyte. Curr Biol *12*, 1982-1991.
16. Emery, G., Hutterer, A., Berdnik, D., Mayer, B., Wirtz-Peitz, F., Gaitan, M.G., and Knoblich, J.A. (2005). Asymmetric Rab 11 endosomes regulate delta

recycling and specify cell fate in the *Drosophila* nervous system. Cell *122*, 763-773.

17. Forrest, K.M., and Gavis, E.R. (2003). Live imaging of endogenous RNA reveals a diffusion and entrapment mechanism for nanos mRNA localization in *Drosophila*. Curr Biol *13*, 1159-1168.
18. Gonzalez-Reyes, A., Elliott, H., and St Johnston, D. (1995). Polarization of both major body axes in *Drosophila* by gurken-torpedo signalling. Nature *375*, 654-658.
19. Gonzalez-Reyes, A., and St Johnston, D. (1998). The *Drosophila* AP axis is polarised by the cadherin-mediated positioning of the oocyte. Development *125*, 3635-3644.
20. Horne-Badovinac, S., and Bilder, D. (2005). Mass transit: epithelial morphogenesis in the *Drosophila* egg chamber. Dev Dyn *232*, 559-574.
21. Huynh, J.R., and St Johnston, D. (2004). The origin of asymmetry: early polarisation of the *Drosophila* germline cyst and oocyte. Curr Biol *14*, R438-449.
22. Jafar-Nejad, H., Andrews, H.K., Acar, M., Bayat, V., Wirtz-Peitz, F., Mehta, S.Q., Knoblich, J.A., and Bellen, H.J. (2005). Sec15, a component of the exocyst, promotes notch signaling during the asymmetric division of *Drosophila* sensory organ precursors. Dev Cell *9*, 351-363.
23. Januschke, J., Gervais, L., Dass, S., Kaltschmidt, J.A., Lopez-Schier, H., St Johnston, D., Brand, A.H., Roth, S., and Guichet, A. (2002). Polar transport in the *Drosophila* oocyte requires Dynein and Kinesin I cooperation. Curr Biol *12*, 1971-1981.

24. Kirilly, D., and Xie, T. (2007). The *Drosophila* ovary: an active stem cell community. Cell Res *17*, 15-25.

25. Lehman, K., Rossi, G., Adamo, J.E., and Brennwald, P. (1999). Yeast homologues of tomosyn and lethal giant larvae function in exocytosis and are associated with the plasma membrane SNARE, Sec9. J Cell Biol *146*, 125-140.

26. Li, B.X., Satoh, A.K., and Ready, D.F. (2007). Myosin V, Rab11, and dRip11 direct apical secretion and cellular morphogenesis in developing *Drosophila* photoreceptors. J Cell Biol *177*, 659-669.

27. Macdonald, P.M., Kerr, K., Smith, J.L., and Leask, A. (1993). RNA regulatory element BLE1 directs the early steps of bicoid mRNA localization. Development *118*, 1233-1243.

28. Mazelova, J., Ransom, N., Astuto-Gribble, L., Wilson, M.C., and Deretic, D. (2009). Syntaxin 3 and SNAP-25 pairing, regulated by omega-3 docosahexaenoic acid, controls the delivery of rhodopsin for the biogenesis of cilia-derived sensory organelles, the rod outer segments. J Cell Sci *122*, 2003-2013.

29. Montell, D.J. (2003). Border-cell migration: the race is on. Nat Rev Mol Cell Biol *4*, 13-24.

30. Neuman-Silberberg, F.S., and Schupbach, T. (1993). The *Drosophila* dorsoventral patterning gene gurken produces a dorsally localized RNA and encodes a TGF alpha-like protein. Cell *75*, 165-174.

31. Neuman-Silberberg, F.S., and Schupbach, T. (1996). The *Drosophila* TGF-alpha-like protein Gurken: expression and cellular localization during *Drosophila* oogenesis. Mech Dev *59*, 105-113.

32. Nilson, L.A., and Schupbach, T. (1999). EGF receptor signaling in *Drosophila* oogenesis. Curr Top Dev Biol *44*, 203-243.

33. Ohlstein, B., Kai, T., Decotto, E., and Spradling, A. (2004). The stem cell niche: theme and variations. Curr Opin Cell Biol *16*, 693-699.

34. Pelissier, A., Chauvin, J.P., and Lecuit, T. (2003). Trafficking through Rab11 endosomes is required for cellularization during *Drosophila* embryogenesis. Curr Biol *13*, 1848-1857.

35. Riggs, B., Rothwell, W., Mische, S., Hickson, G.R., Matheson, J., Hays, T.S., Gould, G.W., and Sullivan, W. (2003). Actin cytoskeleton remodeling during early *Drosophila* furrow formation requires recycling endosomal components Nuclear-fallout and Rab11. J Cell Biol *163*, 143-154.

36. Rom, I., Faicevici, A., Almog, O., and Neuman-Silberberg, F.S. (2007). *Drosophila* Dynein light chain (DDLC1) binds to gurken mRNA and is required for its localization. Biochim Biophys Acta *1773*, 1526-1533.

37. Roth, S. (2003). The origin of dorsoventral polarity in *Drosophila*. Philos Trans R Soc Lond B Biol Sci *358*, 1317-1329; discussion 1329.

38. Roth, S., and Lynch, J.A. (2009). Symmetry breaking during *Drosophila* oogenesis. Cold Spring Harbor Perspect Biol *1*, a001891.

39. Roth, S., Neuman-Silberberg, F.S., Barcelo, G., and Schupbach, T. (1995). cornichon and the EGF receptor signaling process are necessary for both anterior-posterior and dorsal-ventral pattern formation in *Drosophila*. Cell *81*, 967-978.

40. Saunders, C., and Cohen, R.S. (1999). The role of oocyte transcription, the 5'UTR, and translation repression and derepression in *Drosophila* gurken mRNA and protein localization. Mol Cell *3*, 43-54.

41. Schwartz, S.L., Cao, C., Pylypenko, O., Rak, A., and Wandinger-Ness, A. (2007). Rab GTPases at a glance. J Cell Sci *120*, 3905-3910.

42. Serano, T.L., and Cohen, R.S. (1995). A small predicted stem-loop structure mediates oocyte localization of *Drosophila* K10 mRNA. Development *121*, 3809-3818.

43. Serano, T.L., Karlin-McGinness, M., and Cohen, R.S. (1995). The role of fs(1)K10 in the localization of the mRNA of the TGF alpha homolog gurken within the *Drosophila* oocyte. Mech Dev *51*, 183-192.

44. Shirane, M., and Nakayama, K.I. (2006). Protrudin induces neurite formation by directional membrane trafficking. Science *314*, 818-821.

45. Song, X., Zhu, C.H., Doan, C., and Xie, T. (2002). Germline stem cells anchored by adherens junctions in the *Drosophila* ovary niches. Science *296*, 1855-1857.

46. St Johnston, D. (2005). Moving messages: the intracellular localization of mRNAs. Nat Rev Mol Cell Biol *6*, 363-375.

47. Stenmark, H. (2009). Rab GTPases as coordinators of vesicle traffic. Nat Rev Mol Cell Biol *10*, 513-525.

48. TerBush, D.R., Maurice, T., Roth, D., and Novick, P. (1996). The Exocyst is a multiprotein complex required for exocytosis in Saccharomyces cerevisiae. EMBO J *15*, 6483-6494.

49. Theurkauf, W.E., Smiley, S., Wong, M.L., and Alberts, B.M. (1992). Reorganization of the cytoskeleton during *Drosophila* oogenesis: implications for axis specification and intercellular transport. Development *115*, 923-936.

50. Thio, G.L., Ray, R.P., Barcelo, G., and Schupbach, T. (2000). Localization of gurken RNA in *Drosophila* oogenesis requires elements in the 5' and 3' regions of the transcript. Dev Biol *221*, 435-446.

51. Touchot, N., Chardin, P., and Tavitian, A. (1987). Four additional members of the ras gene superfamily isolated by an oligonucleotide strategy: molecular cloning of YPT-related cDNAs from a rat brain library. Proc Natl Acad Sci U S A *84*, 8210-8214.

52. Van De Bor, V., Hartswood, E., Jones, C., Finnegan, D., and Davis, I. (2005). gurken and the I factor retrotransposon RNAs share common localization signals and machinery. Dev Cell *9*, 51-62.

53. Xie, T., and Spradling, A.C. (2000). A niche maintaining germ line stem cells in the *Drosophila* ovary. Science *290*, 328-330.

54. Zerial, M., and McBride, H. (2001). Rab proteins as membrane organizers. Nat Rev Mol Cell Biol *2*, 107-117.

55. Zhang, J., Schulze, K.L., Hiesinger, P.R., Suyama, K., Wang, S., Fish, M., Acar, M., Hoskins, R.A., Bellen, H.J., and Scott, M.P. (2007). Thirty-one flavors of *Drosophila* rab proteins. Genetics *176*, 1307-1322.

56. Zhang, X.M., Ellis, S., Sriratana, A., Mitchell, C.A., and Rowe, T. (2004). Sec15 is an effector for the Rab11 GTPase in mammalian cells. J Biol Chem *279*, 43027-43034.

57. Zimyanin, V.L., Belaya, K., Pecreaux, J., Gilchrist, M.J., Clark, A., Davis, I., and St Johnston, D. (2008). In vivo imaging of oskar mRNA transport reveals the mechanism of posterior localization. Cell *134*, 843-853.

Chapter II

Evidence for a Transport-Trap Mode of *Drosophila melanogaster* *gurken* mRNA Localization

ABSTRACT

The *Drosophila melanogaster gurken* gene encodes a TGF-α-like signaling molecule that is secreted from the oocyte during two distinct stages of oogenesis to define the anteroposterior and dorsoventral axes, respectively, of the follicle cell epithelium that surrounds the oocyte and its 15 anterior nurse cells. Because the *gurken* receptor is expressed throughout the epithelium, axial patterning requires region-specific secretion of Gurken protein, which in turn requires precise subcellular localization of *gurken* transcripts. The first stage of Gurken signaling induces anteroposterior pattern in the follicle epithelium and correlates with the transport of *gurken* transcripts from nurse cells into the oocyte. The second stage of Gurken signaling induces dorsoventral polarity in the follicle epithelium and is dependent on the concentration of *gurken* transcripts at the oocyte's anterodorsal corner. Previous studies, relying predominantly on real-time imaging of injected transcripts, indicated that such concentration requires transport of *gurken* transcripts first to the anterior cortex and then to the anterodorsal corner, followed by anchoring. Such studies further indicated that a single RNA sequence element, called the GLS, mediates both transport steps by facilitating association of *gurken* transcripts with a cytoplasmic dynein motor complex. It was proposed from these findings that the GLS somehow steers the motor complex toward that subset of microtubules that are nucleated around the oocyte nucleus, thus permitting directed transport to the anterodorsal corner.

Here, we re-investigate the role of the GLS using a transgenic fly assay system that includes use of the endogenous *gurken* promoter and biological rescue as well as RNA localization assays. In contrast to previous reports, our studies indicate that the GLS

is required and sufficient for anterior transport only. Our data are consistent with a model in which anterodorsal localization is brought about by repeated rounds of anterior transport, accompanied by specific trapping at the anterodorsal cortex.

INTRODUCTION

The localization of mRNAs to specific subcellular sites is a common mechanism by which cells target proteins to regions where they are needed and/or prevent them from accumulating in places where they may do harm. While localized mRNAs have been described in all examined organisms, genome-wide analyses have been limited to *Drosophila* (Lecuyer et al., 2007), where it has been estimated that 71% of all transcripts are localized. Localized mRNAs encode a variety of proteins types including components of the cytoskeleton, transcription factors, regulators of translation, and even secreted signaling molecules (Lecuyer et al., 2007).

Three distinct, non-mutually exclusive, mechanisms have been described for mRNA localization. These include directed transport on microtubule (MT) or, more rarely, actin tracks, diffusion to a localized anchor, and region-specific mRNA degradation (Becalska and Gavis, 2009; Kugler and Lasko, 2009; Martin and Ephrussi, 2009; Meignin and Davis, 2010; St Johnston, 2005). All three mechanisms are mediated by discrete RNA localization elements (RLEs) that recruit localization machineries to their respective transcripts through specific RNA-protein interactions. The vast majority of characterized RLEs reside in the 5' or 3' untranslated regions (UTRs) of their transcripts, although a few have been mapped to protein coding regions (Martin and Ephrussi, 2009). A fourth mechanism of mRNA localization, transcription from a subset of syncytial nuclei, is transcription-based and does not require RLEs *per se* (Brenner et al., 1990; Meignin and Davis, 2010; Simon et al., 1992).

One of the best systems for studying mechanisms of mRNA localization is the *Drosophila* oocyte whose maturation and patterning is dependent on a cascade of mRNA

localization events (Bastock and St Johnston, 2008). The oocyte develops within an egg chamber composed of an outer, somatically-derived follicle cell epithelium and an inner germline cyst that includes a single posterior oocyte and 15 sister nurse cells (Bastock and St Johnston, 2008). The majority of the mRNAs found in the developing oocyte, mature egg, and early embryo are synthesized in nurse cells during early stages of oogenesis (i.e., stages 1-6) and transported into the oocyte through cytoplasmic bridges, remnants of incomplete cytokinesis during germline cyst formation (Becalska and Gavis, 2009). Such transport is powered by cytoplasmic dynein (Duncan and Warrior, 2002; Januschke et al., 2002), a minus end-directed MT motor protein, and initially results in the accumulation of the transported transcripts at the oocyte's posterior pole, which contains a prominent MT organizing center (MTOC) (Bashirullah et al., 1998; St Johnston, 2005).

Due to their continued association with cytoplasmic dynein and programmed reorganization of the oocyte's MT cytoskeleton, all transported RNAs are relocalized to the oocyte's anterior cortex at stage 7 and form a characteristic ring-like distribution pattern (Cheung et al., 1992; Duncan and Warrior, 2002; Januschke et al., 2002; St Johnston, 2005). The majority of mRNAs persist at the anterior cortex through stage 10, when a final MT reorganization event induces vigorous cytoplasmic streaming (Theurkauf et al., 1992), which causes the RNAs to become dispersed throughout the ooplasm, unless they are anchored to the cell cortex, as is *bicoid* mRNA which encodes a transcription factor morphogen that patterns the anterior end of the future embryo (Bastock and St Johnston, 2008; Berleth et al., 1988; St Johnston, 2005). Several mRNAs, including *nanos* and *oskar*, which encode proteins that pattern the posterior

portion of the future embryo remain at the anterior cortex only transiently, before relocalizing to the oocyte's posterior pole (Ephrussi et al., 1991; Kugler and Lasko, 2009; Lehmann and Nusslein-Volhard, 1986). In the case of *oskar*, relocalization to the posterior pole requires release from, or inactivation of, the dynein motor complex and association with a plus end motor complex that includes Kinesin I (Clark et al., 1997; Januschke et al., 2002; Kugler and Lasko, 2009). The relocalization of *nanos* transcripts is achieved by a diffusion-trap mechanism in which cytoplasmic streaming and Oskar protein serve as a diffusion facilitator and trap, respectively (Forrest and Gavis, 2003).

The *gurken* RNA localization pattern is highly unique, shared only by the transcripts encoded by the *I Factor* retro-transposon (Van De Bor et al., 2005). Following transport into the oocyte and subsequent relocalization to the anterior cortex, *gurken* mRNA is relocalized to the anterodorsal (AD) corner of the cell, forming a characteristic cap above the oocyte nucleus (Neuman-Silberberg and Schupbach, 1993, 1996; Saunders and Cohen, 1999). Previous studies have reported that an RNA element within the *gurken* protein coding region, called the GLS (*gurken* localization sequence), is both required and sufficient for initial, but not persistent, localization of injected *gurken* transcripts to the AD corner of the oocyte (Van De Bor et al., 2005). Such localization was described to be MT- and cytoplasmic dynein-dependent and to occur in a three-step process whereby the RNA is transported first to the anterior cortex and then to the AD corner, followed by anchoring. From these data, it was proposed that MTs nucleated around the oocyte nucleus are somehow different than those nucleated at other regions of the anterior cortex and that the GLS "steers" *gurken* mRNA-cytoplasmic dynein motor complexes toward the former. Here we re-investigate the role of the GLS in *gurken* mRNA localization

using a transgenic fly assay system that includes use of the endogenous *gurken* promoter and both biological rescue and RNA localization assays of GLS activity. In contrast to the previous studies [23], we find that the GLS is required, but not sufficient, for AD localization. Our data are consistent with a model in which the GLS mediates the transport of *gurken* transcripts into the oocyte and, in combination with at least one other RLE, the subsequent localization of the RNA to the oocyte's AD corner. In this model, localization to the AD corner does not involve directed transport to the AD corner, but rather is brought about by repeated rounds of transport to the anterior cortex, coupled with specific anchoring of the transcripts around the oocyte nucleus in the AD corner of the cell.

MATERIALS AND METHODS

Drosophila genetics

Fly culture and crosses were carried out according to standard procedures (Ashburner, 1989). The wild-type stock was w^{1118}. The *gurken* deletion ($grk^{\Delta FRT}$) was made by inducing recombination (Parks et al., 2004) between the FRT insertions (FRT9855 and FRT7069, respectively) of stocks f07069 and d09855 (Harvard Medical School Exelixis collection). The resulting deletion, which extends from 73 nt upstream of the *gurken* transcription start site to ~1100 nt downstream of the *gurken* poly(A) addition site unit was initially identified by non-complementation with grk^{2E} (Schupbach, 1987) and subsequently confirmed by PCR analysis. Homozygous $grk^{\Delta FRT}$ flies are viable, but female sterile (see Text), and maintained over the CyO chromosome balancer. The female sterility is completely rescued by introduction of a genomic copy of the wild-type

gurken gene (see text). Homozygous $grk^{\Delta FRT}$ females were identified by their straight (Cy^{+}) wings. A complete description of all alleles and balancer chromosomes is found at http://flybase.bio.indiana.edu.

P element transformations and transgene constructs

All constructs were cloned into the pCaSpeR4 vector (Pirrotta, 1988) for introduction into the *Drosophila* germline. P-element mediated transformation of w^{1118} flies was carried out as previously described (Saunders and Cohen, 1999; Serano and Cohen, 1995). At least two lines were generated and analyzed for each construct. Most of the transgene lines were maintained as homozygous stocks. Transgene insertions that were homozygous lethal were maintained over the *TM3, Sb* balancer chromosome.

The *K10::GFP* fusion constructs: The starting point for these constructs was a 3.1 kb fully functional *K10* genomic clone that extends from a natural *Asp718 I* restriction site ~850 nt upstream of the transcription start site to a natural *Sal I* site ~400 nt downstream of the poly(A) addition site (Cheung et al., 1992). We then used PCR technology to remove the *K10* translation stop site and insert a 750 nt GFP fragment in-frame with the *K10* protein coding region. Finally, we replaced an ~300 nt *Stu I – Hpa I* restriction fragment in the *K10* 3'UTR that includes the TLS RLE, with a *Bgl II – Xho I* linker. The resulting construct, called *KGFP*, produces readily detectable amounts of RNA and protein that are retained in nurse cells until nurse cell regression at stage 11 (data not shown). All *KGFP* variant constructs (see Fig. 2.2 and Results) were made by inserting appropriate synthetic linker DNAs (sequences available upon request) into the

Bgl II – Xho I sites of *KGFP* and cloned into the *Asp718 I – Xba I* sites of the pCaSpeR4 vector for P element-mediated transformation.

The *grk*^{wt} and *grkGLS*^{mut} rescue constructs: The starting point for these constructs was a 14.1 kb *gurken* genomic fragment that extends from a natural *Asp718 I* site ~7.1 kb upstream of the transcription start site to a synthetic *Spe I* site ~300 nt downstream of the poly(A) addition site. To make *grk*^{wt}, the 14.1 kb genomic fragment was cloned directly into the *Asp718 I – Xba I* sites of the pCaSpeR4 transformation vector. To make *grkGLS*^{mut}, the GLS-containing *Sap I – Hind III* region of *grk*^{wt} was amplified by PCR using "upstream" and "downstream" primer sets. The 3' (bottom strand) primer of the "upstream" primer set and the 5' (top strand) primer of the "downstream" primer set corresponded to the upstream and downstream halves of the GLS, respectively, and overlapped at a synthetic *Sal I* restriction site. The primers were designed to introduce a total of 12 single nucleotide mutations into the GLS (See Fig. 2.3), but targeted wobble positions and thus maintained the wild-type Grk protein sequence (Fig 2.3). Following PCR, the upstream (*Sap I – Sal I*) and downstream (*Sal I – Hind III*) PCR products were substituted for the *Sap I – Hind III* region of *grk*^{wt} in a 3-way ligation reaction. The resulting *grkGLS*^{mut} construct was cloned into the *Asp718 I – Xba I* sites of pCaSpeR4 as above.

Wholemount in situ *hybridization and immunostaining*

Enzyme-linked *in situ* hybridization to wholemount ovaries was carried out according to Tautz and Pfeifle (Tautz and Pfeifle, 1989) with the modifications described in Cheung et al. (Cheung et al., 1992). Digoxigenin-labeled DNA probes were made by

the random priming method (Feinberg and Vogelstein, 1983). The *K10* and *gurken* probes were as previously described (Saunders and Cohen, 1999; Serano and Cohen, 1995). Photographs were taken with a Zeiss Axiophot and digitized by scanning with a Nikon LS-3510 film recorder or captured directly with a Leica DFC300 digital camera. Grk immunostains were carried out as previously described (Cohen et al., 2005; Dollar et al., 2002) with a mouse anti-Grk monoclonal antibody (Queenan et al., 1999) diluted at 1:100 with PBS. Donkey anti-mouse secondary antibodies were purchased from Jackson labs and used at the manufacturer's recommended concentrations. Stained ovaries were mounted in 4% n-propyl gallate (Sigma) in 90% glycerol, 10% phosphate buffered saline. Images were collected on an Olympus 3L Spinning disc or a Zeiss Meta 510 laser scanning confocal microscope.

RESULTS

Identification of a highly conserved sequence element with predicted stem-loop secondary structure in the **gurken** *protein coding region*

It was clear from our previous attempts to map *gurken*'s RLEs that one or more such elements are located in the protein coding portion of the gene (Saunders and Cohen, 1999). While the vast majority of known RLEs do not exhibit strong sequence conservation across species, we reasoned that any RLE in the *gurken* protein coding sequence might since they would be under dual selective pressure, one to maintain a functional protein and another to maintain recognition by the RNA localization machinery. We thus aligned *gurken* gene sequences from six different *Drosophila* species, separated by 10 to 65 million years of evolution, and looked for 40 nucleotides

(nt) or longer sequence elements in the protein coding portion of the gene that were at least 90% identical. As seen in Figs. 2.1A and B, a single such element was identified. Database searches indicated that the identified sequence, which corresponds to amino acid residues 10-31, is the same as the GLS reported by Van de Bor et al. (Van De Bor et al., 2005). As previously recognized by them, the conservation of the GLS among different *Drosophila* species is even more striking at the level of predicted secondary structure. Indeed, all six GLSs are predicted to form the same stem-loop secondary structure (Fig. 2.1C) and to encode the same protein sequence. To address the possibility that the highly conserved nature of the GLS is somehow reflective of codon preference (rather than maintenance of a particular secondary structure), we also examined the GLS of *D. willistoni*, which has a different codon preference than the six species used in our initial alignment (Heger and Ponting, 2007). We found that the *D. willistoni* GLS only differs from the *D. melanogaster* GLS at four nucleotide residues and encodes the exact same predicted secondary structure (Fig. 2.1C). It is also noteworthy, that the codons outside of the GLS vary from species to species, which would not be expected if codon choice was under high selective pressure, e.g., as a means to tightly control Grk protein levels.

The GLS possesses anterior, but not AD, localization activity

To determine if the GLS possesses RNA localization activity we used a transgenic fly assay system. The starting point for these studies was a *K10::GFP* reporter gene construct (called *KGFP*, Fig. 2.2) that contains the *K10* nurse cell enhancer/promoter region and the bulk of the *K10* transcription unit, including the poly(A) addition signal,

but lacks the *K10* RLE (called the TLS) (Serano and Cohen, 1995). As expected, the *KGFP* transgene produced transcripts that exhibited no localization activity (data not shown), i.e., they remained in nurse cells until very late stages (i.e., after stage 11) of oogenesis, when nurse cells indiscriminately dump their entire cytoplasmic contents into the oocyte, in a process known as nurse cell regression. We next inserted a wild-type or truncated copy of the GLS (Fig. 2.3) into the 3'UTR of the *KGFP* reporter and introduced the resulting constructs, called *KGFP+GLS* and *KGFP+GLS*^{trunc}, respectively into flies. We found that *KGFP+GLS* transcripts accumulated in the oocyte beginning at about stage 2 and steadily increased in abundance through about stage 6 or 7, when they became localized to the oocyte's anterior cortex and formed the same ring-like distribution pattern observed for endogenous *gurken* and other transported transcripts (Fig. 2.2C). However, in contrast to wild-type *gurken* transcripts (Fig. 2.2A), the anterior ring of *KGFP+GLS* transcripts persisted through stage 10, and did not refine itself into the AD cap in any of more than 200 examined stages 9 and 10 egg chambers from each of 4 different transgenic lines. As expected, *KGFP+GLS*^{trunc} transcripts exhibited no localization activity (Fig. 2.2D). We tentatively conclude from these findings that the GLS possesses anterior, but not AD, localization activity.

The transport of *KGFP+GLS* transcripts into the oocyte is less robust than the transport of endogenous *gurken* transcripts or the transcripts of *KGFP* transcripts that contain the *K10* TLS (compare Fig. 2.2C to 2.2A and 2.2B). This led us to wonder if the inability of the GLS to mediate AD localization was due to its inability to bind the transport machinery tightly. To address this concern, we inserted a copy of the *K10* TLS into the *KGFP+GLS* reporter construct to make *KGFP+GLS+TLS*. As seen in Fig 2.2E,

KGFP+GLS+TLS transcripts exhibited robust transport into the oocyte and strong anterior localization, indicating that they bind the transport machinery tightly. However, *KGFP+GLS+TLS* transcripts never became enriched at the AD corner of the cell, supporting our earlier conclusion that the GLS lacks AD localization activity.

We next wondered whether the inability of the GLS to mediate AD localization was related to the fact that *KGFP* transcripts, with or without the GLS and/or TLS, are translated. Endogenous *gurken* transcripts are translationally repressed during their relocalization from the anterior cortex to the AD corner (Clouse et al., 2008) and we were concerned that such repression is necessary for relocalization. Consistent with this idea, recent studies have shown that wild-type *gurken* transcripts are highly dynamic, except at sites of translation activation, i.e., the oocyte's AD corner (Jaramillo et al., 2008). The repression of *gurken* translation is thought to be brought about by the binding of a protein complex consisting of Cup, Squid, PABP55B and Bruno to Bruno Response Elements (BREs) located in the 3'UTR of *gurken* mRNA (Clouse et al., 2008). Consistent with this idea, in vivo *gurken* signaling activity is highly responsive to alterations in Bruno expression levels (Filardo and Ephrussi, 2003; Yan and Macdonald, 2004). To determine whether BRE elements confer AD localization activity onto the GLS element, we inserted the same three copies of the BRE from the *oskar* 3' UTR that faithfully repress *oskar* translation (Chekulaeva et al., 2006; Filardo and Ephrussi, 2003) into the *KGFP+GLS* and *KGFP+GLS+TLS* reporter constructs. As seen in Figs. 2.2F and G, the BREs did not alter GLS localization activity, i.e., *KGFP+GLS+BREs* and *KGFP+GLS+TLS+BREs* transcripts were localized to the anterior cortex normally, but never relocalized to the AD corner. We also saw no AD localization when *KGFP*

transcript distribution patterns were assessed by confocal microscopy and fluorescence probes (data not shown) rather than by the enzyme linked detection scheme used in Fig. 2.2. We conclude from these findings that the GLS is unable to mediate AD localization even in the presence of BRE elements. The one caveat to these experiments is that the BRE elements failed to noticeably repress the translation of *K10::GFP* transcripts; we detected similar amounts of GFP fluorescence in the nuclei of flies carrying transgenes with BRE elements as with flies carrying transgenes without BRE elements. Why the BRE elements failed to repress the translation of the *K10::GFP* transcripts is not clear, but these findings suggest that the transport complexes assembled by the GLS alone are somehow different than the ones assembled by intact *gurken* transcripts and that these differences are critical for BRE-mediated translation repression.

While the simplest interpretation of above findings is that the GLS lacks AD localization activity, we cannot rule out the possibility that GLS possesses AD localization activity but that such activity is somehow masked by flanking sequences in the *K10::GFP* reporter transcript. We think this is unlikely for a couple of reasons, however. First, the GLS was inserted into the same general region of the reporter transcript that supports TLS RNA activity, which like that of the GLS appears to rely on the formation of a simple stem-loop secondary structure [24]. Second, the first 25-50 nt that flank the GLS in the *KGFP+GLS, KGP+GLS+TLS, KGP+KGFP+GLS+BREs* and *KGFP+GLS+TLS+BREs* transcripts all differ from one another, yet GLS localization activity remains constant. Another possibility is that AD localization activity is somehow lost when the GLS is moved from a protein coding to a non-protein coding portion of the transcript. While we have not tested this possibility, it is noteworthy that previous studies

have indicated that the GLS "retains" AD localization, even when located downstream of the protein coding portion of a GFP reporter transcript (Van De Bor et al., 2005).

The generation of a **gurken** *RNA null allele*

We next wanted to study the role of the GLS in *gurken* RNA localization and gene function within the context of a more wild-type transcript. To this end, we first set out to generate a *gurken* RNA null allele, so that we could detect *gurken* transgene transcripts without having to mark them with heterologous sequence tags, which could compromise *gurken* gene function. Previously described *gurken* null alleles are not complete deletions and produce significant amounts of *gurken* transcripts (unpublished observations). We were fortunate that the Exelixis stock collection includes lines that carry FRT elements just outside the 5' and 3' ends of the *gurken* transcription unit (see Methods). We successfully used these lines along with one that carries the FLP recombinase to generate a complete deletion allele of the *gurken* gene, called $grk^{\Delta FRT}$. Homozygous $grk^{\Delta FRT}$ flies are viable, but the females are completely sterile and produce egg chambers with no detectable *gurken* transcripts (Fig. 2.4E).

The egg chambers and eggs produced by homozygous $grk^{\Delta FRT}$ flies exhibited severe anteroposterior and dorsoventral patterning defects, consistent with previous studies which have identified two distinct functions for *gurken* during *Drosophila* oogenesis (Gonzalez-Reyes et al., 1995; Grunert and St Johnston, 1996; Nilson and Schupbach, 1999; Roth et al., 1995). The first of these functions is the induction of anteroposterior asymmetry in the follicle cell epithelium that surrounds the nurse cell-oocyte cluster. Following the transport of *gurken* mRNA into the oocyte and translation,

Gurken protein (Grk) is secreted locally and induces neighboring follicle cells to adopt the posterior cell fate (Gonzalez-Reyes et al., 1995; Grunert and St Johnston, 1996; Roth et al., 1995). At stage 7 of oogenesis, posterior follicle cells send a signal back to the oocyte that polarizes the oocyte's MT cytoskeleton, a prerequisite both for the migration of the oocyte nucleus to a point along the oocyte's anterior cortex (Roth et al., 1995), and the transport of *bicoid*, *oskar* and other mRNA that encode embryonic patterning determinants to specific ends of the oocyte (Kugler and Lasko, 2009; St Johnston, 2005). *gurken*'s second function is that of inducing dorsoventral asymmetry in the follicle cell epithelium. Following the relocation of its mRNA to the oocyte's AD corner and translation (Neuman-Silberberg and Schupbach, 1993, 1996), Grk is secreted locally and induces neighboring follicle cells to adopt the dorsal cell fate (Roth, 2003; Serano et al., 1995). Dorsal and ventral (non-induced) follicle cells subsequently differentially signal the oocyte, polarizing the dorsoventral axes of the mature egg and future embryo.

Similar to analyses of other *gurken* null and strong loss-of-function alleles (Schupbach, 1987), we find that $grk^{\Delta FRT}$ females lay very few eggs and those that are laid are completely ventralized, most readily evident by their elongated shape and absence of dorsal appendages on their eggshells (data not shown). Such eggs are also translucent and extremely fragile, suggestive of a general defect in follicle cell differentiation and/or cell fate determination. Also as expected, $grk^{\Delta FRT}$ females exhibited strong defects in the specification of anteroposterior polarity as evident by their inability to support nuclear migration and/or the localization of *K10* transcripts to the anterior cortex of stage 7 oocytes (data not shown). We also found that $grk^{\Delta FRT}$ females produce a high percentage (several per ovariole) of compound egg chambers, i.e., egg chambers that contain two or

more germline cysts encased in a single follicle cell epithelium. All of these phenotypes—female sterility, ventralized and fragile eggs, and compound egg chambers—are due to the loss of *gurken* gene function, since they were completely rescued by the introduction of a wild-type *gurken* transgene, grk^{wt} into the germline (Fig. 2.4C, and see Methods).

The GLS is required for gurken *gene function*

To determine if the GLS is required for normal *gurken* gene function, we created a rescue construct, called $grkGLS^{mut}$, that is identical to grk^{wt}, except for the inclusion of 12 single-base mutations, all within the GLS. All 12 mutations target wobble nucleotides and preserve the encoded protein sequence (Fig. 2.3). Five of the mutations disrupt the predicted base pairing pattern of the GLS (Fig. 2.3) and according to mFOLD (http://mfold.bioinfo.rpi.edu/) are sufficient to destabilize the wild-type structure (data not shown). The other seven mutations disrupt the primary sequence only, but such mutations in other RLEs (e. g., see (Cohen et al., 2005)) are known to compromise RNA localization activities. Four independent lines carrying the $grkGLS^{mut}$ transgene were crossed into a $grk^{\Delta FRT}$ background for analysis. RT-PCR analyses revealed significant (~10-fold) variation in the level of transgene transcript accumulation. Two of the lines exhibited wild-type or near wild-type levels of accumulation and we focused on them for all subsequent analyses. Such analyses revealed no significant differences in the behavior or activities of these two transgenic lines and thus we describe them below as if they are a single line/transgene.

The *grkGLS*^{mut} transgene exhibited no or only weak rescue of the dorsoventral patterning defects of *grk*$^{\Delta FRT}$ flies; ~50% of the recovered eggs (n > 1000 per line) were fully ventralized and similar to those produced by *grk*$^{\Delta FRT}$ flies. The remaining recovered eggs were strongly ventralized, containing a single small appendage on the dorsal midline (Fig. 2.4F). The *grkGLS*^{mut} transgene exhibited much better, but still not complete rescue of the anteroposterior patterning defects of *grk*$^{\Delta FRT}$ flies. Thus while nuclear migration was consistently delayed and sometimes (5-25% of the time) incomplete, most stage 8 and older egg chambers contained a correctly positioned nucleus and exhibited wild-type localization of *K10* mRNA to the anterior cortex (data not shown). We conclude from these data that the GLS is required for *gurken*'s anteroposterior and, especially, dorsoventral patterning activities, both of which are dependent on faithful transport and subcellular localization of *gurken* transcripts. The *grkGLS*^{mut} transgene rescued all other *gurken* activities; *grk*$^{\Delta FRT}$*; grkGLS*^{mut} flies produced virtually no compound egg chambers (only two compound egg chambers were detected in more than 50 examined ovaries or about ~1000 egg chambers from each of the two extensively examined lines), and none of the recovered eggs (n > 1000 per line) were fragile. We also saw a general increase in viability of *grk*$^{\Delta FRT}$*; grkGLS*^{mut} flies compared to *grk*$^{\Delta FRT}$ controls; we recovered many more non-CyO flies from sibling crosses of *grk*$^{\Delta FRT}$*; grkGLS*^{mut}/CyO flies than from sibling crosses of *grk*$^{\Delta FRT}$/CyO flies. We interpret such rescue to mean that mutations in the GLS do not interfere with *gurken* transcription or translation, but rather only mRNA localization.

The GLS is required for the localization of **gurken** *transcripts*

Given the moderate rescue of the anteroposterior patterning defects of $grk^{\Delta FRT}$ ovaries by the $grkGLS^{mut}$ transgene, we expected only modest defects in the transport and anterior localization of $grkGLS^{mut}$ transcripts. Unexpectedly, *in situ* hybridization experiments revealed no enrichment of *gurken* transcripts in stage 1-7 oocytes of $grkGLS^{mut}$; $grk^{\Delta FRT}$ flies, and the transcripts never became concentrated along the oocyte's anterior cortex (Fig. 2.4G). Significantly more $grkGLS^{mut}$ transcripts were detected in later stage (e.g., stage 8-10) oocytes, but this is likely due to diffusion, since the diameter of the cytoplasmic bridges between nurse cells and the oocyte increases dramatically during these stages (unpublished observations). We conclude from these findings that the GLS is required for the transport and anterior localization of *gurken* transcripts, and strongly suspect that this requirement is met by the GLS's ability to recruit a cytoplasmic dynein motor complex. Whether the small amounts of *gurken* transcripts detected in stage 1-7 $grkGLS^{mut}$; $grk^{\Delta FRT}$ oocytes is indicative of residual GLS transport activity, the transport activity of other RLEs in the *gurken* mRNA, and/or diffusion of *gurken* transcripts from nurse cells into the oocyte is not clear from our data, although the complete absence of anterior localization is most supportive of the last possibility. Antibody stains for Grk protein were consistent with the RNA data. Most stage 1-7 egg chambers showed no obvious enrichment of Grk protein in the oocyte or anywhere else in the germline cyst (Fig. 2.4H). Given that most $grkGLS^{mut}$; $grk^{\Delta FRT}$ oocytes supported nuclear migration and *K10* mRNA localization, we further conclude from these analyses that very low levels of *gurken* mRNA and protein are sufficient for

anteroposterior patterning and that such patterning does not require subcellular localization of *gurken* transcripts and/or protein within the oocyte.

The rescue data predicts a stronger requirement for the GLS in the localization of transcripts to the oocyte's AD corner. Thus while the *grkGLS*^{mut} transgene showed moderate rescue of the anteroposterior defects of *grk*$^{\Delta FRT}$ egg chambers and eggs, it exhibited almost no rescue of the dorsoventral patterning defects of *grk*$^{\Delta FRT}$ ovaries (see above). Consistent with this prediction, the *grkGLS*^{mut} transcripts were dispersed throughout the ooplasm in all examined staged 7-10 *grkGLS*^{mut}; *grk*$^{\Delta FRT}$ oocytes. Antibody stains for Grk protein were again consistent with the RNA data in that the vast majority of examined stage 8-10 egg oocytes showed no enrichment of Grk protein around the nucleus or elsewhere in the cell. Surprisingly, however, a few (less than 5%) showed distinct enrichment of Grk protein around the oocyte nucleus (e.g., see Fig. 2.4H). We interpret such enrichment to mean that *gurken* translational activator and/or derepressor proteins are concentrated around the oocyte nucleus, which could also explain the residual dorsoventral patterning activity of the *grkGLS*^{mut} transgene despite its absence of AD RNA localization activity.

DISCUSSION

The major finding of our studies is that the GLS is required but not sufficient for AD localization. We interpret this to mean that AD localization is brought about by the action of the GLS plus one or more additional RLEs, henceforth referred to as AD-RLEs. The nature of the requirement for the GLS in AD localization is not clear, but may simply be that of getting *gurken* transcripts to the oocyte's anterior cortex, where they can

associate (through the action of the AD-RLEs) with the AD localization machinery. Consistent with this view, transgenic RNAs that contain the GLS but no other *gurken* RLEs, e.g., *KGFP+GLS* transcripts (Fig. 2.2C), are transported into the oocyte and subsequently accumulate along the oocyte's anterior cortex, but never become concentrated at the oocyte's AD corner. The transport and anterior localization pattern of *KGFP+GLS* transcripts is mirrored by a number of other mRNAs, including *K10* and *Orb* and is completely consistent with the idea that the GLS mediates association of *gurken* mRNA with a minus end motor complex, most probably cytoplasmic dynein. Direct support for this idea comes from real-time imaging and immunoelectron microscopy experiments (Delanoue et al., 2007), which show that *gurken* transcripts form large particles that contain cytoplasmic dynein heavy chain (DHC) and the motor cofactors Egalitarian (Egl) and Bicaudal D (BicD) upon injection into stage 7-9 oocytes. Moreover, the majority of these particles are in close proximity to microtubules and their formation is dependent on the GLS. Finally, it has been shown that Dynein light chain (Ddlc) binds *gurken* mRNA *in vitro* and that such binding is mediated by the 3'UTR, not the GLS (Rom et al., 2007).

How the AD-RLEs mediate the relocalization of *gurken* transcripts from the anterior cortex to the AD corner is not clear, although one simple possibility is that they bind proteins that are (or become) anchored to the oocyte nucleus or to a neighboring structure. Given that some *grkGLS*^{mut} transcripts accumulate in (diffuse into?) the oocyte, yet only very inefficiently become concentrated at the AD corner (or around the nucleus), it would appear that efficient AD localization requires active transport, i.e., AD localization cannot be brought about by diffusion within the oocyte and specific

anchoring at the AD corner of the cell. However, it is not clear as previously suggested (Van De Bor et al., 2005) that such transport needs to be specifically directed toward the AD corner. Rather AD localization could be brought about by repeated rounds of GLS-mediated transport to the anterior cortex (i. e., to the minus ends of the oocyte's MTs), coupled with region-specific anchoring at the AD corner and/or to the nucleus. In this scenario, the AD-RLEs, which could include the GLS, would constitute the RNA component of the anchor complex. Consistent with the notion of anchoring, photo-bleaching and real-time imaging experiments reveal that endogenous and injected *gurken* transcripts are highly dynamic during early and middle stages of oogenesis, but become static coincident with AD localization (Delanoue et al., 2007; Jaramillo et al., 2008). The dynamic to static transition is accompanied by a distinct change in *gurken* particle morphology (Delanoue et al., 2007). Interestingly, this transition requires cytoplasmic dynein, but not other components of the motor complex, e.g., Egl and BicD. These observations have led to the proposal that upon reaching its final destination, the Dynein motor becomes a static anchor and is no longer a functional motor protein.

How do we reconcile our findings with those of previous studies (Van De Bor et al., 2005) which indicate that the GLS mediates directed transport to the oocyte's AD corner? One possibility relates to the fact that such studies utilized either injected RNAs or transgenic RNAs expressed from very strong promoters. Both scenarios are likely to result in the formation of very large transport particles and it may be that such particles are better able to recruit the AD localization machinery than endogenous *gurken* transport particles, e.g., because of a higher number of GLS elements within the particle. It should also be noted that the AD localization activity of injected GLS-containing transcripts is

not nearly as complete as the AD localization of wild-type *gurken* transcripts; wild-type *gurken* transcripts are rarely detected outside the AD corner of stage 9 oocytes, whereas injected transcripts are readily detectable in all regions of the anterior cortex (Van De Bor et al., 2005). Similarly, the AD localization of previously described GLS-containing transgene transcripts is transient in nature, not persisting past stage 9. Taken together, these data indicate that the GLS is not sufficient (even in multiple copies) for wild-type AD localization, and that one or more additional elements are needed for persistent AD localization

It is not clear how cytoplasmic dynein switches from a motor to anchor. Thus while *gurken* transport and anchor particles are morphologically distinct, no proteins have been identified that are specific to one particle or the other. Given that *gurken* transcripts are specifically translated at the AD corner of the oocyte, the switch might be regulated by translation. Consistent with this idea, *gurken* transcripts never become anchored (remain dynamic) in *K10* and *Squid* mutants and are translated all along the anterior cortex (Jaramillo et al., 2008). Squid is a normal component of *gurken* transport and anchor particles, but is specifically required for anchoring. Thus, the switch from transport to anchoring might involve some sort of activation of Squid. K10 is an attractive candidate here as it binds Squid in vitro (Norvell et al., 1999). Moreover, K10 is concentrated in the oocyte nucleus and thus could provide the necessary asymmetry to the system. The one obvious caveat to this scenario is that K10 appears to be strictly nuclear and tightly associated with the oocyte's chromatin. Squid, while predominantly a cytoplasmic protein, is also detected in the nucleus and has been shown to interact with transportin, a nuclear import protein in vitro (Norvell et al., 1999). The activation of

Squid and *gurken* anchoring could thus be brought about by specific modification of Squid in the oocyte nucleus by K10.

ACKNOWLEDGEMENTS

We thank Jaya Arora with help in the construction of the *gurken* null allele. We thank Vicki Corbin for comments on the manuscript and the Bloomington and Harvard Medical Schools Stock centers for flies. Finally, we thank David Moore for excellent help with confocal microscopy.

Figure 2.1 Conservation and predicted secondary structure of the GLS. (**A**) Sequence alignment of the *gurken* transcription unit displayed using the Vista Browser at http://pipeline.lbl.gov/cgi-bin/gateway2 (Nielsen et al., 2010). The estimated years in millions (MYA) of evolution between *D. melanogaster* and each of the other five species is from Heger and Ponting (Heger and Ponting, 2007). The most highly conserved region is circled and includes the first 39 nt of the GLS. The last 25 nt of the GLS map to the 3' side of the abutting intron. The arrow indicates the direction of transcription. The red shaded region corresponds to a putative transposable element. The numbers at the bottom of the graph indicate nucleotide position along the chromosome. (**B**) The 5' end of the *gurken* mRNA, where the green dot denotes the translation start site, the red arrows the boundaries of the GLS, and the asterisk the position of the intron. The nucleotides beneath the aligned sequence blocks highlight differences between the *D. Willistoni* and *D. melanogaster* sequences. (**C**) Predicted secondary structure of the GLS, with non-conserved residues shown in red.

FIGURE 2.1

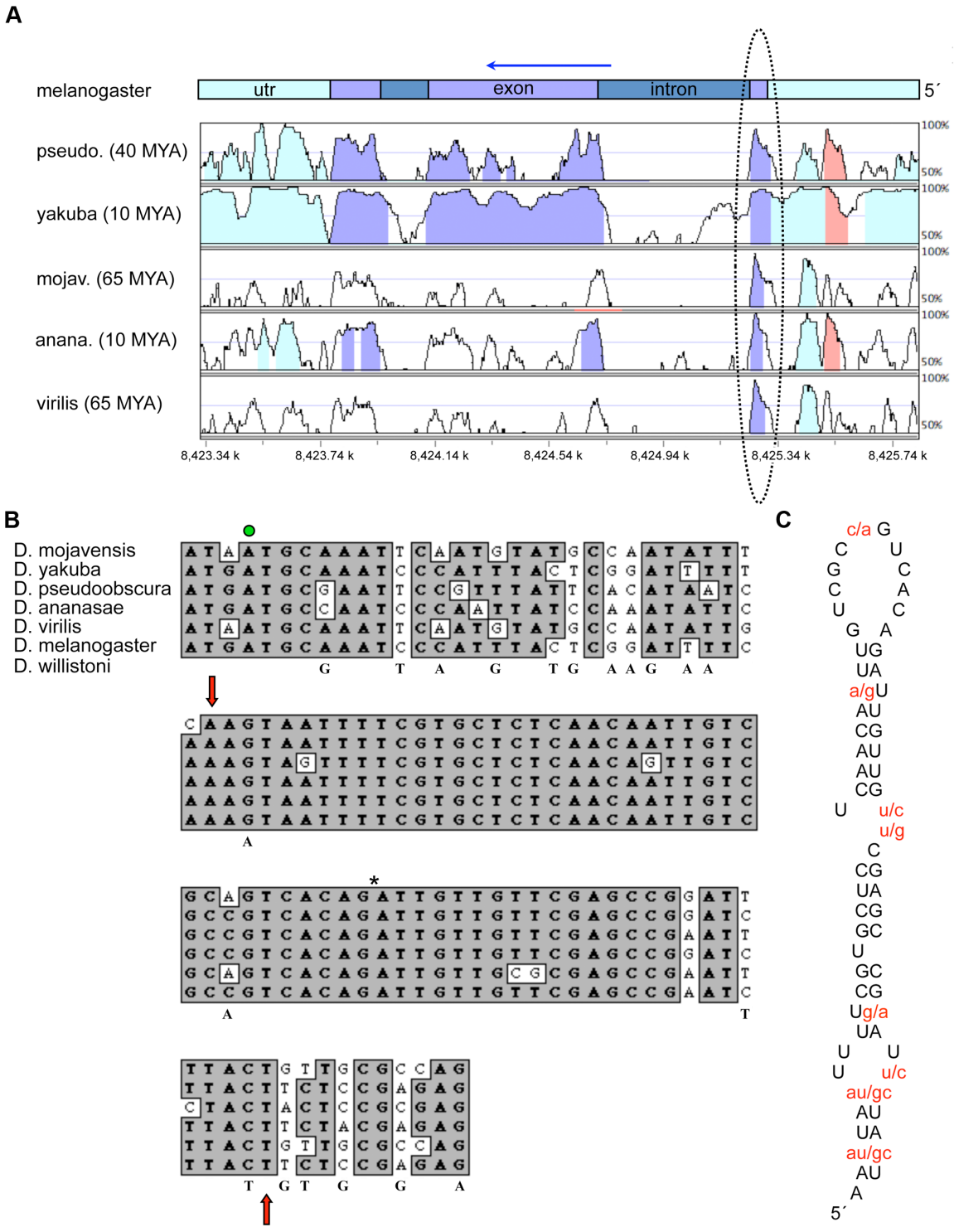
A
melanogaster
utr
exon
intron
5´
pseudo. (40 MYA)
yakuba (10 MYA)
mojav. (65 MYA)
anana. (10 MYA)
virilis (65 MYA)
100%
50%
8,423.34 k
8,423.74 k
8,424.14 k
8,424.54 k
8,424.94 k
8,425.34 k
8,425.74 k
B
D. mojavensis
D. yakuba
D. pseudoobscura
D. ananasae
D. virilis
D. melanogaster
D. willistoni
C
c/a G
C U
G C
C A
U C
G A
UG
UA
a/gU
AU
CG
AU
AU
CG
U u/c
u/g
C
CG
UA
CG
GC
U
GC
CG
Ug/a
UA
U U
U u/c
au/gc
AU
UA
au/gc
AU
A
5´

Figure 2.2 The GLS is sufficient for anterior, but not anterodorsal localization within the *Drosophila* oocyte. RNA distribution patterns of wild-type *gurken* transcripts (**A**) and *K10::GFP* reporter transcripts (**B-G**) as revealed by wholemount *in situ* hybridization (see Methods). Individual ovarioles are shown, with older egg chambers oriented to the right. The transgenes (**B-G**) are noted in the individual panels. The structure of the transgenes and expression summary is shown beneath the *in situ*s.

Figure 2.2

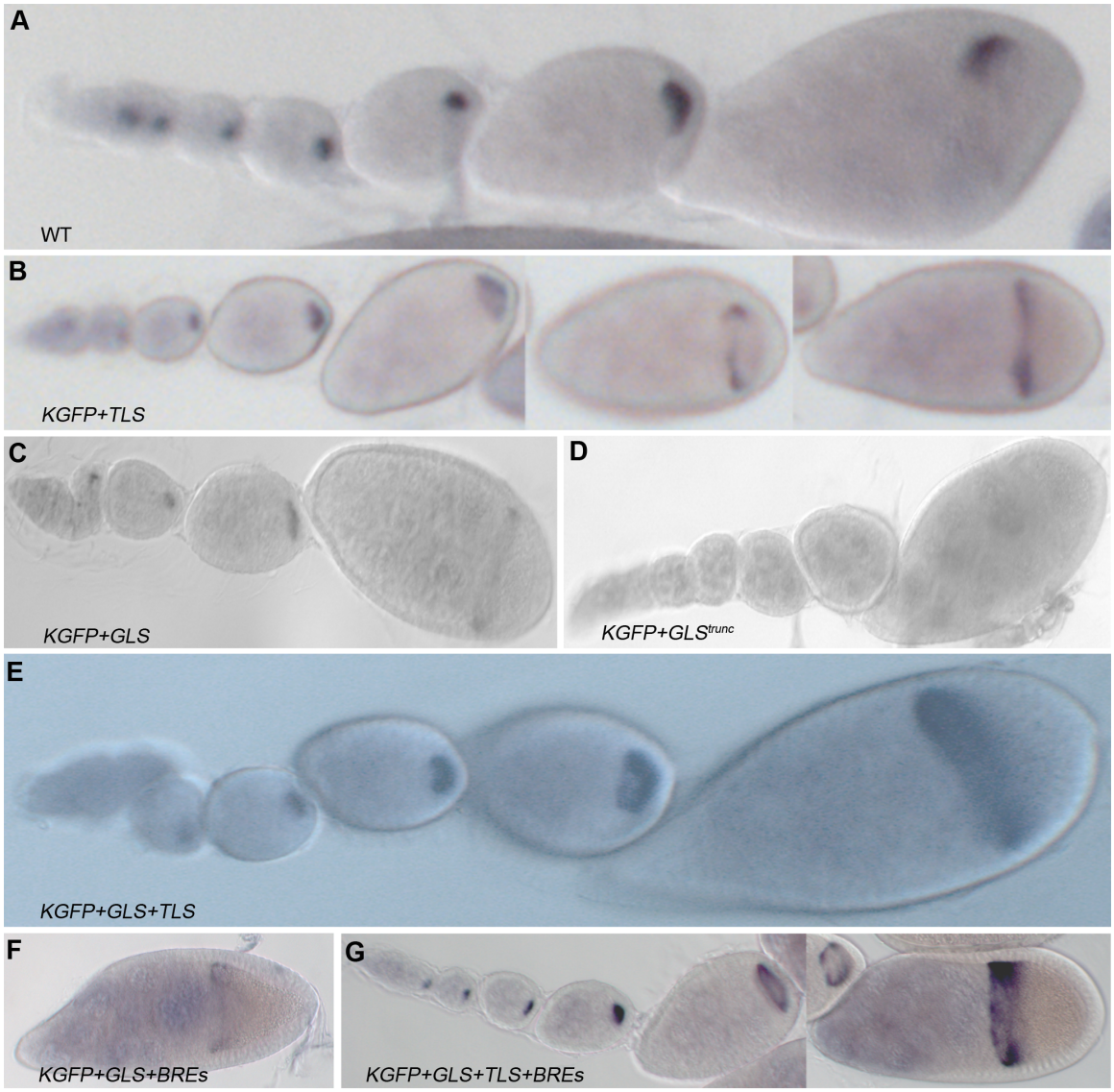
A
WT
B
KGFP+TLS
C
KGFP+GLS
D
KGFP+GLS^trunc
E
KGFP+GLS+TLS
F
KGFP+GLS+BREs
G
KGFP+GLS+TLS+BREs
K10 genomic fragment
ATG
TAG
TLS
pA
GFP
GLS
BRE
GLS^trunc
Localization
Oocyte (stage1-6)
Anterior (stage 7)
AD
KGFP+TLS ++++ ++++ -
KGFP - - -
KGFP+GLS ++ ++ -
KGFP+GLS^trunc - - -
KGFP+GLS+TLS ++++ ++++ -
KGFP+GLS+BREs ++ ++ -
KGFP+GLS+TLS+BREs ++++ ++++ -

Figure 2.3 Structure of GLS variants. The wild-type GLS is shown at the left for comparison. The GLS mutant (referred to as *grkGLS*^{mut} in Text) contains 12 point mutations (shown in red), which are predicted to disrupt the predicted base pairing pattern of the GLS at five sites (circled). None of the 12 mutations affect the protein coding sequence as shown at the bottom portion of the figure.

Figure 2.3

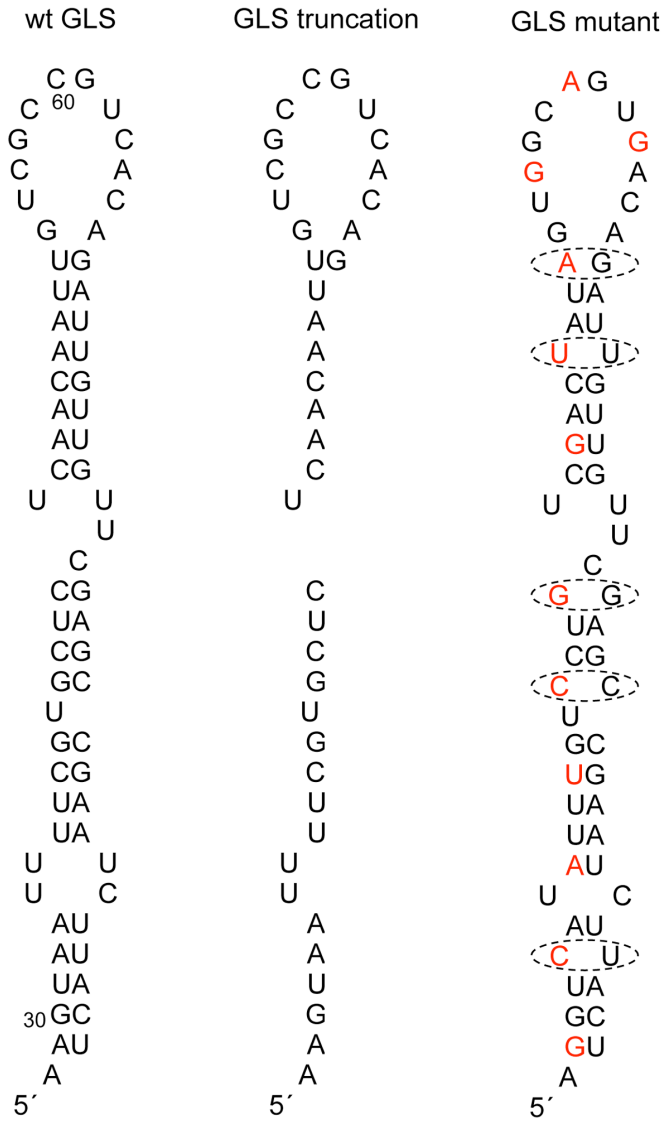

	30				40			50				60	
wt	AAA	GTA	AUU	UUC	GUG	CUC	UCA	ACA	AUU	GUC	GCC	GUC	
GLS mutant	AAG	GTC	AUA	UUU	GUC	CUG	UCG	ACU	AUA	GUG	GCA	GUG	
protein	Lys	Val	Ile	Phe	Val	Leu	Ser	Thr	Ile	Val	Gly	Val	

Figure 2.4 The GLS is required for *gurken* RNA localization and gene function. (**A-B**) Wild-type expression patterns of endogenous *gurken* RNA (**A**) and protein (**B**) as revealed by whole mount *in situ* hybridization and immunofluorescence, respectively. Anterodorsal localization of transcripts and protein is only apparent in the rightmost egg chambers, which are stage 8 and 9, respectively. (**C-E**) The *gurken* RNA and protein distribution patterns of *gurken* null mutants ($grk^{\Delta FRT}$) carrying the wild-type *gurken* transgene, grk^{wt} (**C-D**) or no transgene (**E**). (**F-H**) $grk^{\Delta FRT}$ eggs and egg chambers (from *gurken* null mothers) carrying the $grkGLS^{mut}$ transgene. (**F**) Left panel: representative $grk^{\Delta FRT}$; $grkGLS^{mut}$ egg exhibiting a completely ventralized phenotype, i.e., complete loss of dorsal appendage material. Right panel; anterior end of a $grk^{\Delta FRT}$; $grkGLS^{mut}$ egg exhibiting a strong, but not complete, ventralized phenotype. Note, for example the short, fused dorsal appendage. (**G**) $grk^{\Delta FRT}$; $grkGLS^{mut}$ ovariole following *in situ* hybridization with *gurken* probe. Transcripts are dispersed throughout the germline cysts with only slight enrichment in the oocyte and no subcellular localization. (**H**) $grk^{\Delta FRT}$; $grkGLS^{mut}$ ovariole following immunofluorescence using an anti-Grk antibody. The protein is generally dispersed throughout the germline cysts, although slight enrichment around the oocyte nucleus is seen in rare stage 10 and 11 egg chambers.

Figure 2.4

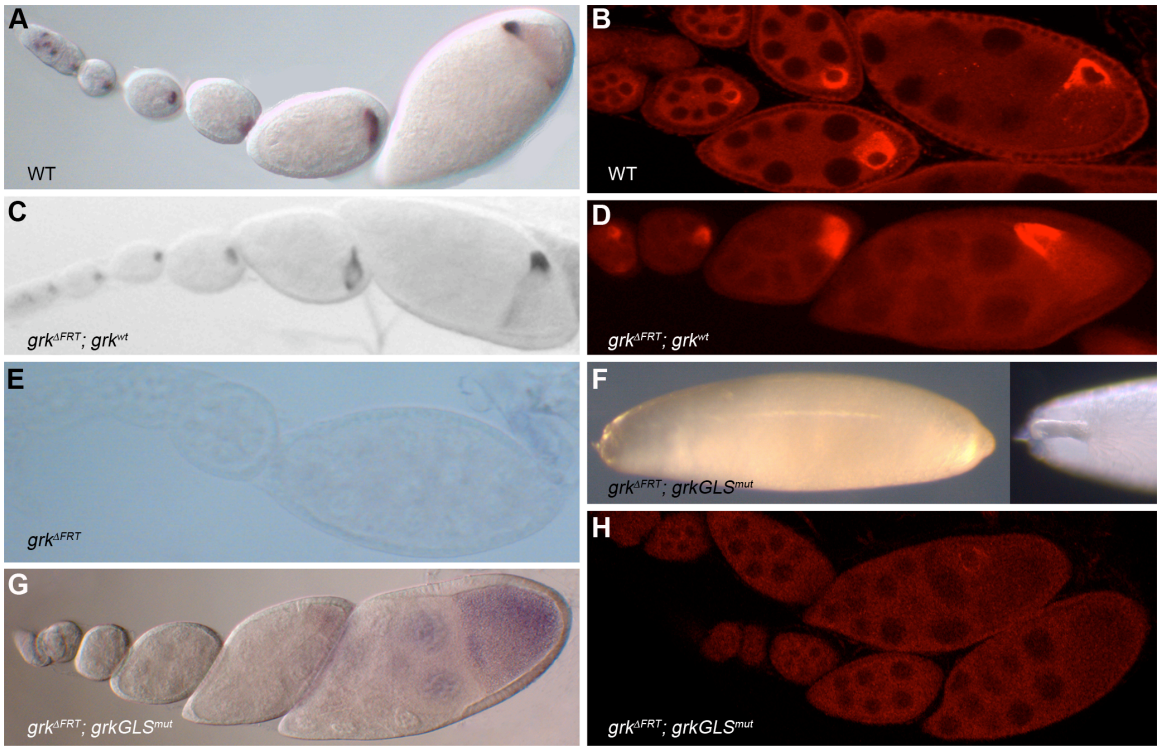
A
WT
B
WT
C
grk^ΔFRT; grk^wt
D
grk^ΔFRT; grk^wt
E
grk^ΔFRT
F
grk^ΔFRT; grkGLS^mut
G
grk^ΔFRT; grkGLS^mut
H
grk^ΔFRT; grkGLS^mut

REFERENCES

1. Ashburner, M. (1989). *Drosophila* (Cold Spring Harbor, N.Y., Cold Spring Harbor Laboratory).
2. Bashirullah, A., Cooperstock, R.L., and Lipshitz, H.D. (1998). RNA localization in development. Annu Rev Biochem *67*, 335-394.
3. Bastock, R., and St Johnston, D. (2008). *Drosophila* oogenesis. Curr Biol *18*, R1082-1087.
4. Becalska, A.N., and Gavis, E.R. (2009). Lighting up mRNA localization in *Drosophila* oogenesis. Development *136*, 2493-2503.
5. Berleth, T., Burri, M., Thoma, G., Bopp, D., Richstein, S., Frigerio, G., Noll, M., and Nusslein-Volhard, C. (1988). The role of localization of bicoid RNA in organizing the anterior pattern of the *Drosophila* embryo. EMBO J *7*, 1749-1756.
6. Brenner, H.R., Witzemann, V., and Sakmann, B. (1990). Imprinting of acetylcholine receptor messenger RNA accumulation in mammalian neuromuscular synapses. Nature *344*, 544-547.
7. Chekulaeva, M., Hentze, M.W., and Ephrussi, A. (2006). Bruno acts as a dual repressor of oskar translation, promoting mRNA oligomerization and formation of silencing particles. Cell *124*, 521-533.
8. Cheung, H.K., Serano, T.L., and Cohen, R.S. (1992). Evidence for a highly selective RNA transport system and its role in establishing the dorsoventral axis of the *Drosophila* egg. Development *114*, 653-661.

9. Clark, I.E., Jan, L.Y., and Jan, Y.N. (1997). Reciprocal localization of Nod and kinesin fusion proteins indicates microtubule polarity in the *Drosophila* oocyte, epithelium, neuron and muscle. Development *124*, 461-470.
10. Clouse, K.N., Ferguson, S.B., and Schupbach, T. (2008). Squid, Cup, and PABP55B function together to regulate gurken translation in *Drosophila*. Dev Biol *313*, 713-724.
11. Cohen, R.S., Zhang, S., and Dollar, G.L. (2005). The positional, structural, and sequence requirements of the *Drosophila* TLS RNA localization element. RNA *11*, 1017-1029.
12. Delanoue, R., Herpers, B., Soetaert, J., Davis, I., and Rabouille, C. (2007). *Drosophila* Squid/hnRNP helps Dynein switch from a gurken mRNA transport motor to an ultrastructural static anchor in sponge bodies. Dev Cell *13*, 523-538.
13. Dollar, G., Struckhoff, E., Michaud, J., and Cohen, R.S. (2002). Rab11 polarization of the *Drosophila* oocyte: a novel link between membrane trafficking, microtubule organization, and oskar mRNA localization and translation. Development *129*, 517-526.
14. Duncan, J.E., and Warrior, R. (2002). The cytoplasmic dynein and kinesin motors have interdependent roles in patterning the *Drosophila* oocyte. Curr Biol *12*, 1982-1991.
15. Ephrussi, A., Dickinson, L.K., and Lehmann, R. (1991). Oskar organizes the germ plasm and directs localization of the posterior determinant nanos. Cell *66*, 37-50.

16. Feinberg, A.P., and Vogelstein, B. (1983). A technique for radiolabeling DNA restriction endonuclease fragments to high specific activity. Anal Biochem *132*, 6-13.

17. Filardo, P., and Ephrussi, A. (2003). Bruno regulates gurken during *Drosophila* oogenesis. Mech Dev *120*, 289-297.

18. Forrest, K.M., and Gavis, E.R. (2003). Live imaging of endogenous RNA reveals a diffusion and entrapment mechanism for nanos mRNA localization in *Drosophila*. Curr Biol *13*, 1159-1168.

19. Gonzalez-Reyes, A., Elliott, H., and St Johnston, D. (1995). Polarization of both major body axes in *Drosophila* by gurken-torpedo signalling. Nature *375*, 654-658.

20. Grunert, S., and St Johnston, D. (1996). RNA localization and the development of asymmetry during *Drosophila* oogenesis. Curr Opin Genet Dev *6*, 395-402.

21. Heger, A., and Ponting, C.P. (2007). Variable strength of translational selection among 12 *Drosophila* species. Genetics *177*, 1337-1348.

22. Januschke, J., Gervais, L., Dass, S., Kaltschmidt, J.A., Lopez-Schier, H., St Johnston, D., Brand, A.H., Roth, S., and Guichet, A. (2002). Polar transport in the *Drosophila* oocyte requires Dynein and Kinesin I cooperation. Curr Biol *12*, 1971-1981.

23. Jaramillo, A.M., Weil, T.T., Goodhouse, J., Gavis, E.R., and Schupbach, T. (2008). The dynamics of fluorescently labeled endogenous gurken mRNA in *Drosophila*. J Cell Sci *121*, 887-894.

24. Kugler, J.M., and Lasko, P. (2009). Localization, anchoring and translational control of oskar, gurken, bicoid and nanos mRNA during *Drosophila* oogenesis. Fly (Austin) *3*, 15-28.

25. Lecuyer, E., Yoshida, H., Parthasarathy, N., Alm, C., Babak, T., Cerovina, T., Hughes, T.R., Tomancak, P., and Krause, H.M. (2007). Global analysis of mRNA localization reveals a prominent role in organizing cellular architecture and function. Cell *131*, 174-187.

26. Lehmann, R., and Nusslein-Volhard, C. (1986). Abdominal segmentation, pole cell formation, and embryonic polarity require the localized activity of oskar, a maternal gene in *Drosophila*. Cell *47*, 141-152.

27. Martin, K.C., and Ephrussi, A. (2009). mRNA localization: gene expression in the spatial dimension. Cell *136*, 719-730.

28. Meignin, C., and Davis, I. (2010). Transmitting the message: intracellular mRNA localization. Curr Opin Cell Biol *22*, 112-119.

29. Neuman-Silberberg, F.S., and Schupbach, T. (1993). The *Drosophila* dorsoventral patterning gene gurken produces a dorsally localized RNA and encodes a TGF alpha-like protein. Cell *75*, 165-174.

30. Neuman-Silberberg, F.S., and Schupbach, T. (1996). The *Drosophila* TGF-alpha-like protein Gurken: expression and cellular localization during *Drosophila* oogenesis. Mech Dev *59*, 105-113.

31. Nielsen, C.B., Cantor, M., Dubchak, I., Gordon, D., and Wang, T. (2010). Visualizing genomes: techniques and challenges. Nat Methods *7*, S5-S15.

32. Nilson, L.A., and Schupbach, T. (1999). EGF receptor signaling in *Drosophila* oogenesis. Curr Top Dev Biol *44*, 203-243.

33. Norvell, A., Kelley, R.L., Wehr, K., and Schupbach, T. (1999). Specific isoforms of squid, a *Drosophila* hnRNP, perform distinct roles in Gurken localization during oogenesis. Genes Dev *13*, 864-876.

34. Parks, A.L., Cook, K.R., Belvin, M., Dompe, N.A., Fawcett, R., Huppert, K., Tan, L.R., Winter, C.G., Bogart, K.P., Deal, J.E.*, et al.* (2004). Systematic generation of high-resolution deletion coverage of the *Drosophila* melanogaster genome. Nat Genet *36*, 288-292.

35. Pirrotta, V. (1988). Vectors for P-mediated transformation in *Drosophila*. Biotechnology *10*, 437-456.

36. Queenan, A.M., Barcelo, G., Van Buskirk, C., and Schupbach, T. (1999). The transmembrane region of Gurken is not required for biological activity, but is necessary for transport to the oocyte membrane in *Drosophila*. Mech Dev *89*, 35-42.

37. Rom, I., Faicevici, A., Almog, O., and Neuman-Silberberg, F.S. (2007). *Drosophila* Dynein light chain (DDLC1) binds to gurken mRNA and is required for its localization. Biochim Biophys Acta *1773*, 1526-1533.

38. Roth, S. (2003). The origin of dorsoventral polarity in *Drosophila*. Philos Trans R Soc Lond B Biol Sci *358*, 1317-1329; discussion 1329.

39. Roth, S., Neuman-Silberberg, F.S., Barcelo, G., and Schupbach, T. (1995). cornichon and the EGF receptor signaling process are necessary for both anterior-posterior and dorsal-ventral pattern formation in *Drosophila*. Cell *81*, 967-978.

40. Saunders, C., and Cohen, R.S. (1999). The role of oocyte transcription, the 5'UTR, and translation repression and derepression in *Drosophila* gurken mRNA and protein localization. Mol Cell *3*, 43-54.

41. Schupbach, T. (1987). Germ line and soma cooperate during oogenesis to establish the dorsoventral pattern of egg shell and embryo in *Drosophila* melanogaster. Cell *49*, 699-707.

42. Serano, T.L., and Cohen, R.S. (1995). A small predicted stem-loop structure mediates oocyte localization of *Drosophila* K10 mRNA. Development *121*, 3809-3818.

43. Serano, T.L., Karlin-McGinness, M., and Cohen, R.S. (1995). The role of fs(1)K10 in the localization of the mRNA of the TGF alpha homolog gurken within the *Drosophila* oocyte. Mech Dev *51*, 183-192.

44. Simon, A.M., Hoppe, P., and Burden, S.J. (1992). Spatial restriction of AChR gene expression to subsynaptic nuclei. Development *114*, 545-553.

45. St Johnston, D. (2005). Moving messages: the intracellular localization of mRNAs. Nat Rev Mol Cell Biol *6*, 363-375.

46. Tautz, D., and Pfeifle, C. (1989). A non-radioactive in situ hybridization method for the localization of specific RNAs in *Drosophila* embryos reveals translational control of the segmentation gene hunchback. Chromosoma *98*, 81-85.

47. Theurkauf, W.E., Smiley, S., Wong, M.L., and Alberts, B.M. (1992). Reorganization of the cytoskeleton during *Drosophila* oogenesis: implications for axis specification and intercellular transport. Development *115*, 923-936.

48. Van De Bor, V., Hartswood, E., Jones, C., Finnegan, D., and Davis, I. (2005). gurken and the I factor retrotransposon RNAs share common localization signals and machinery. Dev Cell *9*, 51-62.

49. Yan, N., and Macdonald, P.M. (2004). Genetic interactions of *Drosophila* melanogaster arrest reveal roles for translational repressor Bruno in accumulation of Gurken and activity of Delta. Genetics *168*, 1433-1442.

Chapter III

Cloning and Characterization of the Putative Rab11 effector, dRip11

ABSTRACT

Rab11, a small GTPase, functions critically in the establishment and maintenance of cell polarity by trafficking of vesicles from recycling endosome to the plasma membrane. It mediates multiple trafficking steps and it traffics different cargos in different cells, both by interacting with unique set of effector molecules. Here, I characterize a putative Rab11 effector, *Drosophila* Rab11-family interacting protein (dRip11). First, I show that dRip11 binds to Rab11 in vitro. Second, I identify a region within the Rab11 protein that is required for binding to dRip11. Third, I show that dRip11 has overlapping expression pattern with Rab11 in GSCs and border cells within the *Drosophila* ovary. Finally, I describe my attempt to generate and analyze dRip11 mutations.

INTRODUCTION

In order to understand the details of Rab11 function, I set out to identify effector molecules that work with Rab11 in regulating trafficking events. There are two structural classes of Rab11-family interacting proteins (Rab11-FIPs) (Horgan and McCaffrey, 2009). Class I proteins have a N-terminal C2 domain and include Rip11, FIP2 and Rab-coupling protein (RCP), while Class II proteins have EF-hand domains and include FIP3 and FIP4. Both classes have a highly conserved 20 amino acid Rab11-binding domain (RBD) in their C-terminal end and like the majority of other Rab effector proteins, have an overall α-helical coiled-coil structure.

We used yeast two-hybrid screens (University of *Wisconsin* Molecular Interaction Facility, Madison, *WI*) to identify candidate Rab11 binding partners and got a significant hit with CG6606. Protein BLAST searches identified CG6606 as an ortholog of human Rab11-FIP2. CG6606/ Rab11-FIP2, henceforth referred to as dRip11 (*Drosophila* Rab11-family interacting protein 2) (Prekeris et al., 2000), is the only Class I Rab11 effector in *Drosophila* (Li et al., 2007).

In this chapter, I describe studies to clarify the role of dRip11 in the ovary. I confirm the binding between dRip11 and Rab11 by a GST-pull down assay. I also mapped the domain in Rab11 that is responsible for such binding using different Rab11 mutant proteins as bait. Finally, I used antibody staining to show that dRip11 is expressed abundantly in the ovary, including in germline stem cells (GSCs) and in migrating border cells.

MATERIALS AND METHODS

Generation of GST-tagged Rabs and His-tagged dRip11 proteins

GST-Rab11: The entire protein-coding region of Rab11 as described in (Dollar et al., 2002) was cloned between *Xho I* and *Asp718 I* site of pGEX(B)XA vector for purification of GST-Rab11.

Chimera proteins Rab11-2 and Rab2-11: The entire Rab2 coding region was amplified from GH01619 (BDGP EST project) using PCR (forward primer containing an *Xho I* site: CTCTCTCGAGATGTCCTACGCGTACTTGTTC and reverse primer containing an *Asp718 I* site: CTCTGGTACCCTACTAGCAGCAGCCACTGTTTGC) and was cloned into the same vector as described above. To make Rab11-2, the amino half of Rab11 was amplified and fused to the carboxy half of Rab2 at a common *Spe I* site near the middle of the two proteins. A reciprocal strategy was used to make Rab2-11. For Rab2-11, PCR fragments from the first 270bp of the Rab2 coding region (forward primer: CTCTCTCGAGATGTGGTACGCGTACTTGTTC; reverse primer: CTCTCACTAGTAAGGCGCCAGCAGCTCCGCGGTA) were combined with PCR fragment from the second 390bp of the Rab11 coding region (forward primer: CTCTCTACTAGTCTATGACATTGCCAAGCAT; reverse primer: CTCTGGTACCTCATCACTGACAGCACTGTTTGCG). For Rab11-2, PCR fragments used were the first 300bp of the Rab11 coding region (forward primer: GGATCAGCCGCCCTCGAGATGGGT; reverse primer: CTCTGACTAGTAGGGCCCCCACGGCACCGCGGTA) and 410bp of the second half of the Rab2 coding region (forward primer:

CTCTTTACTAGTGTACGACATCACGCGACGG; reverse primer: CTCTGGTACCCTACTAGCAGCAGCCACTGTTTGC).

High resolution Rab11-Rab2 chimera proteins (GST-Rab11M1, GST-Rab11M2, …, GST-Rab11M11): Different high resolution Rab11-Rab2 chimeric proteins (as described in Xu et al., unpublished data) were cloned into the same pGEX(B)XA vector individually for purification of GST-Rab11Ms. Each such protein contained 6-10 Rab2 amino acids within the context of an otherwise intact Rab11 backbone.

His-dRip11 and His-dRip11Ala: For generation of His-dRip11 protein, GM01994 (BDGP GM_pBS library) was used. It encodes the 314 amino acid carboxyl end of dRip11 including Rab11 binding domain (RBD) (Fig. 3.1). The dRip11 fragment was cloned into pET-14b. For dRip11Ala mutant, 8 amino acids in RBD were substituted by Alanine residues using PCR.

Protein purification, pull-down assay and western blot

For protein purification, *E. Coli* BL21(DE3) cells expressing either pGEX(B)XARab for GST-Rab proteins or pET-14bdRip11 and pET-14bdRip11Ala for His-tag proteins were grown at 30˚C until OD600 was 0.6. I then added 0.01g/50ml IPTG to the culture and incubated it at 15˚C, with continuous shaking overnight. Cells were harvested by centrifugation and lysed in 1.5ml non-denaturing lysis buffer (NDLB) (25mM Tris PH 8.0, 100mM NaCl, 1mM β-mercaptoethanol, 0.1% Triton-100, 10% glycerol) with 0.5mg/ml lysozyme on ice for 1hr. After sonication, the cell lysates were

centrifuged (Beckman Coulter Optima TL-100 Ultracentrifuge) at 50,000g for 0.5hr at 4˚C and the supernatant was collected for further purification. For GST-tagged protein, Glutathione Sepharose 4 Fast Flow (Amersham Bioscience) beads were used and GST-tag proteins were purified according to manufacture's recommended protocol, except the final cleavage step was not performed. For His-tagged proteins, Ni-NTA His•Bind Superflow™ (Novagen) was used and manufacture's manual was followed.

For pull-down assays, 5µl of His-tag protein and 5µl of GST-tag protein with Glutathione Sepharose beads attached were incubated in 1ml NDLB for 2hr at 4˚C on a Nutator (Fisher Scientific). For a negative control, equal amounts of Glutathione Sepharose beads alone were incubated with 5µl of His-tag protein. The beads were isolated by centrifugation and washed 4 times with 0.5ml NDLB. Bead-bound proteins were resuspended in 10µl NDLB and 10µl of SDS sample buffer was added. Standard SDS-PAGE procedure was followed and proteins were transferred to nitrocellulose.

Western blot was carried out following standard protocol (Maniatis, 1982) using mouse monoclonal anti-His HRP (1:5000, abcam) and ECL plus Western Blotting Detectin System (Amersham Bioscience) according to manufacture's instructions.

Fly stocks

Fly culture and crosses were carried out according to standard procedures (Ashburner, 1989). The wild-type stock was w^{1118}. Four different P-element recessive lethal *dRip11* alleles (*PL12, PL63, PL72, PL7202*) were obtained from the Bloomington

Stock Center. Another P-element recessive lethal allele *dRip11*^{KG02485} was from Li et al. (Li et al., 2007). All dRip11 alleles were balanced over FM7c.

Construction of transgenic flies expressing dRip11::GFP

I made two *dRip11::GFP* constructs using the RED/ET recombination system (Gene Bridges, Inc., CA). Both constructs contained the same 735bp *GFP* insert but differed in its placement within the *dRip11* ORF (Fig. 3.1); in *dRip11::nGFP*, *GFP* was inserted immediately downstream of the start codon ATG, whereas in *dRip11::cGFP*, *GFP* was inserted immediately upstream of the stop codon TAA. The resulting CaSpeR4 P element transformation vector carrying either *dRip11::nGFP* or *dRip11::cGFP* was microinjected into w^{1118} flies following standard procedures (Rubin and Spradling, 1982; Spradling and Rubin, 1982). Five independent *dRip11::nGFP* lines and two independent *dRip11::cGFP* lines were established, each with a single copy of the transgene. All transgenic lines were viable and maintained as homozygous stocks.

Immunocytochemistry and confocal microscopy

Ovaries were fixed and immunostained as previously described (Bogard et al., 2007; Dollar et al., 2002). Primary antibodies were used at the following concentration: rat anti-Rab11 (1:500) (Dollar et al., 2002); rabbit anti-GFP (1:250; Invitrogen); rat anti-dRip11 (1:1000; unpublished data); mouse anti-FasIII (1:50; Hybridoma bank); mouse anti-Hts (1B1) (1:10; Hybridoma bank). Secondary antibodies were purchased from The Jackson Laboratoty and used at the manufacturer's recommended concentrations. Stained

ovaries were mounted in 4% n-propyl gallate (Sigma) in 90% glycerol, 10% PBS (phosphate buffered saline). Images were collected on Olympus 3L Spinning disc or Zeiss Meta 510 laser scanning confocal microscopes.

RESULTS

dRip11 is a Rab11 binding partner

Yeast two-hybrid assays identified dRip11 as the only binding partner of *Drosophila* Rab11. To confirm the binding between *Drosophila* dRip11 and Rab11, I carried out *in vitro* binding using a GST pull-down assay with full-length Rab11 (50kDa) and His-tagged dRip11 protein (40kDa) containing the putative Rab11 binding domain (RBD) (Fig. 3.1). As shown in Figure 3.2A, His-dRip11 binds to GST-Rab11. To confirm that the putative RBD is responsible for the binding, I used a dRip11 mutant with altered RBD in the binding assay (see Methods). This mutant protein failed to bind to GST-Rab11 in vitro (data not shown). I conclude that *Drosophila* dRip11 binds to Rab11 via its C-terminal RBD. I also tested the binding between dRip11 and Rab11 with or without GTPγ-NH-P (10^{-6}M) because theoretically dRip11 binds to active GTP-bound form of Rab11 instead of inactive GDP-bound form. The presence of GTPγ-NH-P, however, did not make any difference in the binding. Whether this is because Rab11 does not need to be in the GTP-bound form to bind dRip11 or because purified GST-Rab11 is pre-bound to GTP is not clear from my studies.

Rab11 amino acid 38-42 is responsible for dRip11 binding

To determine which part of Rab11 binds to dRip11, I initially made two Rab11-Rab2 chimera proteins. The overall 3-D fold of Rab2 is virtually identical to Rab11. However, they localize to different compartments within a cell and share no common effector molecules. As expected, His-dRip11 does not bind to Rab2 (Fig. 3.2B). The two Rab11-Rab2 chimera proteins I made are Rab11-2 with the N-terminal half of Rab11 fused with C-terminal half of Rab2, and Rab2-11, with the N-terminal half of Rab2 fused with the C-terminal half of Rab11. When I made the chimera proteins, I chose the region in the middle of the protein that is the same in both Rab11 and Rab2 so that both chimera proteins can fold properly. As shown from the binding assay, dRip11 binds to Rab11-2, but not Rab2-11 (Fig. 3.2B). I conclude from these data that the N-terminal half of Rab11 (amino acid 1-100) is responsible for its binding to dRip11.

To map more precisely the dRip11 binding domain of Rab11, I tested 11 additional Rab11-Rab2 chimeric proteins for binding to dRip11. Each chimeric protein had a full-length Rab11 backbone, and a 6-10 amino acid stretch composed of Rab2 sequences (Fig. 3.2D and data not shown). Only one Rab11-2 chimera (Rab11 M1), with amino acid substitutions from 38-42, failed to bind dRip11 (Fig. 3.2C and data not shown). I conclude, amino acid 38-42 in Rab11 is responsible for the binding between Rab11 and dRip11.

dRip11::GFP transgenes rescue lethality of dRip11 alleles

To better characterize the function of dRip11, we made two dRip11::GFP transgene constructs using dRip11 genomic fragment containing the endogenous dRip11 promotor, one with GFP at the N-terminus of dRip11 and the other with GFP at the C-terminus (Fig. 3.1). We recovered several lines of each transgene with stable, single copy insertions. All the transgenes are fully functional, as they rescued all five dRip11 lethal alleles.

dRip11 expressions in spectrosome/fusome and border cells

Next we examined the expression patterns of dRip11 during *Drosophila* oogenesis. We use a rat anti-dRip11 antibody to determine the expression patterns of endogenous dRip11 in wild-type oocytes, or rabbit anti-GFP to examine the dRip11::GFP expression in dRip11::GFP transgenic flies. Both antibodies showed that dRip11 is expressed strongly in the germarium and in border cells.

In the germarium, dRip11 is expressed abundantly in the spectrosome and in the fusome (Fig. 3.3D, red; Fig. 3.3E, green), which were identified by co-staining with antibodies against Hu-li tai shao (hts) (Fig. 3.3G) (Petrella et al., 2007; Yue and Spradling, 1992). Rab11 is also expressed in the spectrosome/fusome (Fig. 3.3B, F) and has overlapping expression with dRip11 (Fig. 3.3C, H).

In stage 9 and older egg chambers, dRip11 is expressed in the border cells (Fig. 3.4, 3.5). Rab11 again have overlapping expression with dRip11 in border cells (Fig. 3.5).

DISCUSSION

In this study, I confirmed the in vitro binding between *Drosophila* dRip11 and Rab11, which was shown in vertebrate systems (Prekeris et al., 2000) and in our previous yeast two-hybrid screens (University of Wisconsin Molecular Interaction Facility, Madison, WI). In addition, I mapped the domain in Rab11 that is responsible for such binding. I also investigated the expression pattern of dRip11 and found that dRip11 and Rab11 have overlapping expression pattern in germarium and in border cells.

Given the extensive role of Rab11 in membrane trafficking, and the fact that Rabs work with effector molecules in each of its trafficking steps, identifying Rab11's binding partner is the first step in finding those effectors and is important in elucidating its detailed function in membrane trafficking. While there are examples of effectors that bind to GDP-bound form of Rab, almost all the effector molecules prefer the GTP-bound form (Shirane and Nakayama, 2006; Stenmark, 2009). There are two regions in Rab11 called switch 1 and switch 2 that have different conformation depending on the nucleotide binding states (GTP- or GDP-bound). In fact, Rab11 M1 that fails to bind to dRip11 has amino acid changes (see Materials and Methods) within switch 1 region. Although each Rab protein has similar switch regions, while the conformation differences within the switch regions between each Rabs confer the specificity of effector binding.

Previous studies in our lab pointed out that Rab11 functions in germline stem cell maintenance (Bogard et al., 2007) and in polar cell fate specification (Xu et al., unpublished data). The overlapping expression of dRip11 and Rab11 in the germline stem cell and in border cells suggests a role for dRip11 as a Rab11 effector in germline stem cell maintenance and in border cells.

Given the localization results presented here, there was a strong prediction that dRip11 mutants would be defective in GSC maintenance and/or in border cell migration. However, examination of dRip11 mutants revealed no such defects. We interpret this to mean that there might be other Rab11 effector protein(s) that act redundantly with dRip11 in those processes. Alternatively, the dRip11 alleles we tested may not be strong enough. In order to get a null dRip11 mutant, I set out to make a deletion of the whole dRip11 gene using the FRT-FLP system (Parks et al., 2004). However, I never recovered such mutants and suspect that one or more of the FRT stocks that we used are defective; the FRT elements may, for example, be mutated in a way that severely reduces their ability to recombine with each other.

Figure 3.1 Diagram of dRip11 genomic structure and subclones used in this study. (**A**) Genomic structure of dRip11, with mRNA and protein coding regions shown as red and green boxes, respectively. (**B**) The 314 amino acid C-terminal region used in GST pull-down assay with Rab11. As described in the Text, this region contains the putative Rab11 binding domain, and binds Rab11 in vitro. (**C**) Diagram of the N- and C-terminal dRip11::GFP fusion constructs.

FIGURE 3.1

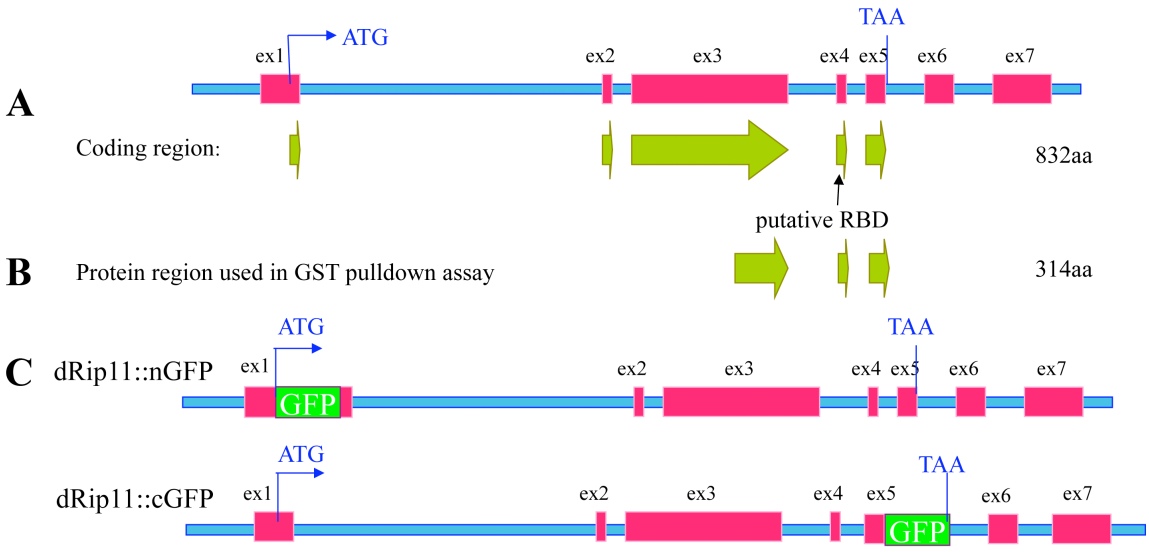
A
ATG
TAA
ex1
ex2
ex3
ex4
ex5
ex6
ex7
Coding region:
832aa
putative RBD
B
Protein region used in GST pulldown assay
314aa
C
dRip11::nGFP
ATG
TAA
GFP
dRip11::cGFP
ATG
TAA
GFP

Figure 3.2 Identification of the dRip11 binding domain in Rab11. (**A**) Western blot control experiment using anti-His antibody showing that His-dRip11 (arrow) binds (is pull-down by) Rab11 protein that is attached to beads use a GST-tag. Control lane (His-dRip11+beads) shows that His-dRip11 is not pulled down by beads alone. (**B**) Western blot experiment using anti-His antibody showing that the amino-terminal half of Rab11 mediates binding to His-dRip11. The structures of the Rab11-Rab2 fusion proteins are described in Methods and are also shown in **D**. The arrow indicates the position of the His-dRip11 protein. Higher molecular weight proteins represent a dRip11 dimer as they are eliminated when Dithiothreitol (*DTT*) is added to the binding reaction (data not shown). The stronger binding of Rab11-2 than Rab11 to dRip11 was due to the degradation of Rab11 in storage buffer, while Rab 11-2 was freshly made at the time of this particular pull down assay. (**C**) Western blot experiment using anti-His antibody showing that amino acids 38-42 of Rab11 mediate binding to His-dRip11 because Rab11 M1 with amino acids 38-42 substituted showed no binding to His-dRip11. The absent binding was not due to its absence of expression because Rab11 M1 showed same level of expression as the other mutant (M) proteins (data not shown). The structures of the different Rab11 mutant (M) proteins are described in Methods and are also show in **D**. The arrow indicates the position of the His-dRip11 protein. The lower molecular weight proteins in alternative lanes were from another binding experiment, and did not interfere with the binding between His-dRip11 and different Rab11 mutants. (**D**) Structure of the GST-Rab11 fusion proteins used in the GST pull-down experiments shown in **A**, **B**, **C**.

Figure 3.2

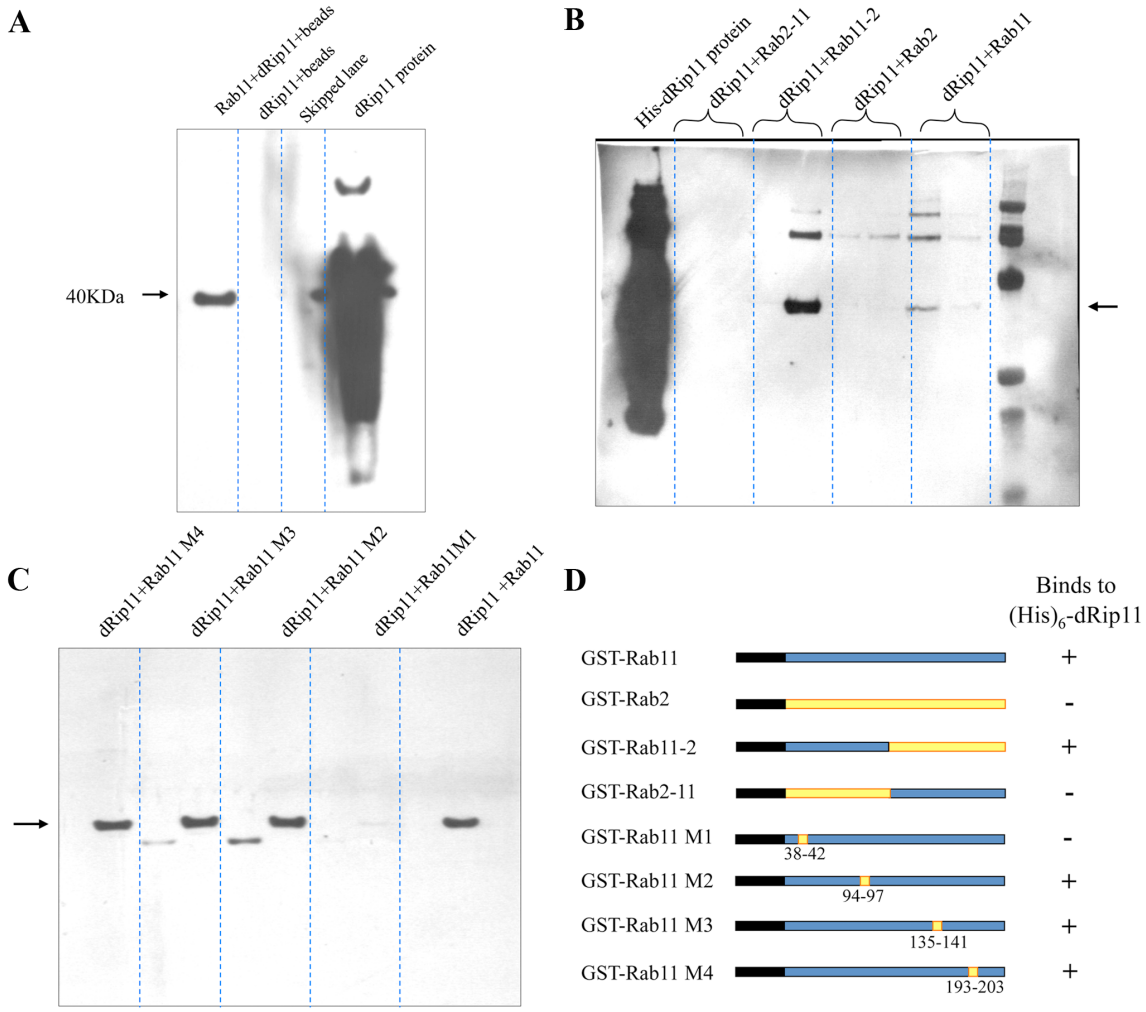
A
Rab11+dRip11+beads
dRip11+beads
Skipped lane
dRip11 protein
40KDa
B
His-dRip11 protein
dRip11+Rab2-11
dRip11+Rab11-2
dRip11+Rab2
dRip11+Rab11
C
dRip11+Rab11 M4
dRip11+Rab11 M3
dRip11+Rab11 M2
dRip11+Rab11M1
dRip11 +Rab11
D
Binds to
(His)6-dRip11
GST-Rab11
+
GST-Rab2
-
GST-Rab11-2
+
GST-Rab2-11
-
GST-Rab11 M1
-
38-42
GST-Rab11 M2
+
94-97
GST-Rab11 M3
+
135-141
GST-Rab11 M4
+
193-203

Figure 3.3 dRip11 and Rab11 both are expressed in the fusome. (**A**-**C**) wild-type germarium and young (stage 1-3) egg chambers following antibody staining for endogenous dRip11 (red, **A**) and Rab11 (green, **B**) protein. The merged image is shown in **C**. Both proteins are enriched at the anterior end of germarium and have a staining pattern consistent with expression in the fusome. (**D**) Diagram of germarium (Bogard et al. 2007). The bar beneath the diagram depicts germarial regions 1, 2a, 2b and 3. Region 3 corresponds to a stage 1 egg chamber. TF: terminal filament, CC: cap cell, ESC: escort cell, FC: follicle cell. Black: germline stem cell (GSC), red: spectrosome (in GSC)/ fusome (in cystoblast or cyst), green: oocyte, blue: ring canal. (**E**-**H**) dRip11::GFP transgenic germarium following antibody staining for GFP (green, **E**), Rab11 (blue, **F**), Hu-li tai shao (red, **G**). The merged image is shown in **H**. Hu-li tai shao staining marks the fusome (arrow head). dRip11 and Rab11 are both enriched in the fusome.

Figure 3.3

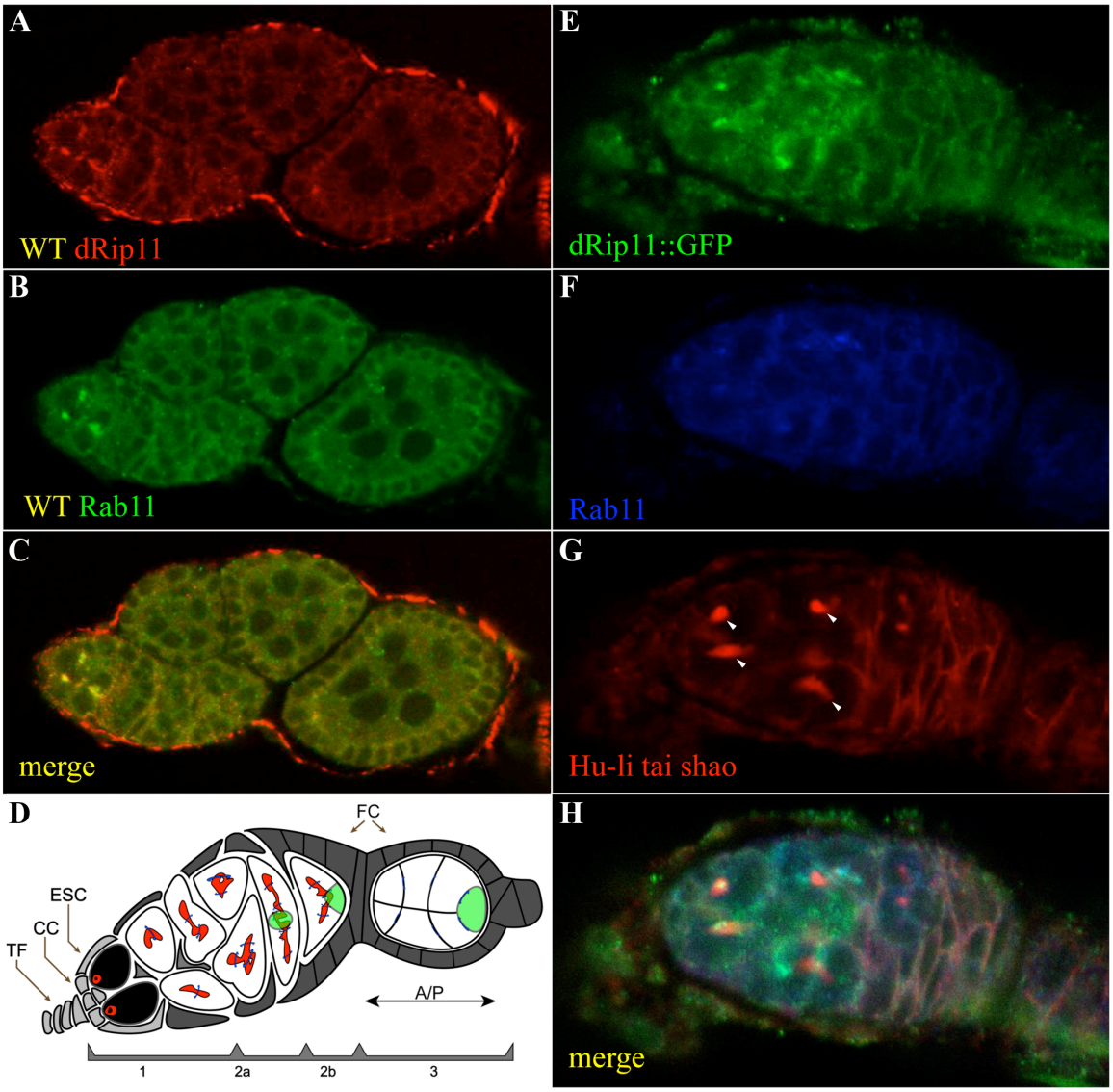
A
WT dRip11
E
dRip11::GFP
B
WT Rab11
F
Rab11
C
merge
G
Hu-li tai shao
D
FC
ESC
CC
TF
A/P
1
2a
2b
3
H
merge

Figure 3.4 Wholemount immunostaining showing strong expression of dRip11 in border cells. (**A**) Wild-type stage 10 egg chambers following antibody staining for endogenous dRip11 (green), dRip11 expresses in border cells, especially at the leading edge. (**B**, **C**) dRip11::GFP transgenic stage 10 egg chambers following antibody staining for dRip11::GFP (red). dRip11::GFP expresses in border cells in different lines of dRip11::GFP transgenic egg chambers; such expression is the same as in **A**.

O: oocyte, bc: border cell cluster, nc: nurse cells, fc: follicle cells.

Figure 3.4

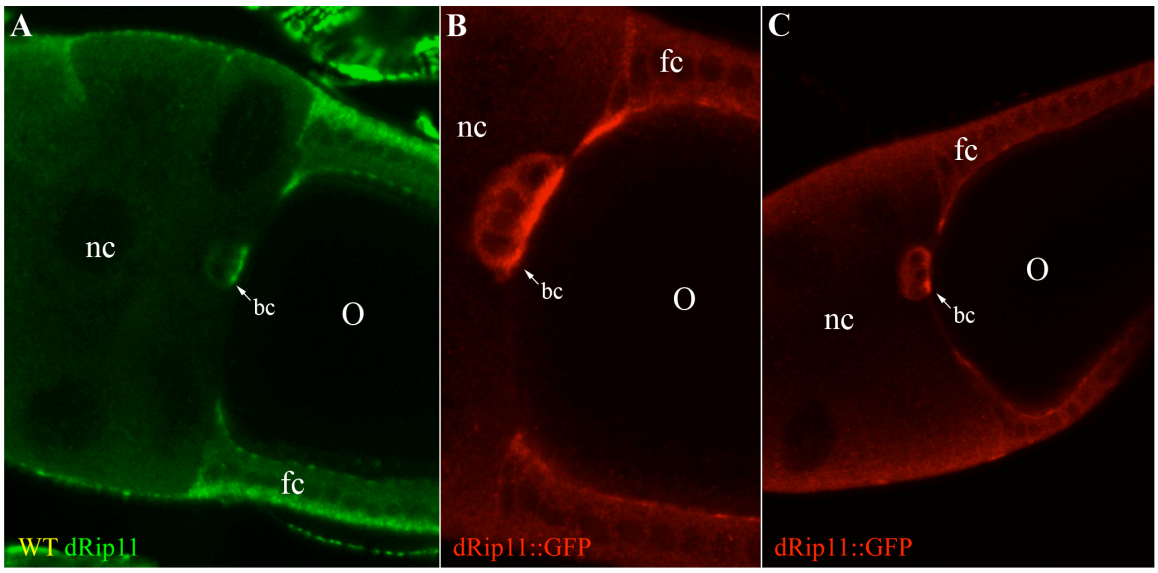
A
nc
bc
O
fc
WT dRip11
B
fc
nc
bc
O
dRip11::GFP
C
fc
O
nc
bc
dRip11::GFP

Figure 3.5 dRip11 and Rab11 colocalize during all stages of border cell migration towards the oocyte. dRip11::GFP transgenic egg chambers (stage 9-10) following antibody staining for dRip11::GFP (green, **A**, **B**, **C**), Rab11 (red, **A′**, **B′**, **C′**). The merged image is shown in **A′′**, **B′′**, **C′′**. During border cell migration, dRip11 and Rab11 colocalize before the border cells delaminated from the anterior follicle epithelium (**A**, **A′**, **A′′**), during the process of migration (**B**, **B′**, **B′′**) and when they reach the oocyte (**C**, **C′**, **C′′**). Arrowhead points to the border cell cluster.

Figure 3.5

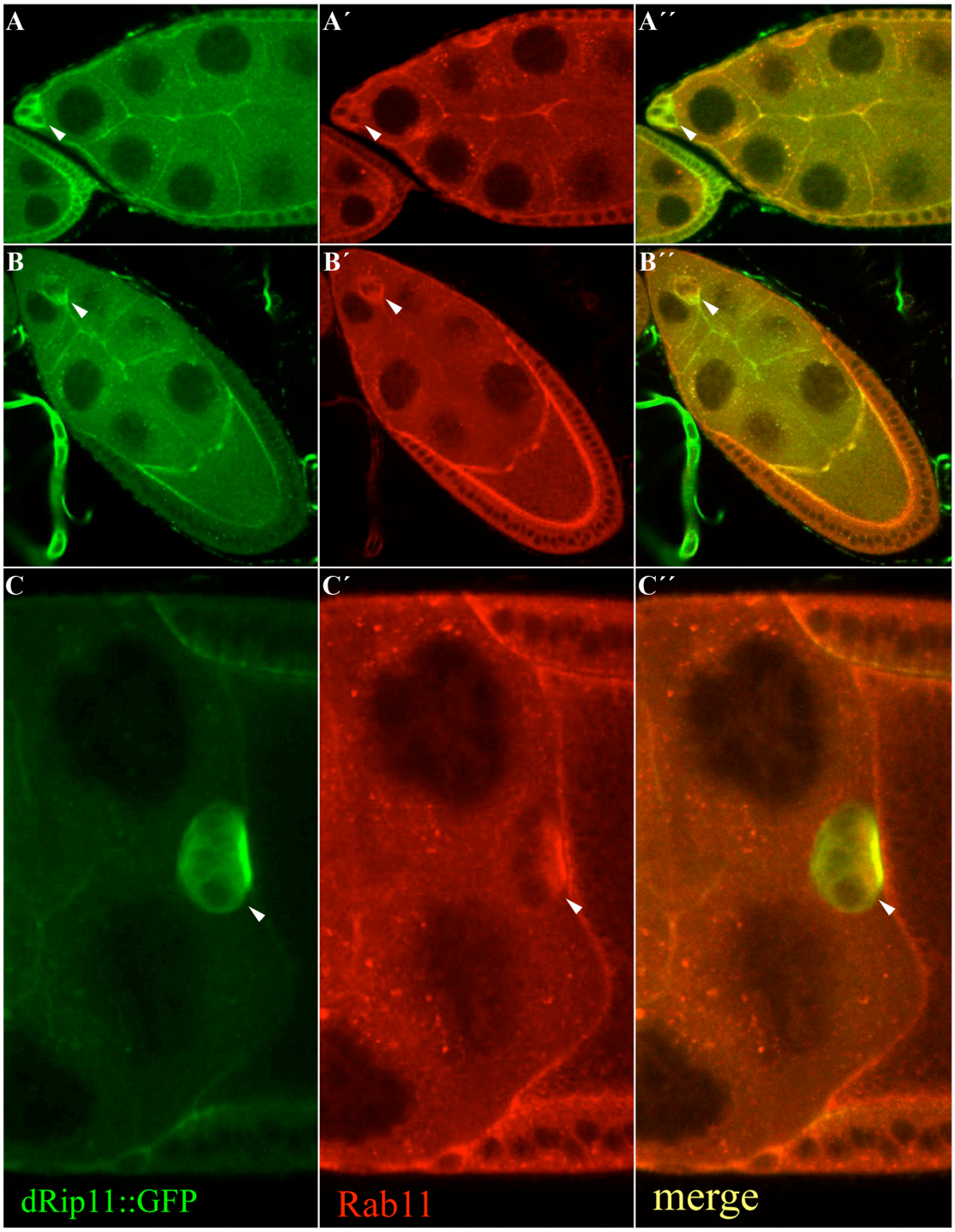

REFERENCES

1. Ashburner, M. (1989). *Drosophila* (Cold Spring Harbor, N.Y., Cold Spring Harbor Laboratory).
2. Bogard, N., Lan, L., Xu, J., and Cohen, R.S. (2007). Rab11 maintains connections between germline stem cells and niche cells in the *Drosophila* ovary. Development *134*, 3413-3418.
3. Dollar, G., Struckhoff, E., Michaud, J., and Cohen, R.S. (2002). Rab11 polarization of the *Drosophila* oocyte: a novel link between membrane trafficking, microtubule organization, and oskar mRNA localization and translation. Development *129*, 517-526.
4. Horgan, C.P., and McCaffrey, M.W. (2009). The dynamic Rab11-FIPs. Biochem Soc Trans *37*, 1032-1036.
5. Li, B.X., Satoh, A.K., and Ready, D.F. (2007). Myosin V, Rab11, and dRip11 direct apical secretion and cellular morphogenesis in developing *Drosophila* photoreceptors. J Cell Biol *177*, 659-669.
6. Maniatis, T. (1982). Molecular cloning : a laboratory manual (Cold Spring Harbor, N.Y., Cold Spring Harbor Laboratory).
7. Parks, A.L., Cook, K.R., Belvin, M., Dompe, N.A., Fawcett, R., Huppert, K., Tan, L.R., Winter, C.G., Bogart, K.P., Deal, J.E.*, et al.* (2004). Systematic generation of high-resolution deletion coverage of the *Drosophila* melanogaster genome. Nat Genet *36*, 288-292.

8. Petrella, L.N., Smith-Leiker, T., and Cooley, L. (2007). The Ovhts polyprotein is cleaved to produce fusome and ring canal proteins required for *Drosophila* oogenesis. Development *134*, 703-712.
9. Prekeris, R., Klumperman, J., and Scheller, R.H. (2000). A Rab11/Rip11 protein complex regulates apical membrane trafficking via recycling endosomes. Mol Cell *6*, 1437-1448.
10. Rubin, G.M., and Spradling, A.C. (1982). Genetic transformation of *Drosophila* with transposable element vectors. Science *218*, 348-353.
11. Shirane, M., and Nakayama, K.I. (2006). Protrudin induces neurite formation by directional membrane trafficking. Science *314*, 818-821.
12. Spradling, A.C., and Rubin, G.M. (1982). Transposition of cloned P elements into *Drosophila* germ line chromosomes. Science *218*, 341-347.
13. Stenmark, H. (2009). Rab GTPases as coordinators of vesicle traffic. Nat Rev Mol Cell Biol *10*, 513-525.
14. Yue, L., and Spradling, A.C. (1992). hu-li tai shao, a gene required for ring canal formation during *Drosophila* oogenesis, encodes a homolog of adducin. Genes Dev *6*, 2443-2454.

Chapter IV

Discussion

This thesis addresses questions fundamental to how egg chambers are made: How are the different cell types that compose the egg chamber determined? How do those cells come together to form an egg chamber and communicate with each other to control egg chamber maturation and the production of egg cells that are sufficiently patterned so as to be able to specify the major body axes of the future embryo?

In Chapter 2, I contribute to our understanding of oocyte patterning through investigating the cis-acting RNA sequence elements that control the transport and anterodorsal (AD) localization of *gurken* mRNA. In contrast to previous injection-based assay systems (Van De Bor et al., 2005), my studies utilized a transgenic assay system and allowed me to definitively address the question of whether the GLS is needed for *gurken* gene function as well as to provide accurate information regarding the mechanism of GLS function. My studies show first that the GLS is essential for *gurken* gene function. My studies also show that the GLS is required for *gurken* RNA transport and AD localization. In contrast to the injection studies, my studies indicate that the GLS does not mediate directed transport to the oocyte's AD corner, but rather only transport to the anterior cortex. The simplest interpretation of these findings is that AD localization is brought about by repeated transport to the anterior cortex, coupled with specific trapping of *gurken* transcripts at the AD corner. Finally, my data indicate that anterior transport is mediated by the GLS, while trapping at the AD corner is mediated by other RNA localization elements (RLEs), which may or may not work in conjunction with the GLS. Several questions remain unknown regarding the mechanisms of gurken mRNA localization and are worthy of future study. These include: 1) the identity of the additional RLEs required for trapping at the AD corner; 2) the physical nature of the trap

and an understanding of how it is localized; and 3) how RNA localization is coupled to translational control and whether such coupling is dependent on the fact that the GLS, unlike the vast majority of other examined RLEs, resides in the protein coding portion of the transcript.

In Chapter 3, I contribute to the understanding of egg chamber formation by analyzing the function of the putative Rab11 effector protein, dRip1. Rab11 functions in various locations during oogenesis: in germline stem cells (GSCs) for the maintenance of GSC identity, in somatic stem cells for the differentiation of epithelial cells and the specification of the polar cell fate, and in the oocyte for the organization of the posterior compartment and *oskar* mRNA localization. My studies show that dRip11 binds Rab11 in vitro. I also show that dRip11 colocalizes with Rab11 in GSCs and in border cells, suggesting a role for dRip11 as a Rab11 effector in GSC maintenance and in border cell migration. However, dRip11 mutants revealed no defects in GSC maintenance and in border cell migration. This could due to the redundancy in Rab11's effectors function in those processes and/or the weakness of dRip11 alleles. Unfortunately, my effort in making a completely null dRip11 mutant was not successful. I suspect that one or more of the FRT stocks that we used are defective. Several questions remain unanswered regarding the function of Rab11 effectors and are worthy of investigations. These include: 1) what roles does dRip11 play in oogenesis, whether it functions in GSC maintenance and/or border cell migration, or other processes; 2) what are the other effectors that work with Rab11 in various oogenesis stages, and how do they work together in each of the processes. A candidate effector of Rab11 in epithelial cell differentiation and polar cell specification is nuclear fallout (nuf), as it shows strong

expression in somatic stem cells, follicle cell precursors and is colocalized with Rab11 in those cells.

REFERENCES

1. Van De Bor, V., Hartswood, E., Jones, C., Finnegan, D., and Davis, I. (2005). gurken and the I factor retrotransposon RNAs share common localization signals and machinery. Dev Cell *9*, 51-62.

APPENDIX

Chapter V

Rab11 maintains connections between germline stem cells and niche cells in the *Drosophila* ovary

SUMMARY

All stem cells have the ability to balance their production of self-renewing and differentiating daughter cells. The germline stem cells (GSCs) of the *Drosophila* ovary maintain this balance through physical attachment to anterior niche cap cells and stereotypic cell division, whereby only one daughter remains attached to the niche. GSCs are attached to cap cells via adherens junctions, which also appear to orient GSC division through capture of the fusome, a germline-specific organizer of mitotic spindles. Here we show that the Rab11 GTPase is required in the ovary to maintain GSC-cap cell junctions and to anchor the fusome to the GSC's anterior cortex. Thus *rab11*-null GSCs detach from niche cap cells, contain displaced fusomes, and undergo abnormal cell division, leading to an early arrest of GSC differentiation. Such defects likely reflect a role for Rab11 in E-cadherin trafficking as E-cadherin accumulates in Rab11-positive recycling endosomes (REs) and E-cadherin and Armadillo/β-catenin are both found in reduced amounts on the surface of *rab11*-null GSCs. The Rab11-positive REs through which E-cadherin transits are tightly associated with the fusome. We propose that such association polarizes Rab11's trafficking of E-cadherin and other cargoes toward the GSC's anterior cortex, thus simultaneously fortifying GSC-niche junctions, fusome localization, and asymmetric cell division. These studies bring to focus the important role of membrane trafficking in stem cell biology.

INTRODUCTION

Drosophila oogenesis is an excellent system in which to study stem cell maintenance and differentiation because all of the steps unfold in well-defined compartments. The initial steps occur within the germarium, which is divided along its anterior-posterior axis into 3 morphologically distinct regions (Fig. 5.1A). Two to three germline stem cells (GSCs) are attached by adherens junctions to niche cap cells at the extreme anterior end of germarial region 1 (Song et al., 2002; Kirilly and Xie, 2007). The cap cells and other neighboring niche cells continuously secrete Dpp and Gbb, short-range TGF-β-like signaling molecules that maintain GSC identity through repression of *bam* transcription (Xie and Spradling, 1998; Xie and Spradling, 2000; Song et al., 2004). Each GSC divides along its anterior-posterior axis to produce another GSC, which remains attached to the cap cells, and a posterior cystoblast, which is displaced from the niche and free to differentiate. The axis of GSC division is determined by the membrane- and spectrin-rich fusome, which anchors one pole of the mitotic spindle to the GSC's anterior cortex (McGrail and Hays, 1997; Deng and Lin, 1997; de Cuevas et al., 1998). A small amount of fusome is donated to the cystoblast where it guides four stereotypic rounds of incomplete cell division, resulting in a germline cyst of 16 cells interconnected by cytoplasmic bridges, called ring canals (Huynh and St Johnston, 2004). In germarial region 2A, Orb, BicD and other cell fate determinants become enriched in the cell with the most fusome material, committing it to differentiate as the oocyte, while each of the other 15 cells adopts a nurse cell fate (Huynh and St Johnston, 2004). The oocyte is positioned at the posterior end of the germline cyst in region 2B through E-cadherin-mediated adhesion to neighboring somatic follicle cells (Gonzales-Reyes and St

Johnston, 1998; Godt and Tepass, 1998). Finally, in germarial region 3, the germline cyst is encased in an epithelium of somatic follicle cells to give the stage 1 egg chamber, the basic unit of all subsequent steps of oogenesis (Huynh and St Johnston, 2004).

RESULTS AND DISCUSSION

Rab11 associates with the fusomes of GSCs and developing germline cysts

Our first clue that Rab11 plays important roles in early oogenesis came from immunostain experiments which revealed strong expression of endogenous Rab11 and a fully functional Rab11::GFP in GSCs, cystoblasts, and young (2- 4- and 8-cell) germline cysts (Fig. 5.1). Strikingly, the proteins were concentrated as discrete dots on the fusome (Fig. 5.1E-L), which electron microscope and photobleaching studies have shown is highly vesicular and rapidly exchanged with other membrane stores (Mahowald, 1972; Snapp et al., 2004). Triple stain experiments showed that some of these dots also contained E-cadherin (Fig. 5.1B-E), which has been shown to transit though Rab11-positive recycling endosomes (REs) en route to the plasma membrane in some cells (Lock and Stow, 2005; Langevin et al., 2005). High magnifications images showed that the Rab11 (and more rarely E-cadherin) dots were often nestled into cavities within the fusome (Fig. 5.1D-E). Such Rab11-harboring cavities were visible in the fusomes of all examined GSCs, cystoblasts, and young germline cysts, not only in the ovary but also in the testes (Fig. 5.1; data not shown). In view of Rab11's well-described enrichment in recycling endosomes (REs) (Dollar et al., 2002; Emery et al., 2005; Lock and Stow, 2005; Riggs et al., 2003; Zhang et al., 2004), we propose that these Rab11- and E-

cadherin-harboring cavities are REs and will hereafter refer to them as FREs (fusome-associated recycling endosomes).

Rab11 is required for maintenance of GSC identity

Previous studies of hypomorphic *rab11* alleles revealed a role for the gene in polarizing the mid-stage oocyte's anterior-posterior axis (Dollar et al., 2002; Jankovics et al., 2001). To investigate the role of Rab11 during early oogenesis, we set out to examine a *rab11* null allele. The one null allele available at the start of these studies proved to be tightly linked to a second site cell lethal mutation, so we made a new one using the FRT-flipase method (Parks et al., 2004). This new allele, called $rab11^{\Delta FRT}$, deletes the *rab11* promoter and the first two exons of the gene, and produces no detectable protein (Fig. 5.1I).

Because $rab11^{\Delta FRT}$ is homozygous lethal, we used the FRT-FLP system (Xu and Rubin, 1993) to generate homozygous *rab11-null* clones that were marked by loss of nuclear GFP. Consistent with a role for Rab11 in the maintenance of GSCs, we recovered a disproportionately small number of *rab11-null* GSCs compared to *rab11-null* germline cysts. To determine the half-life of *rab11*-null GSCs, we calculated the percentage of *rab11-null* GSCs to total GSCs as a function of days after clone induction (ACI). As a control, we made identical calculations for marked clones carrying the wild-type *rab11* allele. Such studies revealed a half-life of 4.0 days for r*ab11-null* GSCs, or ~4-fold less than wild-type (Table 1). We also made clones with the $rab11^{2148}$ hypomorphic allele and calculated a near wild-type half-life of 15.9 days (Table 1). This was the expected result as this allele, which contains a P element insertion in the first

intron, produces apparently normal amounts of Rab11 protein during early oogenesis (Dollar et al., 2002). We conclude from these data that *rab11* is required to maintain GSC identity.

Consistent with previous findings that lost GSCs can be replaced (Kai and Spradling, 2003: Kai and Spradling, 2004), many of the germaria that had lost a *rab11-null* GSC contained a full complement (2 or 3) of wild-type GSCs. One apparent replacement event is shown in Fig. 5.2A-B, where a wild-type GSC is dividing along an axis parallel to the niche and just anterior to a displaced *rab11-null* GSC.

Rab11 GSCs exhibit E-cadherin trafficking defects and have misplaced fusomes

To determine whether the observed defects in GSC maintenance reflect a requirement for Rab11 in E-cadherin trafficking, we compared the distribution of E-cadherin in wild-type and *rab11-null* GSCs. In contrast to wild-type GSCs (Figs. 5.2C-D, white arrows), we found little or no E-cadherin along the anterior surface (i.e., at the GSC-cap cell interface) of *rab11-null* GSCs (n=9) 8-10 days ACI (Fig. 5.2D, yellow arrow). Similar analyses of germaria 2.2 days ACI revealed reduced or no accumulation of E-cadherin along the anterior cortex of 16 of 22 examined *rab11-null* GSCs (Fig. 5.2E). Consistent with the idea that such reductions reflect a loss of adherens junctions, we saw similar strong reductions of Armadillo/β-catenin (data not shown). Concomitant with its reduction along the GSC's anterior surface, increased amounts of E-cadherin (seen as discrete dots) were detected on the fusomes/FREs of *rab11-null* GSCs (Fig. 5.2E, yellow arrow). Thus while wild-type GSCs contained an average of 0.16 dots of E-cadherin per fusome (n=31), *rab11-null* GSCs contained an average of 1.6 dots/fusome

(n=17) (Table 1). We conclude that *rab11* is required for the maintenance of adherens junctions between cap cells and GSCs and propose that such maintenance involves the trafficking of intracellular E-cadherin, and possibly other cargoes, from the FRE to the GSC's anterior surface.

Although the simplest interpretation of the above data is that Rab11 maintains GSC identity through E-cadherin trafficking, we cannot rule out the possibility that the primary role of Rab11 is that of recycling Dpp or other signals required for GSC maintenance and that the observed defects in E-cadherin trafficking are a secondary effect of insufficient signaling. To test this idea, we immunostained mosaic germaria for Bam, whose expression is negatively regulated by Dpp (Xie and Spradling, 1998; Xie and Spradling, 2000; Song et al., 2004). Such studies revealed a normal pattern of Bam expression; Bam was not detected in *rab11-null* GSCs or cystoblasts, but was detected in young (2- to 8-cell) germline cysts (Fig. 5.2G). These data argue strongly against the idea that the primary role of *rab11* is that of facilitating Dpp signaling, in which case *rab11-null* GSCs would be expected to move out of the niche only after they have activated Bam. We conclude from these findings that Rab11 does not affect GSC maintenance or E-cadherin trafficking through regulation of Dpp or other signals that maintain GSC identity via Bam repression.

The *rab11-null* clones also revealed a role for Rab11 in the sub-cellular localization and behavior of the fusome. In wild-type GSCs (Fig. 5.2F, white arrowhead), the fusome is anchored to the anterior cortex and spreads out along the mitotic spindle such that ~1/3 of it extends into, and is ultimately donated to, the cystoblast (Deng and Lin, 1997). In contrast, the fusome of *rab11-null* GSCs (Fig. 5.2F,

yellow arrow) was not anchored to the anterior cortex and, while it spread out along the mitotic spindle during cell division, it was often splayed and generally much less organized. We suspect such splaying results from the detachment of the fusome from the cell cortex, but cannot rule out a more direct role for Rab11 in fusome segregation. Although it is not known how the fusome is attached to the GSC's anterior cortex, it is likely to involve association with intracellular domains of the adherens junctions (Song et al., 2002). If so, Rab11, the fusome/FRE, and the adherens junctions may comprise a tripartite feedback loop whereby each reinforces the subcellular localization/behavior of the other. Specifically, we propose that the association of Rab11 with the fusome/FRE polarizes Rab11's trafficking of E-cadherin toward the GSC-cap cell interface, in turn reinforcing GSC-cap cell junctions, fusome localization, and asymmetric cell division.

Rab11 germline cysts arrest development early and exhibit defects in fusome segregation, oocyte positioning, and bulk membrane trafficking

All *rab11-null* germline cysts arrested development by stage 6 and were of two phenotypic classes. The rarer (~10%), more severely affected class arrested development in region 1 of the germarium, often contained less than 16 cells, and had little or no fusome (Fig. 5.3A-B, D, yellow outlines). Given the splayed fusome phenotype of dividing *rab11-null* GSCs described above, we speculate that this early arrest reflects a role for Rab11 in faithful segregation of the fusome to daughter cystoblasts. Consistent with this idea, mutations in *α-spectrin* and *hu-li tai shao*, which encode components of the fusome, cause a similar early arrest of cyst development (Lin et al., 1994; de Cuevas et al., 1996).

The less affected class of *rab11-null* germline cysts elaborated a normal fusome (Fig. 5.3A, white dashes), but contained clumped ring canals (Figs. 5.3F-G) and arrested development at ~stage 6. Clumped ring canals have also been reported for *sec5, sec6* and *rab6* mutations and have been interpreted to reflect a requirement for these genes in bulk membrane trafficking to the cell surface (Murthy and Schwarz, 2003; Murthy et al., 2005; Coutelis and Ephrussi, 2007). A similar requirement for Rab11 is likely as many of the nuclei of *rab11-null* germline cysts were clumped together or otherwise poorly spaced (not shown). These cysts also exhibited defects in oocyte positioning. Thus while the oocyte is positioned at the posterior end of wild-type germline cysts in germarial region 2B (Fig. 5.3E, white arrowhead), the oocytes of *rab11-null* germline cysts were often in the center (Fig. 5.3E', yellow arrow). Previous studies (Godt and Tepass, 1998; Gonzales-Reyes and St Johnston, 1998) have shown that oocyte positioning is dependent on enriched accumulation of E-cadherin along the oocyte's posterior surface. Consistent with a role for Rab11 in such enrichment, we observed reduced accumulation of E-cadherin along the posterior surface of *rab11*-null oocytes (Fig. 5.3D, yellow arrow) compared to wild-type oocytes (Figs. 5.3C-D, white arrowheads) in region 2B and 3 germline cysts. Nevertheless it is difficult to know whether the observed defects in oocyte positioning in the *rab11-null* germline cysts reflects a role for Rab11 in E-cadherin trafficking, bulk membrane trafficking, or both.

CONCLUSION

Our studies indicate that Rab11 maintains GSC identity through polarized trafficking of E-cadherin and, possibly, other cargoes that reinforce essential GSC-niche

contacts. Our studies further indicate that Rab11 is required for fusome localization and asymmetric GSC division and suggest a feedback linkage between these events and E-cadherin trafficking. While Rab11 has been implicated in the trafficking of E-cadherin in other cells, we know of no other cases where such trafficking has been correlated with a biological response. It will be of interest to determine whether Rab11 is required for the maintenance of stem cells in other systems and whether such maintenance involves E-cadherin trafficking or the trafficking of other adhesion molecules. It will also be of interest to determine the role of Rab11 in other E-cadherin-dependent cell behaviors, particularly since Rab11, at least in *Drosophila*, is expressed in only a small subset of E-cadherin-expressing cells (Xu and Cohen, unpublished).

EXPERIMENTAL PROCEDURES

Drosophila genetics

Fly culture and crosses were carried out according to standard procedures (Ashburner, 1989). The wild-type stock was *w*, or *w histone2::GFP* (Morin et al., 2001). The *rab11* deletion ($rab11^{\Delta FRT}$) was made by inducing recombination (Parks et al., 2004) between the FRT insertions (FRT5377 and FRT1994, respectively) of stocks f05377 and d01994 (Harvard Medical School Exelixis collection). The resulting deletion, which removes the Rab11 promoter and first two exons was initially identified by non-complementation with $rab11^{2148}$ (Dollar et al., 2002) and subsequently confirmed by PCR. The $rab11^{\Delta FRT}$ allele complements a lethal allele of *rtet*, which lies just upstream of *rab11* and close to the FRT insertion of f05377, and produced no protein (Fig. 5.1I). Homozygous mutant clones were generated by crossing *w; rab11-null*/*FRT5377,*

Hrb98::GFP or *w; rab11+/FRT5377, Hrb98::GFP* controls to *y w hsp::FLP*. The *FRT5377, Hrb98::GFP* chromosome was made by recombining the *Hrb98::GFP* transgene from line ZCL058 (Morin et al., 2001; Kelso et al., 2004) onto the FRT5377-containing chromosome and verified by PCR. For most experiments, clones were induced in 2- to 5-day old adults by heat-shocking for 1 hour at 37^{o}C on 2 consecutive days and examined 8 or more days ACI, thus ensuring that all examined *rab11-null* cells were derived from mutant GSCs; germline cysts normally clear the germarium within ~6 days (Song et al., 2002; Xie and Spradling, 1998). For half-life determination, a single large group of 2- to 3-day old adults were heat-shocked twice, 8 hours apart, at 37°C for 1 hour and the number of mutant GSCs and germline cysts were counted 4, 8 or 12 days ACI. Homozygous *rab11-null* and *rab11+* control clones were identified by their lack of GFP staining. The fully functional *Rab11::GFP* transgene is identical to that described in Dollar et al (2002), except for the omission of the N-terminal His-tag.

Immunocytochemistry and confocal microscopy

Ovaries were fixed and immunostained as previously described (Dollar et al., 2002), except EM-grade formaldehyde was substituted for paraformaldehyde in the fixative. Primary antibodies were used at the following concentrations: Rat anti-Rab11 (1:500) (Dollar et al., 2002); Rabbit anti-Rab11 (1:250) (Satoh et al., 2004); E-cadherin (1:40; Hybridoma bank); GFP (1:250; Invitrogen); α-spectrin (1:10; Hybridoma Bank); Hts/1b1 (1:4; Hybridoma Bank); Orb (6H4) (1:20; Hybridoma Bank); Vasa (1:5000) (Williamson and Lehman); HtsRC (1:4; Hybridoma Bank); BamC (1:500;) (McKearin and Ohlstein, 1995). Secondary antibodies were purchased from Jackson labs and used at

the manufacturer's recommended concentrations. Stained ovaries were mounted in 4% n-propyl gallate (Sigma) in 90%glycerol, 10% phosphate buffered saline. Images were collected on an Olympus 3L Spinning disc or Zeiss Meta 510 laser scanning confocal microscopes.

ACKNOWLEDGEMENTS

We thank Sui Zhang for excellent technical assistance and Cristin Gustafson with help in the construction of the *rab11* null allele. We thank Vicki Corbin for comments on the manuscript and Don Reddy, Ting Xie, Lynn Cooley, Ruth Lehman, Hugo Bellen, the Bloomington Stock Center, and Doug Dimlich for antibodies and fly stocks. Finally, we thank David Moore for excellent help with confocal microscopy. This work was support by NIH grant R01 GM068022-01 to RSC.

Figure 5.1 Rab11 is enriched on the fusome of GSCs and germline cysts.

(**A**) Diagram of the *Drosophila* germarium. Niche terminal filament (TF), cap (CC), and escort stem (ESC) cells are shown in gray. The fusome (red) is tightly associated with the anterior cortex of germline stem cells (GSCs) (black) and extends throughout the cytoplasm of germline cysts (white). Other symbols: oocyte (green); somatic follicle cells (FC); ring canals (blue crescents). (**B**-**E**) Region 1 of a wild-type germarium immunostained for E-cadherin (green), Rab11 (red), and the fusome marker, α-spectrin (blue). Merged image (**E**). Scale bar equals 10 microns and anterior is to the left in this and all subsequent figures. A single GSC is outlined in **B**, with the break in the tracing revealing strong E-cadherin staining at the GSC-cap cell interface. The smaller dot of E-cadherin staining (arrow) superimposes with Rab11 on the fusome (arrows in **C** and **D**, respectively). (**F**-**H**) Wild-type germarial regions 1 & 2 immunostained for Rab11 (red), and α-spectrin (blue). Merged image (**G**). Strong accumulation of Rab11 is apparent on the GSC (arrowhead) and germline cyst's (arrow) fusome. (**I**-**J**) Mosaic germarium immunostained for nGFP (green), Rab11 (red) and α-spectrin (blue) showing the absence of Rab11 protein in *rab11-null* (GFP negative) cells. (**J**) Rab11 channel only. (**K**-**L**). Rab11::GFP transgenic germarial region 1 immunostained for GFP (red) and α-spectrin (blue). Arrowheads denote strong Rab11::GFP expression on the fusome.

Figure 5.1

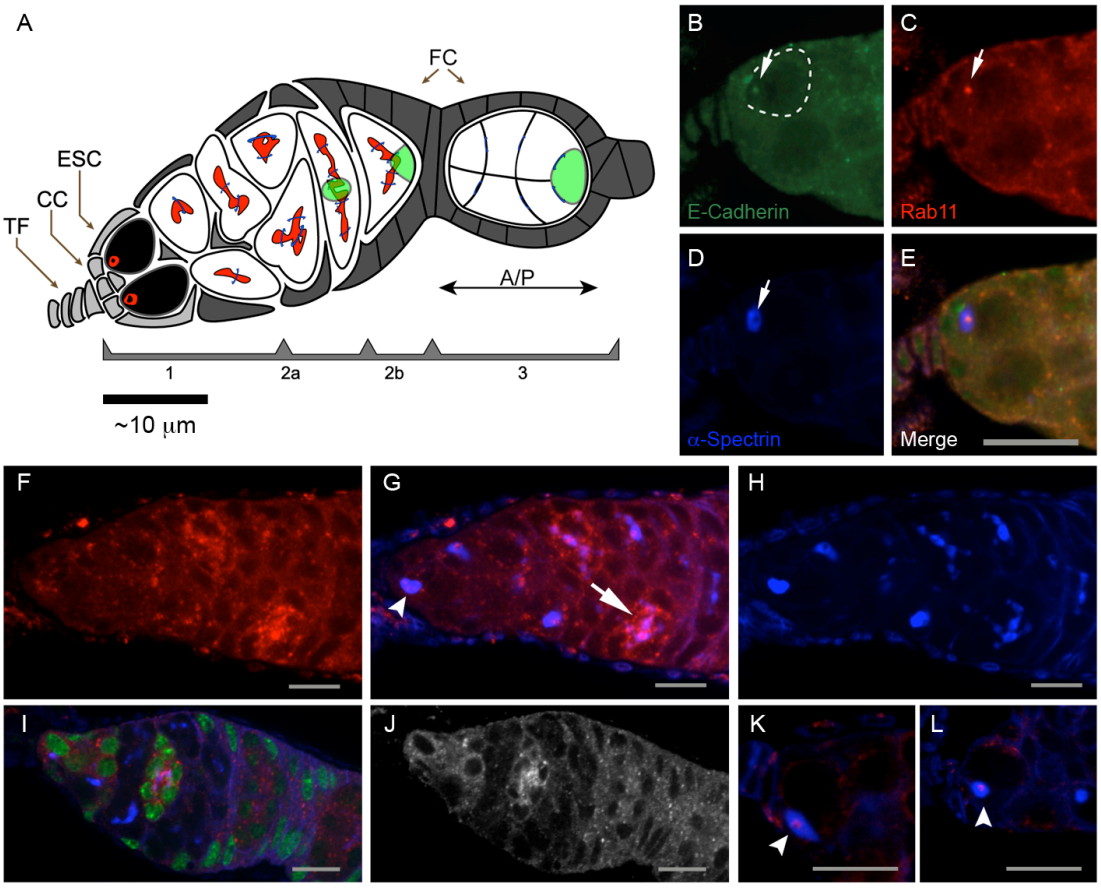
A
FC
ESC
CC
TF
A/P
1
2a
2b
3
~10 μm
B
E-Cadherin
C
Rab11
D
α-Spectrin
E
Merge
F
G
H
I
J
K
L

Figure 5.2 Rab11 is required to maintain E-cadherin at the cap cells-GSC junction and to anchor the fusome to the GSC's anterior cortex.

(**A**, **B**) Region 1 of a mosaic germarium immunostained 8 days after clone induction (ACI) for E-cadherin (red), α-spectrin (blue), and nuclear GFP (nGFP) (green) to mark *rab11-null* clones in this and all subsequent figures. (**A**) A 2-cell *rab11-null* germline cyst is outlined. This is the most anterior mutant cyst in the germarium, and thus, presumably derived from a displaced *rab11-null* GSC (see Text). A dividing wild-type GSC (boxed) is shown at the left and zoomed in (**B**), where the dashed line shows the position of the cap cells. Note that the plane of division (evident by the stretched out fusome) is orthogonal to the germarium's anterior-posterior axis such that both daughter cells remain in the niche, with one filling the vacancy created by the displaced *rab11-null* GSC. (**C**-**E**) Wild-type (**C**) and mosaic (**D**-**E**) germaria immunostained for nGFP (green), E-cadherin (red) and α-spectrin (blue) 2 days ACI. Wild-type and *rab11-null* GSC-cap cell junctions are indicated with arrowheads and arrows, respectively. Note the reduced E-cadherin staining at the three mutant junctions and the increased E-cadherin expression on the mutant fusome, especially in **E**, where three strong dots of staining are evident. (**F**) Dividing *rab11* (arrow) and wild-type (arrowhead) GSCs immunostained for α-spectrin (blue), DAPI (red), Vasa (cytoplasmic green, germline only), and nGFP (green). The DAPI-stained nuclei at the left correspond to cap cells. Note the splayed appearance of the *rab11* GSC fusome and its displacement from the anterior cortex. (**G**). Mosaic germarium immunostained for nGFP (green), α-spectrin (red) and Bam (blue) 2.2 days ACI. The *rab11-null* GSC (outlined in yellow) exhibits only background levels of Bam expression. A wild-type GSC and a 2-cell germline cyst (outlined in white) are shown for comparison.

Figure 5.2

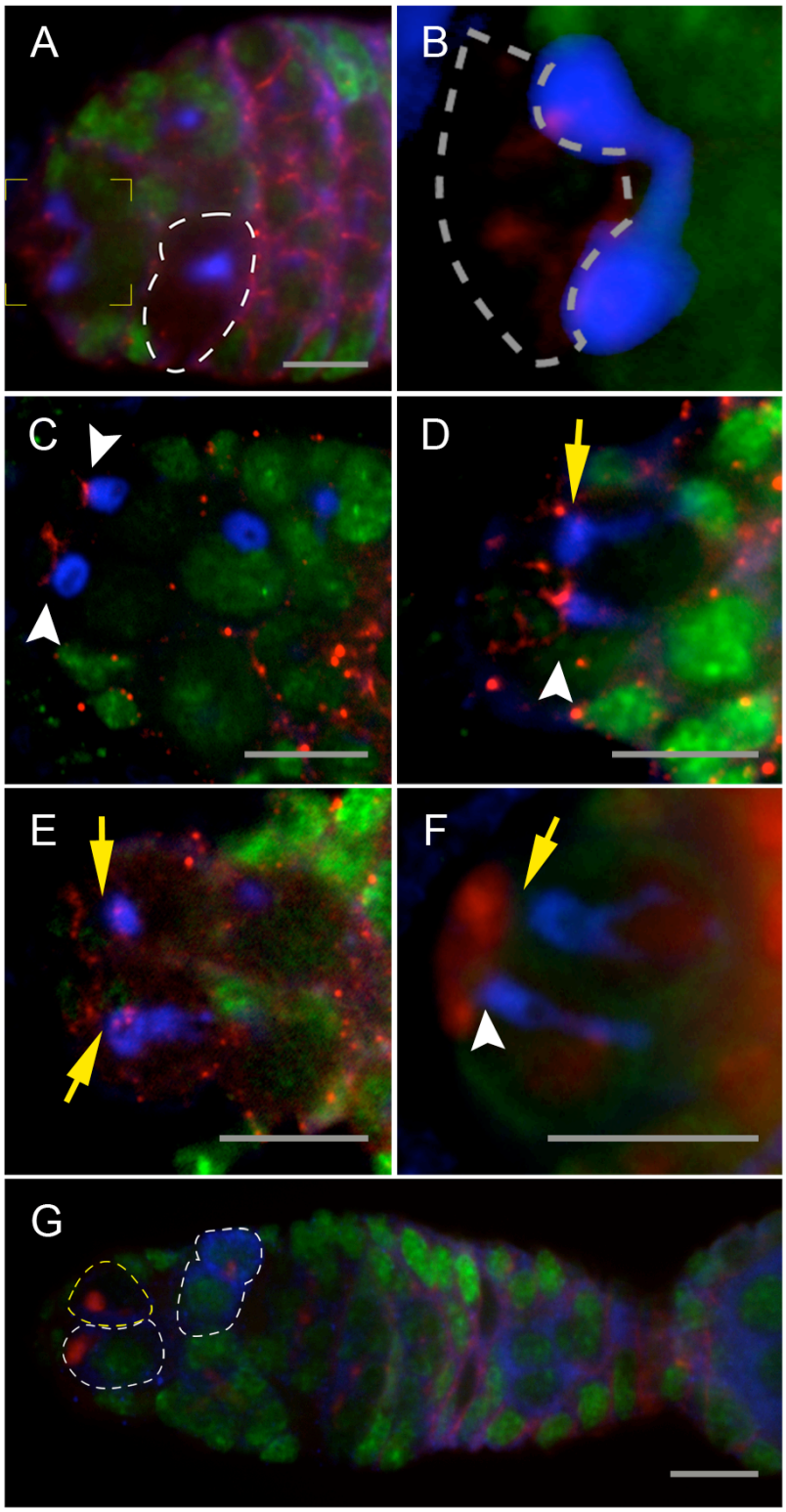

Figure 5.3 Rab11 germline cysts arrest early and display defects in fusome segregation and bulk membrane trafficking.

(**A**) Mosaic germarium immunostained for α-spectrin (red), Vasa (cytoplasmic green), and nGFP (nuclear green). A severely affected *rab11-null* germline cyst with no detectable fusome and a reduced number of germline cells is outlined in yellow. A less affected *rab11-null* germline cyst in which the fusome appears normal is outlined in white. (**B**) Mosaic germarium immunostained for E-cadherin (red), α-spectrin (blue), and nGFP (green). A 5 micron Z-stack is shown to capture all of the fusome. Two severely affected *rab11-null* germline cysts with no fusomes are outlined. A less affected *rab11-null* germline cyst is denoted with the arrow. (**C**) Wild-type germarium immunostained for E-cadherin (red) and α-spectrin (blue). The arrowheads point to the oocyte's posterior surface, where enriched accumulation of E-cadherin is evident, especially in the region 2B oocyte (left arrowhead). (**D**) Mosaic germarium immunostained for E-cadherin (red), α-spectrin (blue), and nGFP (green). The arrow points to a region 2B *rab11-null* oocyte, with greatly reduced E-cadherin accumulation (compare to left arrowhead in panel (**C**)). The arrowhead points to a wild-type region 3 oocyte, where enriched E-cadherin expression is still apparent. A severely affected, *rab11-null* germline cyst similar to those seen in (**B**) is outlined. (**E**, **E'**) Mosaic germarium immunostained for Orb (red) and nGFP (green). The bracketed area in (**E**) is shown at a different focal plane in (**E'**). Note the strong Orb expression in the wild-type region 2A and 2B oocytes (arrowheads). Strong Orb expression is also seen in the region 3 of *rab11-null* germline cyst (arrow), but it is concentrated at the center of the egg chamber, rather than at the posterior pole. (**F**, **G**) Mosaic germarium immunostained for nGFP (green) and HtsRC (red) to label ring canals. (**F**) Left arrow points to a *rab11-null* germline cyst, with clumped ring canals. The right arrow points to a mosaic germline cyst, where the ring canals are only clumped in the *rab11-null* (GFP negative) portion. (**G**) Germarium with a completely *rab11-null* germline. All ring canals are clumped in center of the cysts.

Figure 5.3

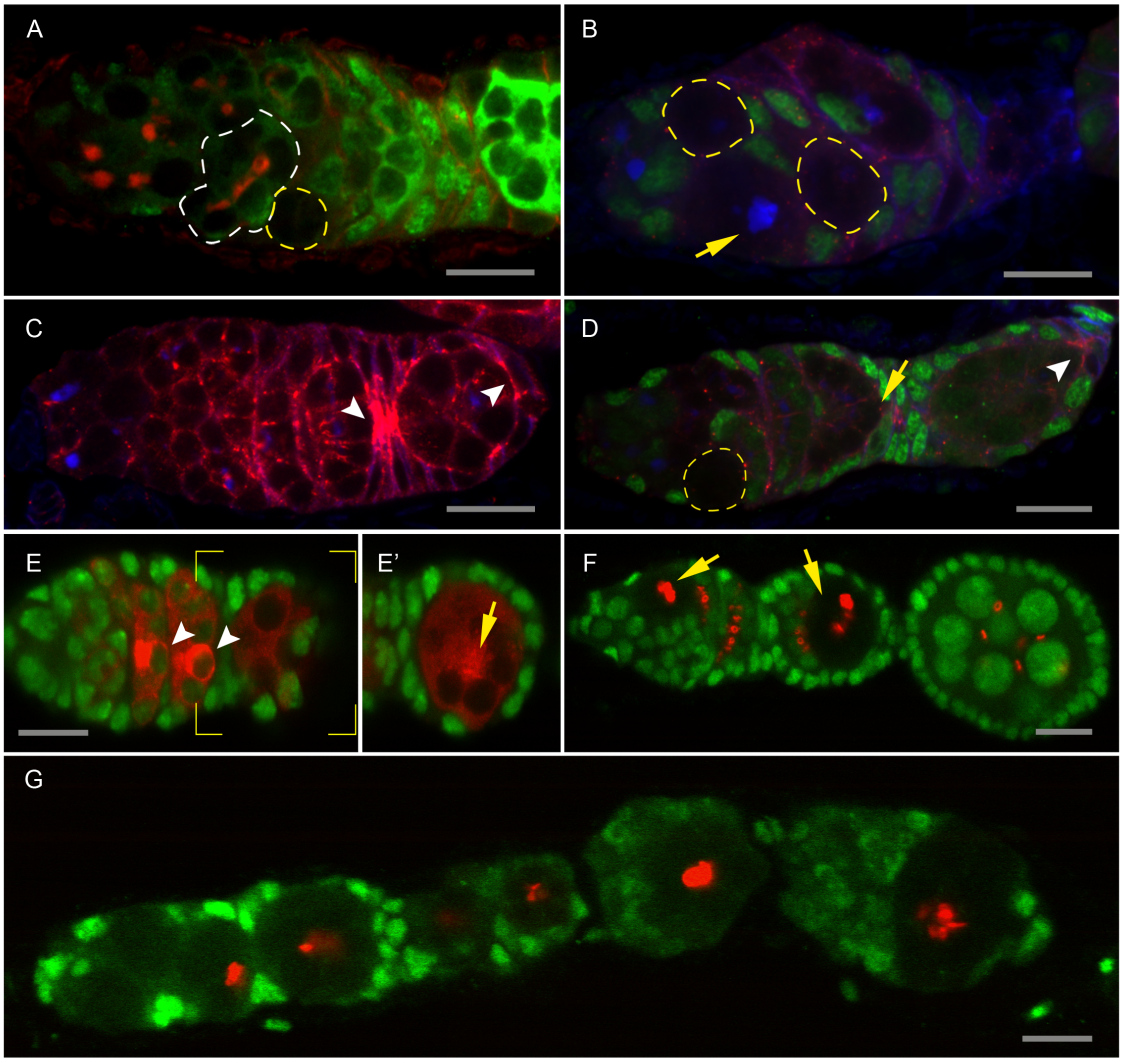

Table 5.1 *rab11-null* GSCs have a 4-fold shorter half-life than *rab11*+ controls

	% marked GSCs (total number of GSCs counted)			
	Days after clone induction			
genotype of marked clones	4	8	12	Half-life
FRT5377, rab11-null	14.5(186)	7.5 (240)	3.5 (144)	4.0 days
FRT82B, *rab11*^{2148}	16.1 (87)	12.6 (238)	11.8 (144)	15.9 days*
FRT5377, rab11+	12.3 (81)	ND	9.4 (607)	16.2 days*

*calculation based on the assumption that GSC loss occurs randomly, and thus linearly over time.

REFERENCES

1. **Ashburner, M.** (1989). *Drosophila: A laboratory Handbook.* Cold Spring Harbor: Cold Spring Harbor Laboratory Press.
2. **Coutelis, J.-B., and Ephrussi, A.** (2007). Rab6 mediates membrane organization and determinant localization during *Drosophila* oogenesis. *Development* **134**, 1419-1430.
3. **de Cuevas, M., and Spradling, A.C.** (1998). Morphogenesis of the *Drosophila* fusome and its implications for oocyte specification. *Development* **125***,* 2781-2789.
4. **de Cuevas, M., Lee, J.K., and Spradling, A.C.** (1996). Alpha-spectrin is required for germline cell division and differentiation in the *Drosophila* ovary. *Development* **122***,* 3959-3968.
5. **Deng, W., and Lin, H.** (1997). Spectrosomes and fusomes anchor mitotic spindles during asymmetric germ cell divisions and facilitate the formation of a polarized microtubule array for oocyte specification in *Drosophila*. *Dev. Biol.* **189,** 79--94.
6. **Dollar, G.L., Struckhoff, E., Michaud J., and Cohen R.S. (2002)**. *Gurken*-independent polarization of the *Drosophila* oocyte; Rab11-mediated organization of the posterior pole. *Development* **129***,* 517-526.
7. **Emery, G., Hutterer, A., Berdnik, D., Mayer, B., Wirtz-Peitz, F., Gaitan, M.G., amd Knoblich, J.A.** (2005). Asymmetric Rab11 endosomes regulate delta recycling and specify cell fate in the *Drosophila* nervous system. *Cell* **122***,* 763-773.
8. **Godt, D., and U. Tepass, U.** (1998). *Drosophila* oocyte localization is mediated by differential cadherin-based adhesion. *Nature* **395***,* 387-391.

9. **Gonzales-Reyes, A., and St Johnston, D**. (1998). The *Drosophila* AP axis is polarised by the cadherin-mediated positioning of the oocyte. *Development* **125***,* 3635-3644.

10. **Huynh, J.-R., and St Johnston, D.** (2004). The origin of asymmetry: early polarization of the *Drosophila* germline cyst and oocyte. *Curr. Biol.* **14***,* R438-R449.

11. **Jankovics, F., Sinka, R. and Erdélyi, M**. (2001). An interaction type of genetic screen reveals a role of the rab11 gene in *oskar* mRNA localization in the developing *Drosophila* oocyte. *Genetics* **158***,* 1177-1188.

12. **Kai, T., and Spradling, A.** (2003). An empty *Drosophila* stem cell niche reactivates the proliferation of ectopic cells. *Proc. Natl. Acad. Sci. USA* **100***,* 4633-4638.

13. **Kai, T., and Spradling, A.C.** (2004). Differentiating germ cells can revert into functional stem cells in *Drosophila* melanogaster ovaries. *Nature* **428***,* 564-569.

14. **Kelso, R. J., Buszczak, M., Quinones, A.T., Castiblanco, C., Mazzalupo, S., and Cooley, L.** (2004.) Flytrap, a database documenting a GFP protein-trap insertion screen in *Drosophila* melanogaster. *Nucl. Acids Res*. **32***,* D418-420.

15. **Kirilly, D., and Xie, T.** (2007). The *Drosophila* ovary: an active stem cell community. *Cell Research* **17***,* 15-25.

16. **Langevin, J., Morgan, M.J., Rossé, C., Racine, V., Sibarita, J-B., Aresta, S., Murthy, M., Schwarz, T., Camonis, J., and Bellaîche.** (2005). *Drosophila* Exocyst Components Sec5, Sec6, and Sec15 Regulate DE-Cadherin Trafficking from Recycling Endosomes to the Plasma Membrane. *Dev. Cell* **9**, 365-376.

17. **Lin, H., Yue., L., and Spradling, A.C.** (1994). The *Drosophila* fusome, a germline-specific organelle, contains membrane skeletal proteins and functions in cyst formation. *Development* **120***,* 947-956.

18. **Lock, J.G., and Stow, J.L.** (2005). Rab11 in Recycling Endosomes Regulates the Sorting and Basolateral Transport of E-Cadherin. *Mol. Biol. Cell* **16***,* 1744-1755.

19. **Mahowald, A.P.** (1972). Ultrastructural observations of oogenesis in *Drosophila*. *J. Morphol.* **137,** 29-48.

20. **McGrail, M., and Hays, T.** (1997). The microtubule motor cytoplasmic dynein is required for spindle orientation during cell divisions and oocyte differentiation. *Development* **124**, 2409 –2419.

21. **McKearin, D., and Ohlstein, B.** (1995). A role for the *Drosophila* bag-of-marbles protein in the differentiation of cystoblasts from germline stem cells. *Development* **121***,* 2937-2947.

22. **Morin, X., Daneman, R., Zavortink, M., and Chia, W**. (2001). A protein trap strategy to detect GFP-tagged proteins expressed from their endogenous loci in *Drosophila*. *Proc. Natl. Acad. Sci. USA* **98***,* 15050-15055.

23. **Murthy, M., and Schwarz, T.L.** (2003). The exocyst component Sec5 is required for membrane traffic and polarity in the *Drosophila* ovary. *Development* **131**, 377-386.

24. **Murthy, M., Ranjan, R., Denef, N., Higashi, M.E., Schupbach, T., and Schwarz, T.L**. (2005). Sec6 mutations and the *Drosophila* exocyst complex. *J. Cell Sci.* **118***,* 1139-1150.

25. **Parks A.L., Cook K.R., Belvin, M., Dompe, N.A., Fawcett, R., Huppert, K., Tan, L.R, Winter. C.G., Bogart, K.P., Deal, J.E., et al.** (2004). Systematic generation of high-resolution deletion coverage of the *Drosophila melanogaster* genome. *Nat. Genet.* **36***,* 288-292.

26. **Riggs, B., Rothwell, W., Mische, S., Hickson, G.R.X., Matheson, J., Hays, T.S., Gould, G.W., and Sullivan, W.** (2003). Actin cytoskeleton remodeling during early *Drosophila* furrow formation requires recycling endosomal components Nuclear-fallout and Rab11. *J. Cell Biol.* **163***,* 143154.

27. **Satoh, A.K., O'Tousa, J.E., Ozaki, K., and Ready, D.F.** (2005). Rab11 mediates post-Golgi trafficking of rhodopsin to the photosensitive apical membrane of *Drosophila*. *Devlopment* **132***, 1487-1498.*

28. **Shulman J.M., and St Johnston, D**. (1999). Pattern formation in single cells. *Trends Cell Biol.* **9***,* 60-64.

29. **Snapp, E.L., Iida, T., Frescas, D., Lippincott-Schwartz, J., and Lilly, M.A.** (2004). The fusome mediates intercellular ER connectivity in *Drosophila* ovarian cysts. *Mol. Biol. Cell* **15,** 4512-4521.

30. **Song, X., Wong, M.D., Kawase, E., and Xie, T.** (2004). Bmp signals from niche cells directly repress transcription of a differentiation-promoting gene, bag of marbles, in germline stem cells in the *Drosophila* ovary. *Development* **131***,* 1353-1364.

31. **Song, X., Zhu, C.H., Doam, C., and Xie, T.** (2002). Germline stem cells anchored by adherens junctions in the *Drosophila* ovary niches. *Science* **296***,* 1855-1857.

32. **Williamson, A., and Lehman, R.** (1996). Germ cell development in *Drosophila*. *Annu Rev Cell Dev Biol*, **12**, 365–391.

33. **Xie, T., and Spradling, A.C.** (1998). Decapentaplegic is essential for the maintenance and division of germline stem cells in the *Drosophila* ovary. *Cell* **94**, 251-260.

34. **Xie, T., and Spradling, A.C.** (2000). A Niche Maintaining Germ Line Stem Cells in the *Drosophila* Ovary. *Science* **290**, 328-330.

35. **Xu, T., Rubin, G.M.** (1993). Analysis of genetic mosaics in developing and adult *Drosophila* tissues. *Development* **117**, 1123-1237.

APPENDIX

Chapter VI

Multiple distinct roles for the Rab11 GTPase within the somatic cells that comprise the *Drosophila* egg chamber

SUMMARY

The *Drosophila* egg chamber is derived from germ-line and somatic stem cells and provides an excellent system in which to study the specification and differentiation of cell fates and their organization into functional units. We showed previously that the Rab11 GTPase, which traffics vesicles from recycling endosomes to the plasma membrane, is required cell autonomously to maintain germ-line stem cell (GSC) identity and to orient the oocyte-nurse cell germ-line cyst within its surrounding somatic epithelium. These requirements are met in part through Rab11's ability to traffic E-cadherin to specific surfaces of GSCs and oocytes and thus fortify important contacts between them and neighboring somatic cells. Here we investigate the role of Rab11 in somatic follicle stem cells (FSCs), which give rise to the epithelial cells that cover germ-line cysts as well as to polar cells, which serve as signaling centers during egg chamber maturation, and to stalk cells, which form single-cell wide bridges or stalks between adjacent egg chambers. We show that *rab11-null* FSCs are viable and maintain their identity, but only give rise to stalk and polar-like cells. Stains for activated caspase activity indicate that pre-epithelial cells are specified, but die via programmed cell death before egg chamber formation. The *rab11-null* stalk cells fail to organize themselves into functional stalks, revealing an additional role for Rab11 in stalk cell differentiation and/or adhesion. The induction of *rab11-null* epithelial cells, following epithelial cell specification indicates that Rab11 is also a suppressor of neoplastic-like cell growth. The *rab11-null* epithelial cells arrest differentiation early, assume a highly aberrant cell morphology, delaminate from the epithelium, and invade the neighboring germ-line cyst. These defects are associated with incomplete E-cadherin localization and a general loss of cell polarity, which may also explain the observed defects in epithelial viability, polar cell specification, and stalk cell organization.

INTRODUCTION

The *Drosophila* egg chamber consists of a germ-line cyst, composed of a single oocyte and 15 nurse cells, surrounded by a monolayer epithelium (Fig. 6.1A; and see ref. (Bastock and St Johnston, 2008)). Egg chambers are produced and mature in assembly-line fashion along the anteroposterior axis of the ovariole, the basic structural unit of the *Drosophila* ovary. Each ovariole is divided into an anterior compartment or germarium, which is subdivided into regions 1-3, and a posterior compartment or vitellarium. Germ-line cysts are derived from germ-line stem cells (GSCs), while the surrounding epithelium is derived from somatic follicle stem cells (FSCs). The FSCs also give rise to specialized cells at the anterior and posterior ends of the epithelium known as polar cells, and to stalk cells, which form single-cell wide bridges between adjacent egg chambers (Fig. 6.1A; and see ref. (Kirilly and Xie, 2007)). Two or three GSCs lie at the extreme anterior end of each germarium (in region 1), where they are anchored via adherens junctions (AJs) to cap cells, which together with neighboring terminal filament and escort cells constitute the GSC niche (Kirilly and Xie, 2007; Song et al., 2002). The AJs are maintained by the trafficking of E-cadherin from the fusome, a germ-line specific organelle, to the GSC's anterior surface (Bogard et al., 2007; Deng and Lin, 1997; Song et al., 2002). Such trafficking requires Rab11 and is facilitated by the close proximity of the fusome to the cytoplasmic side of the AJs (Bogard et al., 2007). The fusome also plays an important role in directing GSC division along the anteroposterior axis of the germarium by anchoring one pole of the mitotic spindle to the GSC's anterior cortex (Song et al., 2004; Xie and Spradling, 1998, 2000). Such anchoring ensures that only one daughter cell inherits the AJs and remains in the niche where it can continue to receive Dpp/BMP4 and other signals essential for maintenance of GSC identity (de Cuevas and Spradling, 1998; Deng and Lin, 1997; McGrail and Hays, 1997).

The posterior daughter, called the cystoblast, is born outside of the signaling range of the niche and initiates a differentiation program that includes four rounds of mitotic division. Each round of mitotic division is accompanied by incomplete cytokinesis such that the 16 cells that comprise the mature germ-line cyst are interconnected to one another by 15 cytoplasmic bridges, called ring canals (Bastock and St Johnston, 2008). The two first-generation cells contain four ring canals each, the two second-generation cells three canals each, the four third-generations cells two canals each, and the eight fourth-generation cells one canal each.

Germ-line cyst divisions and oocyte determination are both dependent on proper segregation, growth and fusion of the fusome (de Cuevas and Spradling, 1998; Deng and Lin, 1997). During GSC division, about one-third of the fusome is donated to the cystoblast. The donated fusome orients the first round of cystoblast division by capturing one pole of the mitotic spindle. New fusome material, called a fusome plug, is laid down at the mid-body of the first mitotic spindle and acts as a physical barrier to cytokinesis (de Cuevas and Spradling, 1998; Deng and Lin, 1997; Huynh and St Johnston, 2004). The fusome plug subsequently fuses with the original fusome material to form a contiguous organelle that extends through the ring canal of the two-cell cyst. One of these cells contains more fusome material than the other as it contains all of the original material plus half of the plug. During the next round of division, each end of the fusome (one in each of the 2 cells) captures a single pole of the mitotic spindle and the whole process of fusome plug formation and fusion is repeated. In this way, the final 16-cell cyst is interconnected by a single branched fusome, with one cell (the original one) containing more fusome material than all of the others and it is always this cell that is selected to differentiate as the oocyte (Huynh and St Johnston, 2004).

In contrast to the strict lineage-dependent mechanism of oocyte determination, somatic cell fates and oocyte positioning are determined through a cascade of cell-cell interactions. Shortly after oocyte determination, the germ-line cyst enters germarial region 2a, where it encounters two FSCs and the differentiating descendants of such cells, which include precursors for the polar/stalk cell lineage as well as for the epithelial cell lineage (Kirilly and Xie, 2007; Lopez-Schier, 2003; Nystul and Spradling, 2010; Tworoger et al., 1999; Zhang and Kalderon, 2001). About 16 pre-epithelial cells, subsequently wrap around the cyst and begin to polarize and form a conventional epithelium (Nystul and Spradling, 2010). Six to eight pre-stalk/polar cells then migrate inward along the germ-line cyst's anterior surface, simultaneously pushing the cyst into germarial region 3 and separating it from the adjacent younger (more anterior) cyst. The older (region 3) cyst induces the 2 closest pre-stalk stalk/polar cells via the Delta/Notch pathway to become polar cells (Assa-Kunik et al., 2007; Grammont and Irvine, 2001; Lopez-Schier and St Johnston, 2001; Torres et al., 2003; Vachias et al., 2010). These cells assume a tear-drop shape and embed themselves into the anterior end of the epithelium of the region three cyst, which is also referred to as the stage 1 egg chamber (Fig. 6.1). Once specified, the polar cells signal the remaining 4-6 pre-stalk/polar cells through both the Notch and JAK/STAT pathways to differentiate as stalk cells (Baksa et al., 2002; Ghiglione et al., 2002; Larkin et al., 1996; McGregor et al., 2002). The stalks cells over-express E-cadherin and through competitive homotypic interactions with E-cadherin expressed on the surface of the adjacent region 2b cyst orient that cyst (Gonzalez-Reyes and St Johnston, 1998); the oocyte, which expresses more E-cadherin than the nurse cells due do its increased amount of fusome material, has a selective adhesive advantage and comes to lie at the posterior end of the cyst, adjacent to the stalk (Huynh

and St Johnston, 2004). This process is repeated with each successive egg chamber such that the oocyte is the most-posterior cell within each germ-line cyst.

Following the specification of the anterior polar cells and adjacent stalk the stage 1 (s1) egg chamber buds from the germarium into the main body of the ovariole. Subsequent steps of egg chamber maturation have been divided into 13 morphologically distinct stages (s2-s14) and culminate with the release of the mature egg into the oviduct for fertilization. During s2 or s3, stalk cells at the posterior end of the egg chamber are induced by poorly understood mechanisms to adopt a polar cell fate (Nystul and Spradling, 2010; Torres et al., 2003). These cells remain indistinguishable from the original polar cells at the egg chamber's anterior end until about stage 7, when the oocyte induces them to adopt a posterior cell fate. Such cells subsequently send a signal back to the oocyte that defines the major body axes of the mature egg and future embryo (Bastock and St Johnston, 2008).

Here, we investigate the role of Rab11 in the specification and differentiation of follicle cell fates. We show that Rab11 is required for the viability of pre-epithelial. Homozygous *rab11-null* FSCs give rise to normal numbers of stalk/polar cells, but to few, if any, epithelial cells. None of the *rab11*-null polar and stalk cells are ever incorporated into a mature stalk/egg chamber, however, indicating an additional requirement for Rab11 in polar and stalk cell differentiation. Finally, we show that the loss of Rab11 from cells that have already committed to the epithelial pathway causes a block in differentiation, loss of cell polarity, and the formation of invasive cell masses. As in the germ-line, many of the defects associated with the loss of Rab11 from somatic follicle cells strongly correlate with inefficient trafficking of E-cadherin.

METHODS

Drosophila genetics

Fly culture and crosses were carried out according to standard procedures (Ashburner et al., 2005). The wild-type stock was *w*, *w His2AV::GFP* , or *w Hrb98DE::GFP* (Bogard et al., 2007; Morin et al., 2001). The *rab11-null, rab11*$^{\Delta FRT}$, has been previously described (Bogard et al., 2007). To generate homozygous *rab11*-null clones, we crossed *w; rab11-null/TM3, Sb* females to *y w hsp::FLP; FRT5377, His2AV::GFP /Tm3, Sb* or *y w hsp::FLP; FRT5377, Hrb98DE::GFP* males, where *FRT5337* corresponds to the centromere-proximal FRT insertion element that was used to make the *rab11-null* allele (Bogard et al., 2007). F1 3rd instar larvae or 2- to 3-day adults were heat shocked for 1 hour at 37^{o}C on 2 consecutive days. Cells (in Sb+ adults) homozygous for the *rab11-null* allele were identified by the absence of GFP fluorescence. Two *sec15*-null mutants were used, *sec15*^{1} and *sec15*^{2} (Mehta et al., 2005), and identical results were obtained with each. To generate *sec15*-null clones, we crossed *w; FRT82B sec15-null/TM3, Sb* females to *y w hsp::FLP; FRT82B, His2AV::GFP/ TM3, Sb* males. Two- to three-day, Sb+ F1 adults were then heat shocked as described for the *rab11*-null clones.

Immunocytochemistry and confocal microscopy

Ovaries were fixed and immunostained as described (Bogard et al., 2007; Dollar et al., 2002). Primary antibodies were used at the following concentrations: Rat anti-Rab11 (1:500) (Dollar et al., 2002); Sec15 (1:2000; a gift from H. Bellen), Nuf (1:200) (Riggs et al., 2003), phospho-histone H3 (1:250; Upstate Biotech.), and GFP (1:250; Invitrogen). All other primary antibodies were obtained from the Hybridoma bank and used at the following concentrations: E-cadherin (1:40), Fas3 (1:50); Orb (6H4) (1:20); Fas2 (1:50); Discs Large (1:250), β-integrin (1:2), Notch (C17.9C6) (1:10), and LamC (1:50). Secondary antibodies were purchased from

Jackson labs and used at the manufacturer's recommended concentrations. Apoptotic cells were identified by incubating fixed cells with PhiPhiLux G2D2 (Cal Biochem), which stains activated caspase 3, according to manufacturer's recommended conditions. Stained ovaries were mounted in 4% n-propyl gallate (Sigma) in 90% glycerol, 10% phosphate buffered saline. Images were collected on Olympus 3L Spinning disc or Zeiss Meta 510 laser scanning confocal microscopes.

RESULTS AND DISCUSSION

Rab11 is required for the differentiation of stalk and polar cells

Previous studies of hypomorphic alleles showed that Rab11 is required to polarize the *Drosophila* oocyte, but failed to reveal any requirement for the protein in somatic follicle cells (Dollar et al., 2002; Jankovics et al., 2001). The strong expression of Rab11 and its effectors in somatic follicle cells ((Dollar et al., 2002); and see Fif. 2D,E), spurred us to re-examine Rab11's role in them using the recently described *rab11*-null allele, $rab11^{\Delta FRT}$ (Bogard et al., 2007). Because the $rab11^{\Delta FRT}$ allele is homozygous lethal, we used the FRT-FLP system (Xu and Rubin, 1993) to generate homozygous *rab11*-null clones marked by the loss of nuclear GFP. In initial experiments, clones were analyzed 10-14 days after clone induction (ACI) to ensure that they were derived from *rab11*-null FSCs (Bastock and St Johnston, 2008; Kirilly and Xie, 2007). Roughly half of the analyzed germaria were mosaics, containing both wild-type (GFP-positive) and *rab11*-null (GFP-negative) follicle cells. All of the mutant phenotypes described below were rescued by a wild-type *rab11* transgene (Bogard et al., 2007), and thus, directly attributable to a loss of *rab11* gene activity.

Most of the recovered *rab11*-null cells that had exited the germarium, and thus, were old enough to exhibit commitment to a particular differentiation pathway had adopted a stalk cell fate as evident by their strong expression of Lamin C (LamC) (Fig. 6.1B-B''), a protein that is normally strongly expressed in s2 and older stalk cells, but not in other follicle cells (Song and Xie, 2003). Such cells were defective in terminal differentiation or adhesion, however, as they never organized themselves into a recognizable stalk. Rather the cells aggregated into 4-8 cell clusters that were loosely tethered to the epithelia of s2 and older egg chambers (Fig. 6.1B-B''). The *rab11-null* stalk cells also never upregulated E-cadherin (data not shown). Indeed, immunostains for E-cadherin failed to detect any E-cadherin protein in most *rab11-null* cells and in the rare case where the protein was detected it appeared to be intracellular, rather than on the cell surface (data not shown).

As expected for a defect in stalk cell differentiation, we recovered many compound egg chambers that contained two or more germ-line cysts encased in a single continuous epithelium (Fig. 6.2A,A'). In some cases, a single massive compound egg chamber filled the entire ovariole (Fig. 6.2C). The compound nature of these egg chambers was confirmed by immunostaining for Orb (Tan et al., 2001), which revealed at least 2 oocytes in each case (Fig. 6.2A, A'). More rarely, fused egg chambers were recovered that contained a single, stalkless layer of follicle cells between adjacent germ-line cysts (Fig. 6.2B). A similar combination of compound and fused egg chambers are produced by mutants for the Notch and JAK/STAT pathways, which are required for the specification of polar and stalk cell fates (Grammont and Irvine, 2001; Larkin et al., 1996; Lopez-Schier and St Johnston, 2001; Vachias et al., 2010). About half of the *rab11*-null stalk cell clusters contained one or two cells (denoted with asterisks in Fig. 6.1B',B'') that stained positive for both LamC and Traffic jam (Tj), a protein that is

normally expressed in all undifferentiated and differentiated follicle cells, except stalk cells (Li et al., 2003). Given that wild-type stalk and polar cells are related by lineage (see above), it is likely that these cells are polar or polar-like cells and we will henceforth refer to them as such. Like their wild-type counterparts, the *rab11*-null polar-like cells were embedded in the epithelium (Fig. 6.1B',B'') and physically tethered the stalk cell clusters to the epithelium. We conclude from these findings that Rab11 is required for the differentiation, but not the specification, of the polar/stalk sub-lineage. Consistent with such a role for Rab1, we detected very strong expression of both Rab11 and its effector Nuf1 [30] in putative pre-stalk and pre-polar cells at the junction of germarial regions 2b and 3 (Fig. 6.2D, 2E). As the production of compound and fused egg chambers was independent of the genotype of the germ-line cyst (data not shown), we further conclude that Rab11 controls stalk and polar cell differentiation in a cell autonomous fashion. The basis for the block in polar cell differentiation is not clear from our data, but could reflect poor reception or processing of the Notch signal which is provided by the neighboring germ-line cyst.

Rab11 is required for pre-epithelial cell viability

We recovered few if any *rab11*-null epithelial cells in the above experiments. Indeed, most egg chambers only had one or two candidate *rab11*-null epithelial (i.e., LamC-negative) cells, and none had more than four (Fig. 6.1B-B''). Moreover, such cells behaved more like rogue polar cells than authentic epithelial cells as they never or only rarely divided as evident by their small clone size (1 or 2 cells) and absence of phospho-histone H3 (PH3) expression (Hendzel et al., 1997)(Fig. 6.1B,B'; data not shown). The paucity of *rab11*-null epithelial cells was not due to a defect in FSC maintenance or division as undifferentiated (Tj-positive, LamC-

negative) *rab11*-null cells could be found in germarial regions 2a and 2b up to at least 20 days ACI (e.g., see Fig. 6.1B,B'). Consistent with the idea that *rab11*-null pre-epithelial cells are formed, but die before formation of the epithelium, stains for activated caspase 3 revealed intense labeling along the periphery of young (stage 1 and 2) egg chambers (Fig. 6.3). Such staining was apparent, however, only when carried out 6 or more days ACI. These results suggest that Rab11 perdures for several days ACI and that only small amounts of the proteins are required for cell survival. The results further suggest that Rab11's requirement for epithelial cell survival is transient as most of the observed activated caspase 3 staining is restricted to the epithelial layers of young (stage 1- and 2) egg chambers. Indeed, large *rab11*-null epithelial clones, containing 50 or more cells, were recovered when the experimental design was shifted (i.e., when analysis was moved from 10-14 days ACI to 3-9 days ACI) to favor recovery of clones induced in young (e.g., stage 1 and 2) follicle cells, rather than in FSCs. As described below, such clones revealed additional roles for Rab11 in epithelial cell behavior.

Rab11 and its effector Sec15 are required for epithelial cell differentiation

As seen in Fig. 6.4A-C, Rab11, and its two best characterized effectors, Nuf and Sec15 (Emery et al., 2005; Jafar-Nejad et al., 2005; Mehta et al., 2005; Riggs et al., 2003), are expressed throughout oogenesis in follicle epithelial cells. To study the role of Rab11 in such cells, we sought to induce *rab11*-null clones in cells already committed to the epithelial cell fate, thereby circumventing the above described requirement for *rab11* in pre-epithelial cell survival. To this end, we examined stage 4-9 egg chambers 3-6 days ACI. This approach proved useful as nearly half of the recovered egg chambers contained *rab11*-null epithelial cells. The approach also proved useful for the production of epithelial cells homozygous for a null allele of *sec15*,

which encodes a component of the exocyst and a Rab11 effector required for the docking of vesicles to the plasma membrane (Hsu et al., 2004; Langevin et al., 2005; Zhang et al., 2004). As expected for analysis within 6 days ACI, the vast majority of recovered egg chambers contained a completely wild-type germ-line. Rare egg chambers with a mutant germ-line cyst were not analyzed to eliminate complications in data interpretation.

All of the recovered *rab11*-null epithelial cells exhibited an early arrest of differentiation as evident by their strong expression of Fasciclin 3 (Fas3) (Fig. 6.4D), a protein that is normally strongly expressed only in s3 and younger epithelial cells (Ruohola et al., 1991). Several observations together rule out the alternative possibility that the Fas3-positive *rab11*-null cells are ectopic polar cells, which also maintain strong expression of Fas3. First, the *rab11*-null cells strongly expressed Eyes absent (Eya), a protein that is expressed in all follicle cells except polar cells (Bai and Montell, 2002) (Fig. 6.1B'). Second, the *rab11*-null cells divided until s6 or 7 (Fig. 6.4F,F'), whereas, polar cells do not divide beyond s1. Finally, the *rab11*-null cells did not form border cell clusters. Thus while authentic polar cells recruit ~6 neighboring cells into a migration-competent border cell cluster that delaminates from the epithelium and migrates toward the oocyte during stage 9 (Montell, 2003), the *rab11*-null cells delaminated prior to stage 9, without recruitment of other cells, and migrated in random directions (see below). The *sec15*-null cells also arrested differentiation early as evident by their strong expression of Fas3 (Fig. 6.4G). However, in contrast to the *rab11*-null cells, which survived for ~6 days, nearly half of the *sec15*-null cells were targeted for programmed cell death by 2 days ACI as evident by immunostaining for activated caspase 3 (Fig. 6.4H). While these data are consistent with the idea that Sec15 is an effector of Rab11 in follicle cell differentiation and maintenance (see below) they indicate additional, Rab11-independent, roles for Sec15 in cell viability.

Rab11 behaves as a neoplastic tumor suppressor-like protein in follicle epithelial cells

The *rab11*-null epithelial cells exhibited a variety of neoplastic-like behaviors including, the above mentioned block in differentiation, loss of cell polarity, and invasion into neighboring tissues. The loss of cell polarity was initially apparent in the gross morphology of the mutant cells. By 5 days ACI, all of the *rab11*-null cells were completely rounded up and displaced from the epithelium (Fig. 6.4D,D'). The loss of cell polarity was confirmed by immunostaining for protein markers of cell polarity. Most telling, E-cadherin and Discs large (Dlg), which establish apical-basal membrane polarity through their organization of adherens and septate junctions (Bilder, 2004; Bilder et al., 2000; Bilder and Perrimon, 2000; Tepass et al., 2001), respectively, were absent from the plasma membrane and concentrated in intracellular compartments, or, in the case of Dlg, dispersed throughout the cytoplasm (Fig. 6.4I-J). A complete loss of cell polarity was also indicated by immunostaining for apical (Notch) and basolateral (Fasciclin 2, Fas3, N-cadherin, and β-integrin) membrane proteins (Fig. 6.4I-K). In each case, the protein was missing from the plasma membrane and instead highly enriched in the same intracellular compartments in which E-cadherin accumulated. Previous studies with *Drosophila* revealed a role for Rab11 in maintaining AJs but did not uncover a requirement for Rab11 in maintaining Dlg expression patterns or other components of septate junctions (Roeth et al., 2009). One explanation for this difference is that the embryonic studies used dominant negative and hypomorphic alleles of *rab11*, which may not have completely eliminated Rab11 function.

The invasive behavior of the *rab11*-null cells was aggressive and distinct from that described for mutations in characterized *Drosophila* tumor suppressor genes (tsgs), which include the septate junction organizers, *discs large, scribble,* and *lethal giant large,* and two

regulators of endocytosis, *avalanche*, and *rab5* (Bilder, 2004; Lu and Bilder, 2005). The *rab11*-null cells invaded surrounded tissues as groups that were fully detached from the epithelium and that ranged in size from as few as 2 cells (Fig. 6.4E,I") to well over 50 (Fig. 6.4L). In contrast, previously characterized tsg mutant cells only invade surrounding tissues as large multi-layered sheets that remain attached to the epithelium (Hariharan and Bilder, 2006). In essence, then, the invasive behavior of other tsg mutant cells is akin to tissue over-growth, while that of the *rab11*-null cells more closely parallels the behavior of metastatic tumor cells of higher animals (Chambers et al., 2002). It is also noteworthy that although the majority of recovered *rab11*-null cells delaminated from the apical side of the epithelium, a small percentage of the cells delaminated from the basal side (arrows in Fig. 6.4D, L), as again is typical of metastatic tumor cells (Chambers et al., 2002). We wish to emphasize, however, that the *rab11*-null epithelial cells exhibited no obvious defects in cell proliferation, a defining phenotype of all true tumor suppressor genes; immunostains for phospho-histone 3 show that *rab11*-null cells cease dividing at stage 6/7 of oogenesis, like their wild-type counterparts. However, we also wish to emphasize that *Drosophila*'s previously characterized neoplastic tumor suppress genes have no demonstrable or only subtle requirements in the suppression of follicle cell over-proliferation (Bilder, 2004). Indeed, the requirement for these genes in the suppression of over-proliferation comes almost entirely from analyses of larval tissues, most notably imaginal discs. Whether suppression of over proliferation of larval and adult cells is fundamentally different or simply easier to demonstrate in the former is not clear. Unfortunately, we have been unable to recover *rab11*-null clones in imaginal discs and other larval tissues, possibly reflecting unique roles for Rab11 in the survival of such cells. In the absence of a definitive role for Rab11 in the suppression of cell over-proliferation, we propose that Rab11 protein be referred to as neoplastic

tumor suppressor-like.

Consistent with our findings that loss of Rab11 promotes migratory behavior in non-migratory cells, recent studies have shown that reduction of Rab11 increases the motility of cells induced to migrate by wounding or other Rab11-independent means (Jones et al., 2006; Prigozhina and Waterman-Storer, 2006). Paradoxically, Rab11 expression is up-regulated in human skin and breast carcinomas and certain other metastatic cell populations (Cheng et al., 2004; Fan et al., 2004; Gebhardt et al., 2005; Goldenring et al., 1999; Jones et al., 2006; Wang et al., 2004; Yoon et al., 2005). It will be of interest to determine if Rab11 loss and up-regulation interfere with the same or different trafficking pathways and how these pathways affect normal versus cancerous cell migrations. The current difficulty in sorting out Rab11's role in the migration of normal and cancerous cells is the lack of information regarding the identity of Rab11's cargoes and the fate of such cargoes in the absence or over-expression of Rab11. More information in this area is needed as is a more extensive survey of the involvement of Rab11 in the migratory behaviors of normal and cancerous cells.

Acknowledgements

We thank Sui Zhang for excellent technical assistance. We thank Vicki Corbin for comments on the manuscript and Bill Sullivan, Hugo Bellen, and the Bloomington Stock Center for antibodies and fly stocks. Finally, we thank David Moore for excellent help with confocal microscopy.

Figure 6.1 Rab11 is required for the faithful differentiation of polar and stalk cells. (**A**) Diagram of the *Drosophila* germarium and a budded stage 2 (s2) egg chamber. Anterior is to the left in this and all subsequent images, unless otherwise noted. Germarial regions 1-3 re indicated below the diagram, where region 3, corresponds to a stage 1 egg chamber. GSCs (dark yellow) reside at the extreme anterior end of region 1 and give rise to cystoblasts, and 2-, 4-, 8- and 16-cell germ-line cysts (light yellow). Oocyte nucleus, blue circle. FSCs (light green) reside at the 2a/2b junction and give rise to epithelial (grey), polar (red) and stalk (blue) cells. Pre-polar/pre-stalk cells are shown in purple. Follicle cells not yet committed to the polar/stalk or epithelial sub-lineages are shown in white. (**B-B''**) Mosaic germarium with adjacent compound egg chamber immunostained for nuclear nuclear GFP (green), Traffic jam (red), and LamC (blue) 10 days ACI. The *rab11-null* cells are identified by the absence of nuclear GFP. Each panel shows a different focal plane. Putative rogue polar cells are indicated with curved arrows (see Results). Arrow in (**B**) points to a group of uncommitted traffic jam-positive, *rab11*-null follicle cells in germarial region 2B. Most other *rab11*-null follicle cells are LamC-positive indicative of commitment to differentiate as stalk cells. Such cells form clusters (arrowheads), but are not organized into recognizable stalks. Germ-line cells are also LamC-positive, but are distinguishable from the stalk cells by size and position. The asterisks in **B'** and **B''** (close up) denote *rab11*-null LamC- and Tj-positive (polar-like) cells that appear to physically tether the stalk-like cell clusters to the epithelium (see Results).

Figure 6.1

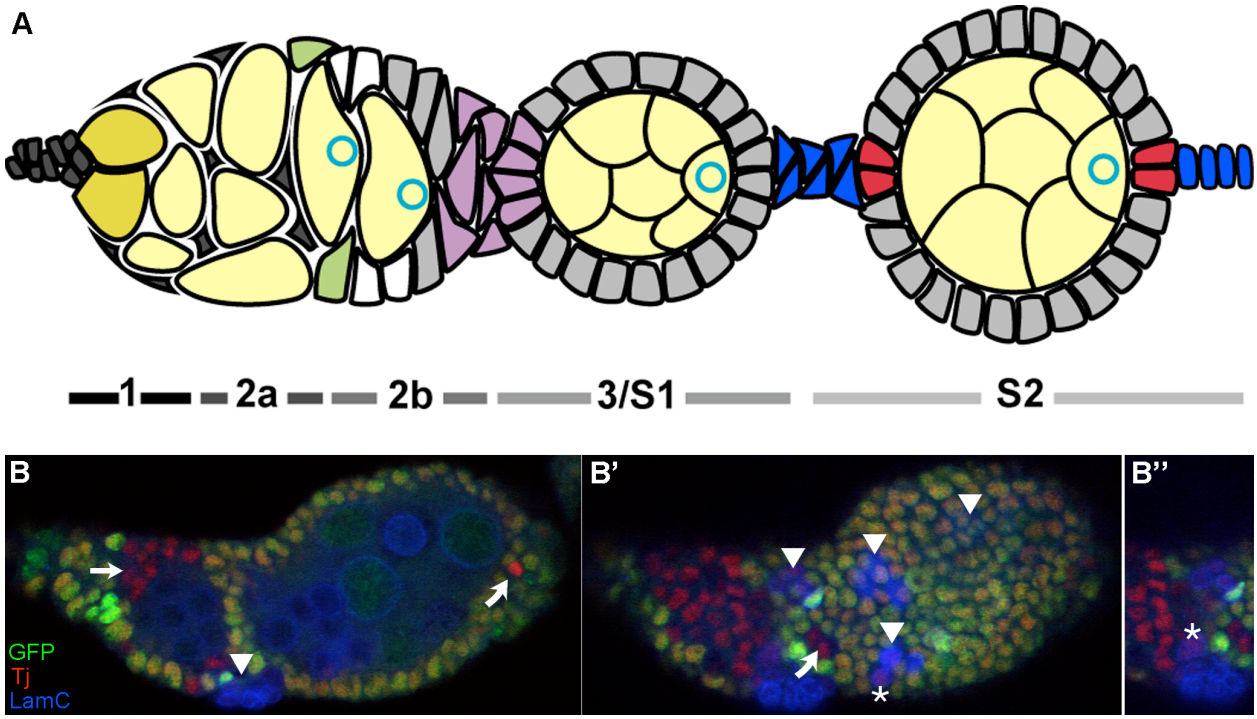

Figure 6.2 The induction of Rab11-null FSCs results in the production of compound and fused egg chambers. (**A**-**C**) Compound and fused egg chambers recovered from females in which rab11-null clones were generated (Methods). (**A**, **A'**) Two different focal planes of a compound egg chamber immunostained for nGFP (green) and the oocyte marker, Orb (red) 10 days ACI. (**B**) Fused egg chamber immunostained for E-cadherin (red) and nGFP (green) 10 days ACI. Anterior at bottom. (**E**) Massive compound egg chamber immunostained for nGFP (green) and lamC (blue). (**F**, **G**) Wild-type germaria immunostained for (**F**) nGFP (green) and Rab11 (red), or (**G**) Nuf (white), a Rab11 effector protein. The arrow in (**F**) points to enriched expression of Rab11 in presumptive pre-stalk/polar cells in region 2B. This region is expanded in (**G**) as stalk cell formation is more advanced in this particular germarium.

Figure 6.2

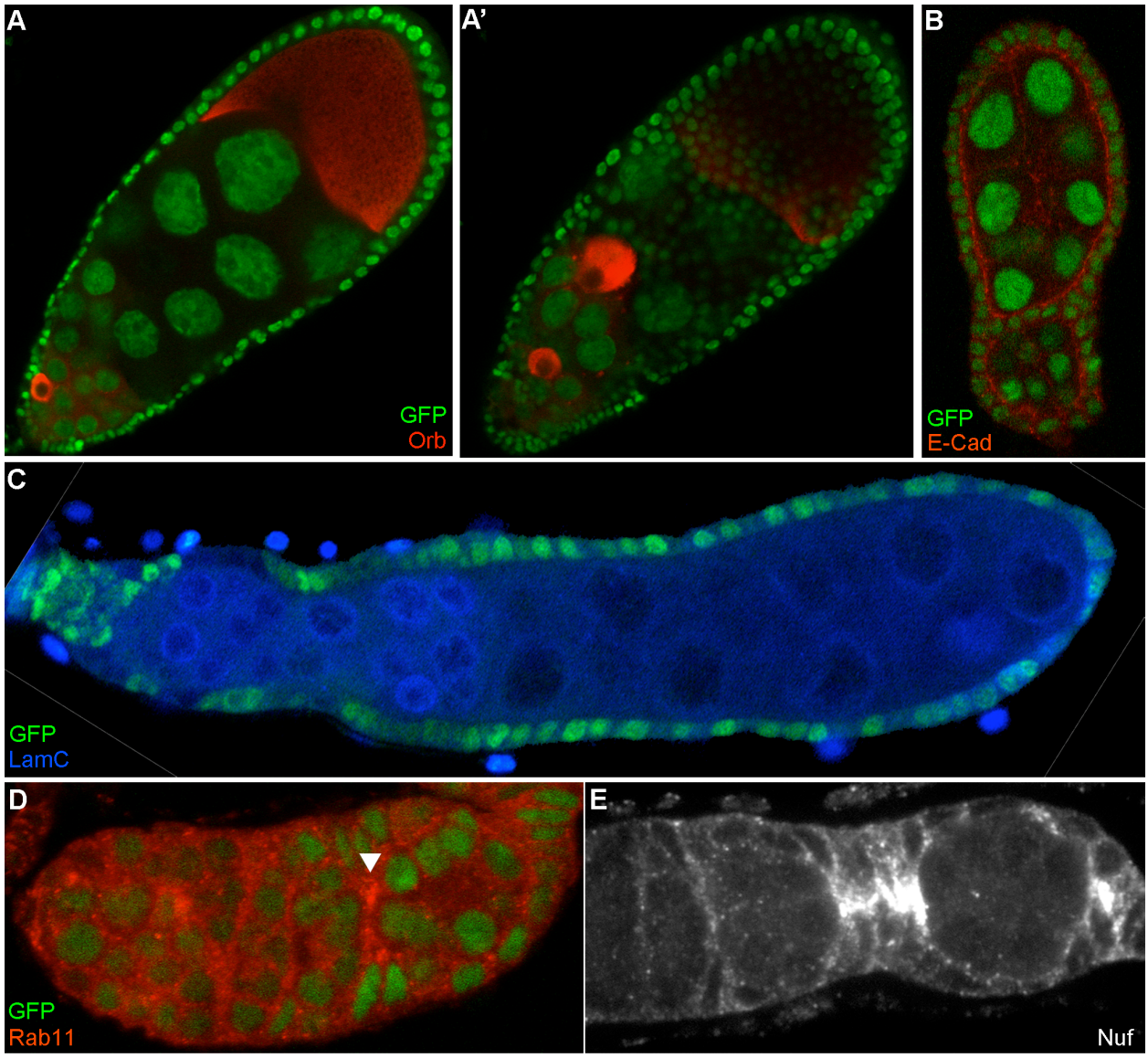

Figure 6.3 Rab11 is required for the survival of pre-epithelial cells. (**A**) A *rab11*+control germarium stained for activated caspase activity (red) and nuclear GFP (see Methods). Selected activated caspase-positive cells are marked with asterisks. The vast majority of such cells in this and other *rab11*+ control germaria are located at the germarial region 1/region 2a junction and almost certainly are escort cells, which are known to undergo programmed cell death following delivery of their associate germ-line cysts to germarial region 2a (Decotto and Spradling, 2005) (**B**) Mosaic germarium following induction of *rab11-null* clones, which are identified by the absence of nuclear GFP. In contrast to control germaria, a significant number of activated caspase-positive cells (denoted with arrows) are observed in posterior regions (i.e., regions 2a, 2b, and 3) of the germarium. All such cells are GFP-negative consistent with a role for Rab11 in their survival. Given that normal or near normal numbers of stalk and polar-like cells are recovered (in older egg chambers), we suspect that these cells are pre-epithelial in nature.

Figure 6.3

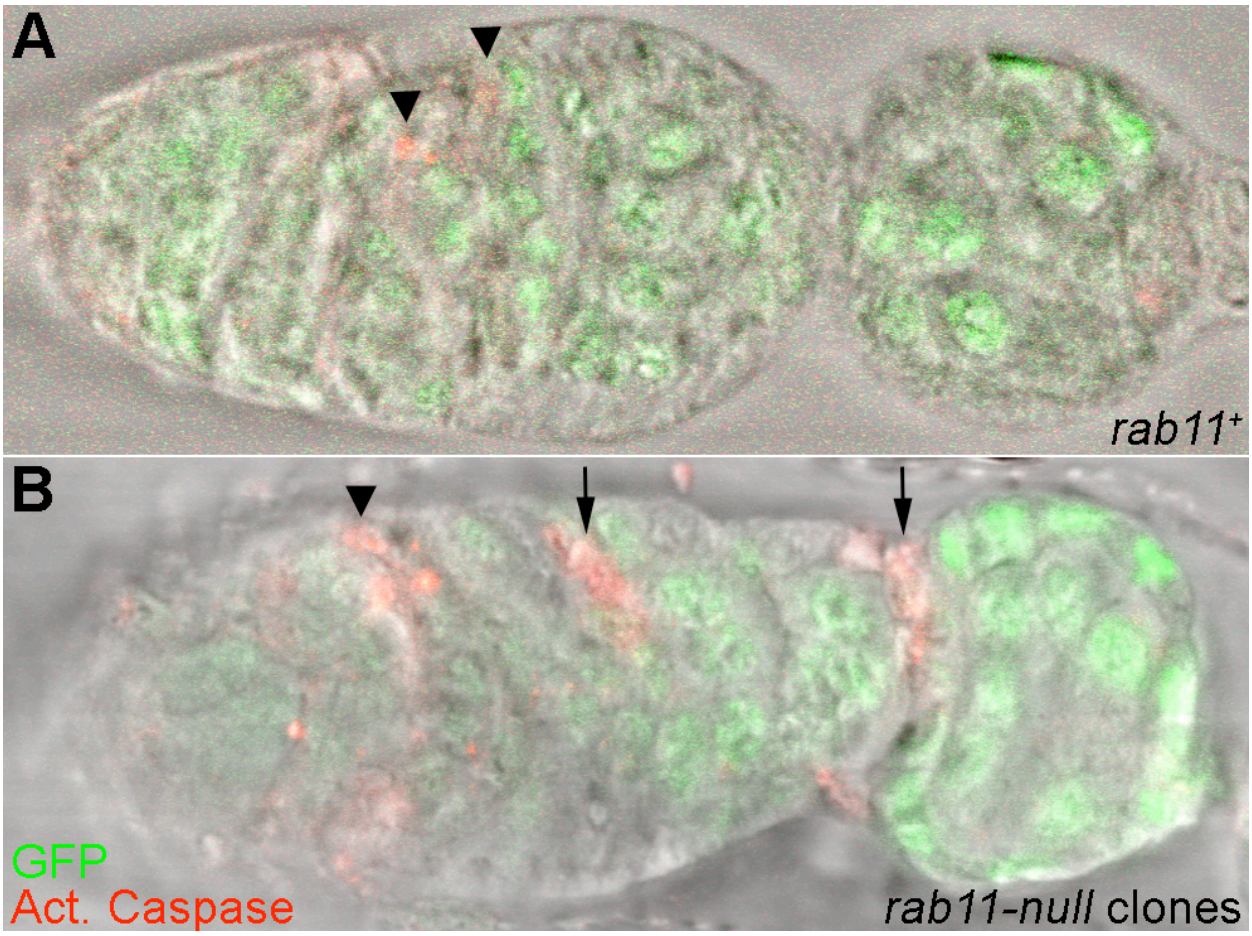

Figure 6.4 Rab11 is required for the differentiation and maintenance of epithelial cells.

(**A**-**C**) Wild-type s8/9 egg chambers immunostained for (**A**) Rab11 (red). (**B**) Nuf (green) and (**C**) Sec15 (red). Magnified views are shown at the bottom of each panel. (**D**) Mosaic s6 egg chamber immunostained for nGFP (green) and Fas3 (red) 4-6 days ACI. The arrows point to *rab11*-null cells that have invaded the basement membrane [see arrow in (**L**) for an additional example. (**D'**) Light micrograph of (**D**). (**E**) Mosaic s7 egg chamber immunostained for nGFP (green), Eyes absent (red), and E-cadherin (blue) 4-6 days ACI. All mutant and wild-type cells, except polar cells (denoted with the arrow), stain positive for Eya. (**F**, **F'**) Mosaic s6/7 egg chamber immunostained for nGFP (green), E-cadherin (red) and phospho-histone H3 3 days ACI. (**F'**) Magnified view. (**G**-**H**) Mosaic s7 *sec15*-null egg chambers immunostained for nGFP (green) 2 days ACI. The egg chamber in (**G**) was also immunostained for Fas3 (red), while the one in (**H**) was stained for activated caspases (red) (see Methods), where the arrow points to an apoptotic cell. (**I**-**L**) Magnified views of mosaic epithelia immunostained for nGFP (green) and (**I**, **I'**) E-cadherin (blue) and Fas2 (red), (**J**) E-cadherin (red) and Discs large (Dlg) (blue), or (**K**) E-cadherin (red) and Notch (blue). Clones (GFP-negative cells) are outlined. Note that E-cadherin, Notch, and Fas2 accumulate in intracellular compartments in the invasive *rab11*-null cells, whereas Dlg is completely dispersed throughout the cytoplasm, or absent. It may also be noted in (**J**) that the polarity defects are more severe in the delaminated *rab11*-null cells (white outlines) that in the non-delaminated ones (yellow outlines). (**L**) Mosaic s7 egg chamber immunostained for β-integrin (red) and nGFP (green) 4-6 days ACI. Nuclear DNA is stained with DAPI (blue). A large mutant clone is outline in white. The arrow points to a smaller clone on the basal side of the epithelium.

Figure 6.4

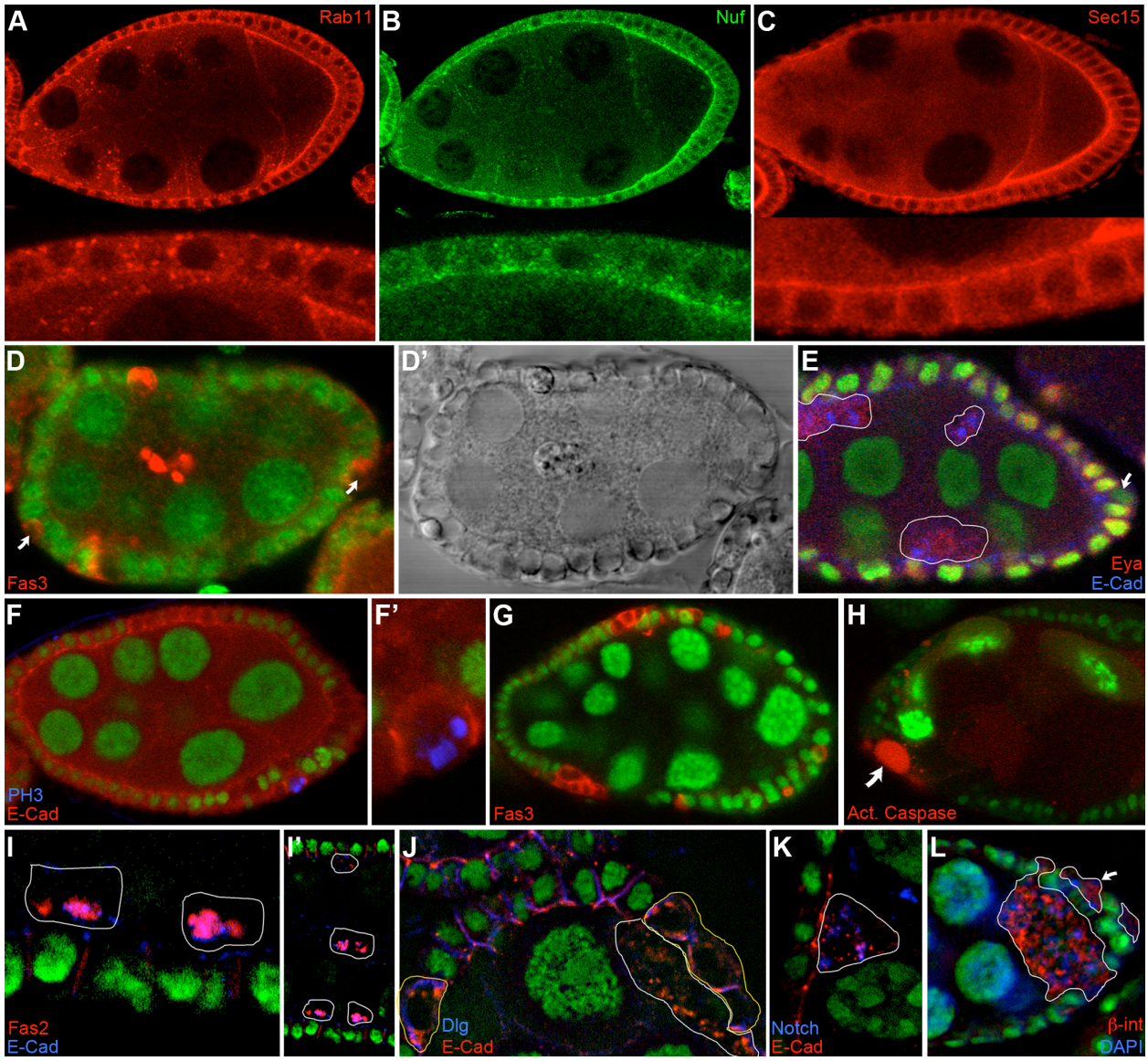
A
Rab11
B
Nuf
C
Sec15
D
Fas3
D'
E
Eya
E-Cad
F
PH3
E-Cad
F'
G
Fas3
H
Act. Caspase
I
Fas2
E-Cad
I'
J
Dlg
E-Cad
K
Notch
E-Cad
L
β-int
DAPI

REFERENCES

1. Ashburner, M., Hawley, R.S., and Golic, K.G. (2005). *Drosophila* : a laboratory handbook, 2nd edn (Cold Spring Harbor, N.Y., Cold Spring Harbor Laboratory Press).
2. Assa-Kunik, E., Torres, I.L., Schejter, E.D., Johnston, D.S., and Shilo, B.Z. (2007). *Drosophila* follicle cells are patterned by multiple levels of Notch signaling and antagonism between the Notch and JAK/STAT pathways. Development *134*, 1161-1169.
3. Bai, J., and Montell, D. (2002). Eyes absent, a key repressor of polar cell fate during *Drosophila* oogenesis. Development *129*, 5377-5388.
4. Baksa, K., Parke, T., Dobens, L.L., and Dearolf, C.R. (2002). The *Drosophila* STAT protein, stat92E, regulates follicle cell differentiation during oogenesis. Dev Biol *243*, 166-175.
5. Bastock, R., and St Johnston, D. (2008). *Drosophila* oogenesis. Curr Biol *18*, R1082-1087.
6. Bilder, D. (2004). Epithelial polarity and proliferation control: links from the *Drosophila* neoplastic tumor suppressors. Genes Dev *18*, 1909-1925.
7. Bilder, D., Li, M., and Perrimon, N. (2000). Cooperative regulation of cell polarity and growth by *Drosophila* tumor suppressors. Science *289*, 113-116.
8. Bilder, D., and Perrimon, N. (2000). Localization of apical epithelial determinants by the basolateral PDZ protein Scribble. Nature *403*, 676-680.
9. Bogard, N., Lan, L., Xu, J., and Cohen, R.S. (2007). Rab11 maintains connections between germline stem cells and niche cells in the *Drosophila* ovary. Development *134*, 3413-3418.

10. Chambers, A.F., Groom, A.C., and MacDonald, I.C. (2002). Dissemination and growth of cancer cells in metastatic sites. Nat Rev Cancer *2*, 563-572.
11. Cheng, K.W., Lahad, J.P., Kuo, W.L., Lapuk, A., Yamada, K., Auersperg, N., Liu, J., Smith-McCune, K., Lu, K.H., Fishman, D.*, et al.* (2004). The RAB25 small GTPase determines aggressiveness of ovarian and breast cancers. Nat Med *10*, 1251-1256.
12. de Cuevas, M., and Spradling, A.C. (1998). Morphogenesis of the *Drosophila* fusome and its implications for oocyte specification. Development *125*, 2781-2789.
13. Decotto, E., and Spradling, A.C. (2005). The *Drosophila* ovarian and testis stem cell niches: similar somatic stem cells and signals. Dev Cell *9*, 501-510.
14. Deng, W., and Lin, H. (1997). Spectrosomes and fusomes anchor mitotic spindles during asymmetric germ cell divisions and facilitate the formation of a polarized microtubule array for oocyte specification in *Drosophila*. Dev Biol *189*, 79-94.
15. Dollar, G., Struckhoff, E., Michaud, J., and Cohen, R.S. (2002). Rab11 polarization of the *Drosophila* oocyte: a novel link between membrane trafficking, microtubule organization, and oskar mRNA localization and translation. Development *129*, 517-526.
16. Emery, G., Hutterer, A., Berdnik, D., Mayer, B., Wirtz-Peitz, F., Gaitan, M.G., and Knoblich, J.A. (2005). Asymmetric Rab 11 endosomes regulate delta recycling and specify cell fate in the *Drosophila* nervous system. Cell *122*, 763-773.
17. Fan, G.H., Lapierre, L.A., Goldenring, J.R., Sai, J., and Richmond, A. (2004). Rab11-family interacting protein 2 and myosin Vb are required for CXCR2 recycling and receptor-mediated chemotaxis. Mol Biol Cell *15*, 2456-2469.

18. Gebhardt, C., Breitenbach, U., Richter, K.H., Furstenberger, G., Mauch, C., Angel, P., and Hess, J. (2005). c-Fos-dependent induction of the small ras-related GTPase Rab11a in skin carcinogenesis. Am J Pathol *167*, 243-253.

19. Ghiglione, C., Devergne, O., Georgenthum, E., Carballes, F., Medioni, C., Cerezo, D., and Noselli, S. (2002). The *Drosophila* cytokine receptor Domeless controls border cell migration and epithelial polarization during oogenesis. Development *129*, 5437-5447.

20. Goldenring, J.R., Ray, G.S., and Lee, J.R. (1999). Rab11 in dysplasia of Barrett's epithelia. Yale J Biol Med *72*, 113-120.

21. Gonzalez-Reyes, A., and St Johnston, D. (1998). The *Drosophila* AP axis is polarised by the cadherin-mediated positioning of the oocyte. Development *125*, 3635-3644.

22. Grammont, M., and Irvine, K.D. (2001). fringe and Notch specify polar cell fate during *Drosophila* oogenesis. Development *128*, 2243-2253.

23. Hariharan, I.K., and Bilder, D. (2006). Regulation of imaginal disc growth by tumor-suppressor genes in *Drosophila*. Annu Rev Genet *40*, 335-361.

24. Hendzel, M.J., Wei, Y., Mancini, M.A., Van Hooser, A., Ranalli, T., Brinkley, B.R., Bazett-Jones, D.P., and Allis, C.D. (1997). Mitosis-specific phosphorylation of histone H3 initiates primarily within pericentromeric heterochromatin during G2 and spreads in an ordered fashion coincident with mitotic chromosome condensation. Chromosoma *106*, 348-360.

25. Hsu, S.C., TerBush, D., Abraham, M., and Guo, W. (2004). The exocyst complex in polarized exocytosis. Int Rev Cytol *233*, 243-265.

26. Huynh, J.R., and St Johnston, D. (2004). The origin of asymmetry: early polarisation of the *Drosophila* germline cyst and oocyte. Curr Biol *14*, R438-449.

27. Jafar-Nejad, H., Andrews, H.K., Acar, M., Bayat, V., Wirtz-Peitz, F., Mehta, S.Q., Knoblich, J.A., and Bellen, H.J. (2005). Sec15, a component of the exocyst, promotes notch signaling during the asymmetric division of *Drosophila* sensory organ precursors. Dev Cell *9*, 351-363.

28. Jankovics, F., Sinka, R., and Erdelyi, M. (2001). An interaction type of genetic screen reveals a role of the Rab11 gene in oskar mRNA localization in the developing *Drosophila* melanogaster oocyte. Genetics *158*, 1177-1188.

29. Jones, M.C., Caswell, P.T., and Norman, J.C. (2006). Endocytic recycling pathways: emerging regulators of cell migration. Curr Opin Cell Biol *18*, 549-557.

30. Kirilly, D., and Xie, T. (2007). The *Drosophila* ovary: an active stem cell community. Cell Res *17*, 15-25.

31. Langevin, J., Morgan, M.J., Sibarita, J.B., Aresta, S., Murthy, M., Schwarz, T., Camonis, J., and Bellaiche, Y. (2005). *Drosophila* exocyst components Sec5, Sec6, and Sec15 regulate DE-Cadherin trafficking from recycling endosomes to the plasma membrane. Dev Cell *9*, 365-376.

32. Larkin, M.K., Holder, K., Yost, C., Giniger, E., and Ruohola-Baker, H. (1996). Expression of constitutively active Notch arrests follicle cells at a precursor stage during *Drosophila* oogenesis and disrupts the anterior-posterior axis of the oocyte. Development *122*, 3639-3650.

33. Li, M.A., Alls, J.D., Avancini, R.M., Koo, K., and Godt, D. (2003). The large Maf factor Traffic Jam controls gonad morphogenesis in *Drosophila*. Nat Cell Biol *5*, 994-1000.

34. Lopez-Schier, H. (2003). The polarisation of the anteroposterior axis in *Drosophila*. Bioessays *25*, 781-791.

35. Lopez-Schier, H., and St Johnston, D. (2001). Delta signaling from the germ line controls the proliferation and differentiation of the somatic follicle cells during *Drosophila* oogenesis. Genes Dev *15*, 1393-1405.

36. Lu, H., and Bilder, D. (2005). Endocytic control of epithelial polarity and proliferation in *Drosophila*. Nat Cell Biol *7*, 1232-1239.

37. McGrail, M., and Hays, T.S. (1997). The microtubule motor cytoplasmic dynein is required for spindle orientation during germline cell divisions and oocyte differentiation in *Drosophila*. Development *124*, 2409-2419.

38. McGregor, J.R., Xi, R., and Harrison, D.A. (2002). JAK signaling is somatically required for follicle cell differentiation in *Drosophila*. Development *129*, 705-717.

39. Mehta, S.Q., Hiesinger, P.R., Beronja, S., Zhai, R.G., Schulze, K.L., Verstreken, P., Cao, Y., Zhou, Y., Tepass, U., Crair, M.C.*, et al.* (2005). Mutations in *Drosophila* sec15 reveal a function in neuronal targeting for a subset of exocyst components. Neuron *46*, 219-232.

40. Montell, D.J. (2003). Border-cell migration: the race is on. Nat Rev Mol Cell Biol *4*, 13-24.

41. Morin, X., Daneman, R., Zavortink, M., and Chia, W. (2001). A protein trap strategy to detect GFP-tagged proteins expressed from their endogenous loci in *Drosophila*. Proc Natl Acad Sci U S A *98*, 15050-15055.

42. Nystul, T., and Spradling, A. (2010). Regulation of epithelial stem cell replacement and follicle formation in the *Drosophila* ovary. Genetics *184*, 503-515.

43. Prigozhina, N.L., and Waterman-Storer, C.M. (2006). Decreased polarity and increased random motility in PtK1 epithelial cells correlate with inhibition of endosomal recycling. J Cell Sci *119*, 3571-3582.

44. Riggs, B., Rothwell, W., Mische, S., Hickson, G.R., Matheson, J., Hays, T.S., Gould, G.W., and Sullivan, W. (2003). Actin cytoskeleton remodeling during early *Drosophila* furrow formation requires recycling endosomal components Nuclear-fallout and Rab11. J Cell Biol *163*, 143-154.

45. Roeth, J.F., Sawyer, J.K., Wilner, D.A., and Peifer, M. (2009). Rab11 helps maintain apical crumbs and adherens junctions in the *Drosophila* embryonic ectoderm. PLoS One *4*, e7634.

46. Ruohola, H., Bremer, K.A., Baker, D., Swedlow, J.R., Jan, L.Y., and Jan, Y.N. (1991). Role of neurogenic genes in establishment of follicle cell fate and oocyte polarity during oogenesis in *Drosophila*. Cell *66*, 433-449.

47. Song, X., Wong, M.D., Kawase, E., Xi, R., Ding, B.C., McCarthy, J.J., and Xie, T. (2004). Bmp signals from niche cells directly repress transcription of a differentiation-promoting gene, bag of marbles, in germline stem cells in the *Drosophila* ovary. Development *131*, 1353-1364.

48. Song, X., and Xie, T. (2003). Wingless signaling regulates the maintenance of ovarian somatic stem cells in *Drosophila*. Development *130*, 3259-3268.

49. Song, X., Zhu, C.H., Doan, C., and Xie, T. (2002). Germline stem cells anchored by adherens junctions in the *Drosophila* ovary niches. Science *296*, 1855-1857.

50. Tan, L., Chang, J.S., Costa, A., and Schedl, P. (2001). An autoregulatory feedback loop directs the localized expression of the *Drosophila* CPEB protein Orb in the developing oocyte. Development *128*, 1159-1169.

51. Tepass, U., Tanentzapf, G., Ward, R., and Fehon, R. (2001). Epithelial cell polarity and cell junctions in *Drosophila*. Annu Rev Genet *35*, 747-784.

52. Torres, I.L., Lopez-Schier, H., and St Johnston, D. (2003). A Notch/Delta-dependent relay mechanism establishes anterior-posterior polarity in *Drosophila*. Dev Cell *5*, 547-558.

53. Tworoger, M., Larkin, M.K., Bryant, Z., and Ruohola-Baker, H. (1999). Mosaic analysis in the *Drosophila* ovary reveals a common hedgehog-inducible precursor stage for stalk and polar cells. Genetics *151*, 739-748.

54. Vachias, C., Couderc, J.L., and Grammont, M. (2010). A two-step Notch-dependant mechanism controls the selection of the polar cell pair in *Drosophila* oogenesis. Development *137*, 2703-2711.

55. Wang, W., Goswami, S., Lapidus, K., Wells, A.L., Wyckoff, J.B., Sahai, E., Singer, R.H., Segall, J.E., and Condeelis, J.S. (2004). Identification and testing of a gene expression signature of invasive carcinoma cells within primary mammary tumors. Cancer Res *64*, 8585-8594.

56. Xie, T., and Spradling, A.C. (1998). decapentaplegic is essential for the maintenance and division of germline stem cells in the *Drosophila* ovary. Cell *94*, 251-260.

57. Xie, T., and Spradling, A.C. (2000). A niche maintaining germ line stem cells in the *Drosophila* ovary. Science *290*, 328-330.

58. Xu, T., and Rubin, G.M. (1993). Analysis of genetic mosaics in developing and adult *Drosophila* tissues. Development *117*, 1223-1237.

59. Yoon, S.O., Shin, S., and Mercurio, A.M. (2005). Hypoxia stimulates carcinoma invasion by stabilizing microtubules and promoting the Rab11 trafficking of the alpha6beta4 integrin. Cancer Res *65*, 2761-2769.

60. Zhang, X.M., Ellis, S., Sriratana, A., Mitchell, C.A., and Rowe, T. (2004). Sec15 is an effector for the Rab11 GTPase in mammalian cells. J Biol Chem *279*, 43027-43034.

61. Zhang, Y., and Kalderon, D. (2001). Hedgehog acts as a somatic stem cell factor in the *Drosophila* ovary. Nature *410*, 599-604.